

Open Quantum Cosmology: A study of two body quantum entanglement in static patch of De Sitter space

Samim Akhtar,^a Sayantan Choudhury,^{1 2 b} Satyaki Chowdhury,^{c,d} Debopam Goswami,^e Sudhakar Panda,^{c,d} Abinash Swain^f

^aDepartment of Physics, Indian Institute of Technology, Madras, Chennai 600036, India.

^bQuantum Gravity and Unified Theory and Theoretical Cosmology Group, Max Planck Institute for Gravitational Physics (Albert Einstein Institute), Am Mühlenberg 1, 14476 Potsdam-Golm, Germany.

^cNational Institute of Science Education and Research, Jatni, Bhubaneswar, Odisha - 752050, India.

^dHomi Bhabha National Institute, Training School Complex, Anushakti Nagar, Mumbai-400085, India.

^eDepartment of Physics, Indian Institute of Technology, Kanpur- 208 016, India.

^fDepartment of Physics, Indian Institute of Technology, Gandhinagar, Palaj, Gandhinagar - 382355, India.

E-mail: samimphysx@gmail.com, sayantan.choudhury@aei.mpg.de,
satyaki.chowdhury@niser.ac.in, debodebopam@gmail.com,
panda@niser.ac.in, abinashswain2010@gmail.com

ABSTRACT: In this work, our prime objective is to study non-locality and long-range effect of two-body correlation using quantum entanglement from the various information-theoretic measure in the static patch of De Sitter space using a two-body Open Quantum System (OQS). The OQS is described by two entangled atoms which are surrounded by a thermal bath, which is modelled by a massless probe scalar field. Firstly, we partially trace over the bath field and construct the Gorini Kossakowski Sudarshan Lindblad (GSKL) master equation, which describes the time evolution of the reduced subsystem density matrix. This GSKL master equation is characterized by two components, these are Spin chain interaction Hamiltonian and the Lindbladian. To fix the form of both of them, using Schwinger-Keldysh formalism we compute the Wightman functions for probe massless scalar field. Using this result along with the large time equilibrium behaviour we obtain the analytical solution for reduced density matrix. Further using this solution we compute Von-Neumann entropy, Rényi entropy, logarithmic negativity, entanglement of formation, concurrence and quantum discord in a static patch of De Sitter space. Finally, we have studied the violation of Bell-CHSH inequality, which is the key ingredient to study non-locality in primordial cosmology.

KEYWORDS: Open Quantum Systems, Quantum dissipation, Quantum entanglement, QFT of De Sitter space, Quantum Information Theory, Theoretical Cosmology.

¹Corresponding author, Alternative E-mail: sayanphysicsisi@gmail.com.

²NOTE: This project is the part of the non-profit virtual international research consortium "Quantum Structures of the Space-Time & Matter" .

Contents

1	Introduction	2
2	Modelling two atomic Open Quantum System (OQS)	6
3	Non unitary time evolution of the reduced subsystem	8
4	Reduced sub system construction	10
4.1	Density Matrix construction	10
4.2	Partial Trace operation	11
5	Effective Hamiltonian Construction	11
6	Quantum Dissipator or Lindbladian Construction	14
7	Bloch Sphere representation of density matrix	15
8	Time evolution of the reduced subsystem density matrix	18
8.1	Large Scale time dependent solution	20
8.2	Arbitrary time dependent solution	22
8.3	Solution of the evolution equations	23
8.4	General solution	24
9	Von Neumann Entanglement Entropy	30
9.1	Bloch sphere representation of Von Neumann Entropy	32
9.2	Von Neumann entropy from OQS of two entangled atoms	33
10	Re'nyi Entropy	35
10.1	Bloch sphere representation of Re'nyi Entropy	37
10.2	Re'nyi entropy from OQS of two entangled atoms	37
11	Logarithmic Negativity	42
11.1	Bloch sphere representation of Logarithmic negativity	43
11.2	Logarithmic negativity from OQS of two entangled atoms	44
12	Entanglement of formation and Concurrence	45
12.1	Bloch sphere representation of Concurrence	47
12.2	Concurrence from OQS of two entangled atoms	48
12.3	Entanglement of formation from OQS of two entangled atoms	50
13	Quantum Discord	52
13.1	Bloch sphere representation of Quantum Discord	53
13.2	Quantum Discord from OQS of two entangled atoms	54

14	Non Locality from Bell CHSH inequality in De Sitter space	56
14.1	Non-locality in Quantum Mechanics	56
14.2	Bell's CHSH inequality violation in De-Sitter Space	59
15	Conclusion	66
A	Geometry of Static Patch of De Sitter space time	69
B	Solution for the bath field equation for probe massless scalar field in Static Patch of De Sitter Space	72
B.1	Finding un-normalized total solution for probe scalar field	72
B.2	Finding un-normalized regular solution for probe scalar field	74
B.3	Finding the normalization constant for the regular solution for probe scalar field	75
B.4	Finding normalized regular solution for probe scalar field	77
C	Quantization of bath modes for probe massless scalar field in Static Patch of De Sitter Space	78
D	Bath Hamiltonian for probe massless scalar field in Static Patch of De Sitter Space	81
D.1	Constructing classical bath Hamiltonian	81
D.2	Constructing quantized bath Hamiltonian	83
E	Quantum states for many body (two atomic) entangled states	88
F	Many body (two atomic) Wightman function for probe massless scalar field in Static Patch of De Sitter Space	90
G	Gorini Kossakowski Sudarshan Lindblad (GSKL) ($C_{ij}^{\alpha\beta}$) matrix	92
G.1	Calculation of $\tilde{A}^{\alpha\beta}$	92
G.2	Calculation of $\tilde{B}^{\alpha\beta}$	94
G.3	Calculation of $C_{ij}^{\alpha\beta}$ matrix elements	94
H	Effective Hamiltonian ($H_{ij}^{\alpha\beta}$) matrix	95
H.1	Calculation of $A^{\alpha\beta}$	95
H.2	Calculation of $B^{\alpha\beta}$	96
H.3	Calculation of $H_{ij}^{\alpha\beta}$ matrix elements	97
I	Calculation of useful integrals	98
I.1	Integral I	98
I.2	Integral II	99
I.3	Integral III	100
I.4	Integral IV	101

1 Introduction

The theory of closed quantum systems is a very popular topic and has already been firmly established. But in practical situations no quantum system can be ideally treated as closed and its interactions with the surroundings cannot be neglected, hence it becomes essential to develop a theoretical framework to treat these non adiabatic interactions and develop a proper understanding of the quantum mechanical system. The knowledge of complete time evolutionary dynamics of a quantum mechanical system requires incorporation of the details of the thermal environment, which paves the way towards the study of *Open Quantum System* [1] (OQS), where the physical system weakly interacts with the environment. In general these interactions with the environment significantly controls the time evolution of the quantum mechanical system and induces the phenomenon of *quantum dissipation*. The dynamics of the reduced subsystem of OQS cannot be described using the unitary time evolution operators after integrating out the bath degrees of freedom from the theory. Correct time evolution of the system requires solving the effective *master equation*, which describes the non-unitary time evolution of the reduced density matrix of the system.

To deal with the subsystem in the context of OQS the entire combination of the system and its surroundings (thermal bath) is together treated as a closed quantum system and hence the evolution equations can be assumed to follow the unitary transformation rules. The prime assumption used in the present context is that the entire system environment combination forms a large closed quantum system. Therefore, its time evolution is governed by a unitary transformation generated by a global Hamiltonian which is made up of subsystem Hamiltonian, bath Hamiltonian and interaction Hamiltonian. Moreover the interaction between the system and the bath is assumed to depend on only the present moment, it carries no past memories at all. In short, the interaction is *Markovian* in nature. The interaction between the system and the surroundings is assumed to be weak which justifies the argument that the only effective change that can be seen over time occurs in the context of OQS. This assumption is generally useful in treating the evolution of the system when the OQS has sufficient time to relax to the equilibrium before being perturbed in presence of interaction between the system and thermal environment. However, in a special situation where the system has very fast or frequent perturbation in presence of system- thermal bath coupling, one needs to consider *Non Markovian* approximation. In this treatment additionally it has been assumed that the system is completely uncorrelated with the surroundings at initial time scale, provided the coupling between the subsystem and the environment is sufficiently weak in nature. The techniques developed in the context of OQS have proven very powerful in the context of quantum optics, statistical mechanics, information theory, thermodynamics, cosmology and biology.

On the other hand, quantum entanglement [2] is probably the most fascinating manifestation of quantum theory in which the beauty of quantum mechanics is truly realized. It is a physical phenomenon that occurs when pairs or groups of particles are generated, interact, or share spatial proximity in ways such that the quantum state of each particle cannot be

from different types of OQS are important topics of research at present [12]. Few of them, namely Von Neumann entanglement entropy, Re'nyi entropy, quantum discord, concurrence and entanglement of formation are calculated in this paper to study the explicit role of quantum entanglement in the reduced subsystem between the two atoms.

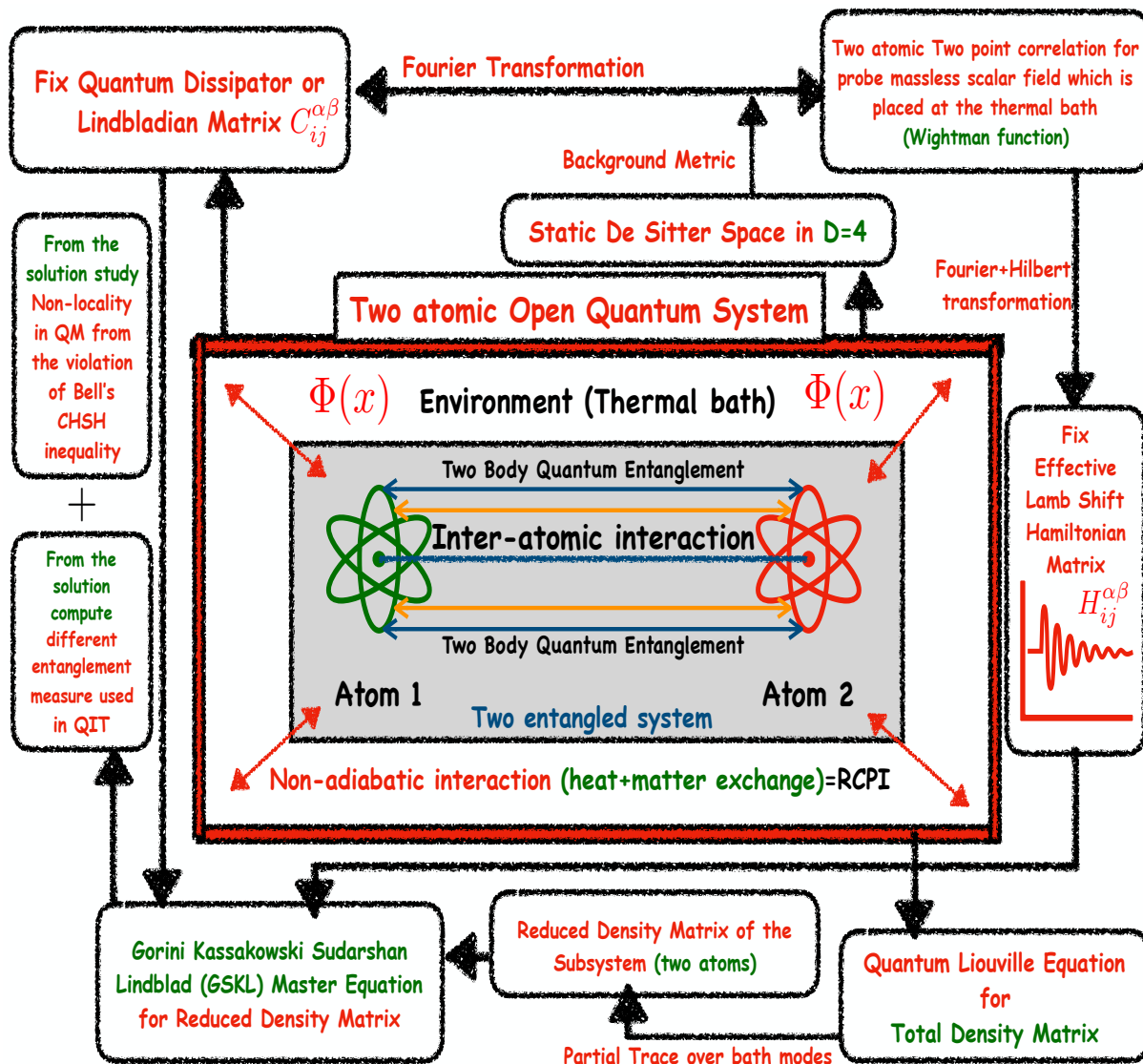


Figure 2. Mnemonic chart for the two atomic (two body) entangled OQS set up.

Many authors have studied the physics of quantum fields in curved spacetime using one and two atomic system in the context of OQS [13–15]. A single detector system weakly interacting with a reservoir in quantized conformally coupled scalar field in De-Sitter space was investigated in the context of OQS in [16]. A similar study was done using two atoms (detectors) in [13] where the authors have studied the evolution of the subsystem only under the effect of the *Lindbladian* operator for different initial states. In that paper the authors have used only concurrence as the measure to quantify entanglement. In this work, however we have studied the evolution of the two atomic subsystem taking into account the contributions from both the prime components of the *master equation*, the

effective Lamb Shift Hamiltonian and the *Lindbladian operator*, which provides a complete solution of the *master equation* and gives us a proper understanding about the complete time evolution of the reduced density matrix of the two atomic subsystem. Further using this result we have computed a number of information theoretic measures to quantify the quantum entanglement. Additionally, we have studied quantum non-locality by establishing Bell's CHSH inequality violation in De Sitter space from the present OQS two atomic set up.

In fig. (1), we have explicitly shown the Penrose diagram representing the static patch of the De Sitter space in which we have placed a two atomic open quantum system which is interacting with a thermal bath non-adiabatically. This diagram represents actually the causal patch of an observer sitting at the north pole, which is represented by $r = 0$ is static coordinate in De Sitter space. Equivalently this can be described in global coordinate with $\theta = 0$. Here the bifurcation Killing horizon for ∂_t is represented by $r = \alpha$ where the parameter $\alpha = \sqrt{\frac{3}{\Lambda}} > 0$ as the cosmological constant $\Lambda > 0$ in De Sitter space. In this context the bifurcation sphere appears just at the middle of the Penrose diagram and in global coordinates it is described by $t = 0$ time slice. However, the other three regions can also be filled by the static coordinate system, which is just like Schwarzschild black holes. In fig. (2), we have presented a mnemonic chart of the computational scheme for the present two atomic OQS set up.

The plan of this paper is as follows. In [section 2](#), we discuss the basics of the OQS. The objective of this section is to familiarize the reader with the prime components of open quantum systems. In [section 3](#), we discuss about the non-unitary time evolution of the reduced subsystem. For OQS, the interactions between the system and its environment make it so that the dynamics of the system cannot be accurately described using unitary operators alone. In [section 4](#), we study the construction of the reduced subsystem. Further, in [section 5](#) and [section 6](#), we show the explicit construction of the two prime components of Gorini Kossakowski Sudarshan Lindblad (GSKL) master equation namely the *effective Lamb Shift part of the Hamiltonian* and the *quantum dissipator operator* or the *Lindbladian*. In [section 7](#), we provide a short introduction on the Bloch sphere representation of the reduced density matrix and explicitly show that it can be expressed in terms of identity matrix and the three Pauli matrices. We also provide a clear mathematical explanation to account for the difference between pure and mixed states in this context. In [section 8](#), we explicitly calculate the analytical solution of the Gorini Kossakowski Sudarshan Lindblad (GSKL) master equation [[17](#), [18](#)] for the case of two entangled atoms which mimics the role of Unruh-De-Witt detectors, which are conformally coupled to a probe massless scalar field which is placed in the thermal bath. We further use the late time equilibrium behaviour as a boundary condition to obtain the analytical solution of the all time dependent components of the reduced density matrix of the two atomic subsystem from the GSKL master equation. In [section 9-13](#), we explicitly calculate various entanglement measures used in the context of quantum information theory now-a-days. To name some we calculate Von Neumann entanglement entropy [[19](#)], Re'nyi entanglement entropy [[20](#)], Logarithmic Negativity [[21](#)], Concurrence [[22](#)], Entanglement of formation [[23](#)] and Quantum discord [[24](#)]. Finally in [section 14](#), we study the concept of non-locality from the violation of Bell-CHSH inequality [[25](#)] in De-Sitter space for the two atomic entangled subsystem in the context of OQS.

2 Modelling two atomic Open Quantum System (OQS)

An OQS is defined to be the one which interacts with the surroundings or environment, which is called *thermal bath*. These interactions are responsible for changing the dynamics of the system and finally give rise to *quantum dissipation* i.e. the information contained in the system is lost to its environment. In reality such system doesn't exist which is completely isolated from its surroundings and hence it becomes a necessary step to develop a theoretical framework to treat these interactions and gain a proper insight of the system.

We are acquainted with the dynamics of *closed* quantum systems (CQS), i.e. with quantum systems that do not suffer from any unwanted interactions with the environment. Although interesting conclusions can be drawn in principle in such idealised physical systems, these observations are tempered by the fact that in real world there are no perfectly closed systems, except perhaps the universe as a whole. Real systems suffer from unwanted interactions with the outside world. We need to develop a theoretical framework in order to have a proper understanding of the dynamics of such quantum mechanical systems. To give an example [12] one can consider a swinging pendulum like that found in mechanical clocks to be an ideal CQS. In this context, the pendulum interacts only very slightly with the rest of the world-its *environment*-mainly through friction. However, to properly describe the full correct dynamics of the pendulum and to give the answer to the question "why it eventually ceases to move one must take into account the damping effects of air friction and imperfections in the suspension mechanism of the pendulum?" one needs to study OQS. This is perfectly correct approach to study the dynamics of interacting quantum system as we know no quantum systems are ever perfectly closed in an ideal sense. An OQS is nothing more than one which has interactions with some environment with system, whose dynamics we wish to neglect usually, or average over the time scale.

It is well known fact that time-dependent *Schrödinger's Equation* describes the time evolution of a quantum state in the context of a CQS. So if our CQS is in some pure state $|\psi(t)\rangle \in \mathcal{H}$ at time t , where \mathcal{H} denotes the Hilbert space of the system, then the time evolution of the state (between two consecutive measurements) is described by the following time evolution equation:

$$\frac{\partial}{\partial t}|\psi(t)\rangle = -i H(t)|\psi(t)\rangle, \quad (2.1)$$

where $H(t)$ is the Hamiltonian operator of the CQS. Here we fix, $\hbar = 1$ in natural units. On the other hand, in the case of mixed states it is useful to introduce the concept of density matrix $\rho(t)$ using which the time evolution of the density operator can be described by the following equation:

$$\frac{d\rho(t)}{dt} = -i[H(t), \rho(t)], \quad (2.2)$$

which sometimes is known as *Quantum Liouville Von Neumann* equation for the CQS. In this context, the time evolution operator is an *unitary operator*. In general, the solution to the *Quantum Liouville Von Neumann* equation can be written as:

$$\rho(t) = \mathcal{U}(t, t_0) = \mathcal{T} \exp \left\{ -i \int_{t_0}^t [H(t'), \rho(t')] dt' \right\} \rho(t_0), \quad (2.3)$$

where $\mathcal{U}(t, t_0)$ is the unitary operator and \mathcal{T} arises from the evolution as a Dyson expansion, when the Hamiltonian H is time-dependent.

The mathematical formalism of *quantum operations* is the key tool for the description of the dynamics of the OQS. It can be used to describe not only nearly closed systems which are weakly coupled to their environments, but also systems which are strongly coupled to their environments, and closed systems that are opened suddenly and subject to measurement. In the present context, two atomic OQS is described by the following global Hamiltonian:

$$H_{\text{Total}}(\tau) = H_{\text{System}}(\tau) \otimes \mathcal{I}_{\text{Bath}} + \mathcal{I}_{\text{System}} \otimes H_{\text{Bath}}(\tau) + H_{\text{Int}}(\tau), \quad (2.4)$$

where, $H_{\text{System}}(\tau)$ represents the two atomic system Hamiltonian, $H_{\text{Bath}}(\tau)$ describes the thermal bath Hamiltonian, which is described by massless probe scalar field [27] which is minimally coupled to gravity in static De Sitter background. $H_{\text{Int}}(\tau)$ signifies the interaction between the thermal bath and the system under consideration in OQS. In static patch of De Sitter space the background space time metric is described by the following infinitesimal line element:

$$ds^2 = \left(1 - \frac{r^2}{\alpha^2}\right) dt^2 - \left(1 - \frac{r^2}{\alpha^2}\right)^{-1} dr^2 - r^2(d\theta^2 + \sin^2\theta d\phi^2) \quad \text{where } \alpha = \sqrt{\frac{3}{\Lambda}} > 0. \quad (2.5)$$

Instead of using the time variable as t in the present context we have introduced a new rescaled time variable τ , which is defined as:

$$\tau = \sqrt{g_{00}} t = \frac{k}{\alpha} t = \sqrt{1 - \frac{r^2}{\alpha^2}} t \quad \text{where } k = \sqrt{\alpha^2 - r^2} > 0. \quad (2.6)$$

In our two atomic OQS set up the system, bath and the interaction Hamiltonian are described by the following expressions [27]:

$$H_{\text{System}}(\tau) = \frac{\omega}{2} \sum_{\alpha=1}^2 \hat{\mathbf{n}}^\alpha \cdot \sigma^\alpha, \quad (2.7)$$

$$H_{\text{Bath}}(\tau) = \int_0^\infty dr \int_0^\pi d\theta \int_0^{2\pi} d\phi \left[\frac{\Pi_\Phi^2(\tau, r, \theta, \phi)}{2} + \frac{r^2 \sin^2 \theta}{2} \left\{ r^2 (\partial_r \Phi(\tau, r, \theta, \phi))^2 + \frac{((\partial_\theta \Phi(\tau, r, \theta, \phi))^2 + \frac{(\partial_\phi \Phi(\tau, r, \theta, \phi))^2}{\sin^2 \theta})}{\left(1 - \frac{r^2}{\alpha^2}\right)} \right\} \right], \quad (2.8)$$

$$H_{\text{Int}}(\tau) = \mu \sum_{\alpha=1}^2 (\hat{\mathbf{n}}^\alpha \cdot \sigma^\alpha) \Phi(\tau, \mathbf{x}^\alpha) = \mu \sum_{\alpha=1}^2 (\hat{\mathbf{n}}^\alpha \cdot \sigma^\alpha) \Phi(\tau, r^\alpha, \theta^\alpha, \phi^\alpha). \quad (2.9)$$

It is important to note that, ω represents the renormalized energy level for two atoms, given by:

$$\omega = \omega_0 + i \times \begin{cases} [\mathcal{K}^{(11)}(-\omega_0) - \mathcal{K}^{(11)}(\omega_0)] & \text{Atom 1} \\ [\mathcal{K}^{(22)}(-\omega_0) - \mathcal{K}^{(22)}(\omega_0)] & \text{Atom 2.} \end{cases} \quad (2.10)$$

Here $\mathcal{K}^{\alpha\alpha}(\pm\omega_0)$ for $\alpha \in \{1, 2\}$ are Hilbert transformations of Wightman function computed from the probe massless scalar field, which we have defined explicitly in later section of this

paper. Also, ω_0 represents the natural frequency of the two identical atoms, which we have fixed [30–34] at ¹:

$$\omega_0 = \frac{i}{k} \left(n + \frac{1}{2} \right) \quad \forall n \in \mathbb{Z} \quad \text{and} \quad k = \sqrt{\alpha^2 - r^2} > 0, \quad \alpha = \sqrt{\frac{3}{\Lambda}} > 0 \quad \text{as} \quad \Lambda > 0, \quad (2.12)$$

for rest of the computation performed in this paper. In this context, the atoms are characterised by the label $\alpha \in [1, 2]$ and $\sigma_i^{\alpha} \forall i \in [1, 2, 3]$ are the Pauli spin matrices. The bath Hamiltonian for the probe massless scalar field have been expressed in the static patch of De Sitter space. Under this assumption of background space time, the massless probe scalar field is minimally coupled to the gravity in this context. Additionally, it is important to mention here that the interaction is controlled by the interaction strength or coupling parameter μ through which the bath degrees of freedom is coupled to the two atomic subsystem. We also consider the weak coupling parameter which will give rise to zero quantum correlation between the atomic subsystem and the thermal bath content i.e. massless probe scalar field at initial time scale. For the description of the OQS we will use the traditional approach of solving the *GSKL Master Equation* which describes the non-unitary time evolution of the reduced density matrix of the subsystem.

3 Non unitary time evolution of the reduced subsystem

The prime objective in this section is to describe the time evolution of an OQS with a GSKL master equation which properly describes non-unitary behaviour and can be obtained by performing partial trace over the bath content i.e. the massless probe scalar field placed at the static patch of the De Sitter background space time.

We assume that the two atomic system and reservoir are initially uncorrelated, i.e.

$$\rho_{\text{Total}}(0) = \rho_{\text{System}}(0) \otimes \rho_{\text{Bath}}(0) + \underbrace{\rho_{\text{Correlation}}(0)}_{=0}. \quad (3.1)$$

However, it is expected that as time evolves the quantum correlations [35] generated due to the non-negligible interaction between the two atomic subsystem and the thermal bath degree of freedom i.e.

$$\rho_{\text{Total}}(\tau) = \rho_{\text{System}}(\tau) \otimes \rho_{\text{Bath}}(\tau) + \underbrace{\rho_{\text{Correlation}}(\tau)}_{\neq 0}. \quad (3.2)$$

Here the exact mathematical form of the quantum correlation part of the total density matrix can only be obtained by solving the *GSKL master equation*.

¹We fix the natural frequency of the two identical atoms by imposing an additional condition:

$$\coth(\pi k \omega_0) = 0 \quad \implies \quad \omega_0 = \frac{i}{k} \left(n + \frac{1}{2} \right) \quad \forall n \in \mathbb{Z}. \quad (2.11)$$

We impose this condition to simplify the mathematical form of GSKL matrix which will fix the *Quantum dissipator* or *Lindbladian* operator.

We define a *dynamical map* $\mathcal{V}(\tau)$ to describe the transformation (or time evolution) of the reduced two atomic subsystem at $\tau = 0$ to some $\tau \geq 0$ as:

$$\rho_{\text{System}}(\tau) = \mathcal{V}(\tau)\rho_{\text{System}}(0) = \text{Tr}_{\text{Bath}} [\mathcal{U}(\tau, 0)(\rho_{\text{System}}(0) \otimes \rho_{\text{Bath}}(0))\mathcal{U}^\dagger(\tau, 0)], \quad (3.3)$$

where $\mathcal{U}(\tau, 0)$ is the unitary operator which gives the evolution of the total OQS, and is given by:

$$\rho_{\text{Total}}(\tau) = \mathcal{U}(\tau, 0)\mathcal{T} \exp\left\{-i \int_0^\tau [H_{\text{Total}}(\tau'), \rho_{\text{Total}}(\tau')]d\tau'\right\}\rho_{\text{Total}}(0), \quad (3.4)$$

If it is allowed to vary, it leads to one-parameter family of dynamical maps with $\mathcal{V}(0)$ being the identity map. The map $\mathcal{V}(t)$ represents a convex-linear, completely positive and trace-preserving *quantum operation*. Considering *Markovian* type of behaviour which is formalized with the help of *semigroup* property:[36]

$$\mathcal{V}(\tau_1)\mathcal{V}(\tau_2) = \mathcal{V}(\tau_1 + \tau_2), \quad \tau_1, \tau_2 \geq 0. \quad (3.5)$$

The time reversal invariance in the dynamics is broken due to the semi group property and provides a suitable starting point for obtaining irreversible dynamics from the *Quantum Liouville equation*. When the quantum dynamical semigroup $\mathcal{V}(t)$ is contracting in nature, we are sure to find a linear map \mathcal{G} , which acts as the generator of the semigroup:

$$\mathcal{V}(\tau) := \exp(\mathcal{G}\tau), \quad (3.6)$$

This finally leads to the following time-evolution equation for the reduced two atomic subsystem, given by:

$$\frac{d}{d\tau}\rho_{\text{System}}(\tau) = \mathcal{G}\rho_{\text{System}}(\tau), \quad (3.7)$$

which is the *Quantum Markovian Master equation*. The construction of the most general form of the linear map generator \mathcal{G} leads to the *GSKL master equation*, which can be written as:

$$\frac{d}{d\tau}\rho_{\text{System}}(\tau) = -i[H_{\text{eff}}(\tau), \rho_{\text{System}}(\tau)] + \mathcal{L}[\rho_{\text{System}}(\tau)], \quad (3.8)$$

where $\mathcal{L}[\rho_{\text{System}}(\tau)]$ is the *quantum dissipator* or the *Lindbladian operator*, which is in general defined as ²:

$$\mathcal{L}[\rho_{\text{System}}(\tau)] = \frac{1}{2} \sum_{\alpha} \gamma_{\alpha} [2\mathcal{D}_{\alpha}\rho_{\text{System}}(\tau)\mathcal{D}_{\alpha}^{\dagger} - \{\mathcal{D}_{\alpha}^{\dagger}\mathcal{D}_{\alpha}, \rho_{\text{System}}(\tau)\}], \quad (3.9)$$

where $\{\mathcal{X}, \mathcal{Y}\} = \mathcal{X}\mathcal{Y} + \mathcal{Y}\mathcal{X}$ denotes an anti-commutator, \mathcal{D}_{α} are the part of the *Lindblad operators* which plays a significant role in the context of OQS and H_{eff} is the effective subsystem Hamiltonian which is constructed after integrating over bath degrees of freedom, representing the coherent part of the dynamics. The term γ_{α} is the Fourier transform of the homogeneous bath correlation functions, which in the present context turn out to be the two atomic Wightman function of the probe massless scalar field. We stress here that the physical assumptions underlying the GSKL form of the Master equation are the:

²The explicit mathematical form of the *quantum dissipator* or the *Lindbladian operator* for the two atomic OQS is written in the later section of this paper. This can be fixed by computing the GSKL matrix elements of the *Lindbladian operator*. These elements are actually the Fourier transform of the two atomic two point Wightman functions which can be computed using *Schwinger Keldysh* technique in the present context. For details see Appendix F and Appendix G.

1. *Born* (Coupling between system and bath is weak),
2. *Markov* (No past memories) and
3. *Rotating Wave Approximation* (fast system dynamics compared to the relaxation time).

4 Reduced sub system construction

4.1 Density Matrix construction

Let us consider a two component system comprising of subsystems A and B , where the subsystem A , our topic of interest is made up of two entangled atoms and the subsystem B forms the thermal bath characterised the massless scalar field. We are interested in the dynamics of A , so we have to somehow eliminate the contributions of the bath degrees of freedom in the evolution equation of the density matrix. This process is generally carried out by an mathematical operation named *Partial trace*.

We assume that the total system (subsystem A +Bath B) evolves according to the Schrödinger equation and that is described by the density matrix $\rho_{\text{Total}}(\tau)$. The Hilbert spaces of the individual components of the system is given by:

$$\mathcal{H}_A = \mathbf{span}\{|i\rangle_A\} \quad \forall \quad i = 0, \dots, d_A - 1 \quad (4.1)$$

$$\mathcal{H}_B = \mathbf{span}\{|j\rangle_B\} \quad \forall \quad j = 0, \dots, d_B - 1 \quad (4.2)$$

where d_A and d_B represent the dimension of Hilbert space of subsystem A and the bath B respectively. Generally, the dimension of the bath is considered to be infinite and the subsystem is considered to be finite dimensional.

The corresponding Hilbert space of the total system will just be written as the tensor product of the individual spaces and is given by:

$$\mathcal{H} = \mathcal{H}_A \otimes \mathcal{H}_B = \mathbf{span}\{|i\rangle_A \otimes |j\rangle_B\}. \quad (4.3)$$

The associated density matrix can be written as:

$$\rho_{\text{Total}} = \sum_a q_a |\Psi_a\rangle \langle \Psi_a| = \sum_a q_a \left(\sum_{i,j} c_{a;ij} |i\rangle_A \otimes |j\rangle_B \right) \left(\sum_{i,j} c_{a;\mu\nu}^* |\mu\rangle_A \otimes |\nu\rangle_B \right), \quad (4.4)$$

where $|\Psi_a\rangle$ represents a particular quantum state and q_a represents the probability weight of the system being in that particular quantum state. In the above representation the quantum state $|\Psi_a\rangle$ is expanded in the basis which spans the Hilbert space \mathcal{H} of the entire system.

Therefore the total density matrix in the combined Hilbert space can be written as:

$$\rho = \sum_{ij\mu\nu} \lambda_{ij\mu\nu} (|i\rangle_A \langle \mu|) \otimes (|j\rangle_A \langle \nu|), \quad (4.5)$$

where

$$\sum_{ij\mu\nu} \lambda_{ij\mu\nu} = \sum_a q_a \sum_{i,j} c_{a;ij} c_{a;\mu\nu}^* \quad (4.6)$$

4.2 Partial Trace operation

To eliminate the contributions of the bath and to construct the reduced density matrix that describes only the subsystem of interest A the operation of taking partial trace on the total density matrix is carried out which basically averages or integrate out the contributions of the components of the bath B from the combined total density matrix.

Partial trace operation is defined as a linear operator that maps from the total Hilbert space to the Hilbert space of A , i.e. $\mathcal{H} \rightarrow \mathcal{H}_A$. Mathematically it is represented by:

$$\text{Tr}_{\text{Bath B}}(\mathcal{M}_A \otimes \mathcal{N}_B) = \mathcal{M}_A \text{Tr}(\mathcal{N}_B) = \mathcal{M}_A \sum_j \langle j | \mathcal{N}_B | j \rangle = \sum_i \langle i | \mathcal{M}_A \otimes \mathcal{N}_B | i \rangle. \quad (4.7)$$

The last expression in the above equation basically represents a partial matrix element, where the matrix element is taken over the second factor (belonging to the second Hilbert space) and the resultant factor is an operator acting on the Hilbert space \mathcal{H}_A .

Thus taking the *partial trace operation* on the total density matrix we can construct the density matrix of the subsystem A as given by[37, 38]³:

$$\rho_A = \rho_{\text{System}} = \text{Tr}_{\text{Bath B}}[\rho_{\text{Total}}]. \quad (4.8)$$

It can very easily be proved that the density matrix of the subsystem A constructed by the above operation satisfies the basic properties of the density matrix which are unit trace and positivity. The density matrix constructed in this way is called the *reduced density matrix* of the subsystem.

5 Effective Hamiltonian Construction

For our system, the effective Hamiltonian can be expressed as

$$\begin{aligned} H_{\text{eff}} &= H_{\text{System}} + H_{\text{Lamb Shift}} \\ &= \underbrace{\frac{\omega}{2} \sum_{\alpha=1}^2 \mathbf{n}^\alpha \cdot \sigma^\alpha}_{\text{Two Atomic System}} - \underbrace{\frac{i}{2} \sum_{\alpha\beta=1}^2 \sum_{ij=1}^3 H_{ij}^{\alpha\beta} (\mathbf{n}_i^\alpha \cdot \sigma_i^\alpha)(\mathbf{n}_j^\alpha \cdot \sigma_j^\alpha)}_{\text{Lamb Shift=Heisenberg spin chain}} \end{aligned} \quad (5.1)$$

where the first term in the effective Hamiltonian, physically represents the Hamiltonian of the two atomic system whereas the second term is known as the *Lamb Shift Hamiltonian*[14, 43], which characterizes the *atomic Lamb Shift* that occurs due to the interaction between

³In the present context, the reduced density matrix of the subsystem is described by the tensor product of density matrices of two atoms. Here each of the atomic density matrices can be represented by the Bloch vector representation. However after taking the tensor product the reduced subsystem density matrix can't be expressed in terms of the Bloch sphere. In that case the entangled reduced density matrix of the subsystem is parametrised by three time dependent parameters $a_{0i}(\tau)$, $a_{i0}(\tau)$ and $a_{ij}(\tau)$ where $i, j = 1, 2, 3$ or $i, j = +, -, 3$, which we actually fix by solving the *GSKL master equation*. But this can only be done once we fix the effective Hamiltonian and the *Lindbladian operator* by determining the *Lamb Shift* matrix and the *GSKL matrix* from the Fourier and Hilbert transform of the Wightman function computed from massless scalar field (bath) placed in the static De Sitter gravitational background. For more details see the rest of the sections of this paper along with Appendix F, Appendix G and Appendix H.

the massless free probe scalar field with the two atomic system under consideration in the background of static De Sitter space. It actually measures a shift in the energy levels due to this interaction.

Here \mathbf{n}^α and \mathbf{n}^β represent the normal unit vectors of the two atoms under consideration in the present OQS set up. The angles between the normal unit vectors and Pauli spin matrices are characterized by the three *Euler Angles* α, β and γ . However, we consider here that these *Euler angles* for two atoms are different to get more general result.

Therefore the *Lamb Shift Hamiltonian* can be re-expressed in terms of *Euler angles* as:

$$\begin{aligned} H_{\text{Lamb Shift}} &= -\frac{i}{2} \sum_{\alpha\beta=1}^2 \sum_{ij=1}^3 H_{ij}^{\alpha\beta} (\mathbf{n}_i^\alpha \cdot \sigma_i^\alpha) (\mathbf{n}_j^\beta \cdot \sigma_j^\beta) \\ &= -\frac{i}{2} \sum_{\alpha\beta=1}^2 \sum_{ij=1}^3 H_{ij}^{\alpha\beta} \cos(\alpha_i^\alpha) \cos(\alpha_j^\beta) \sigma_i^\alpha \sigma_j^\beta. \end{aligned} \quad (5.2)$$

In this present context, we define the following sets of Pauli operators for the two atoms using tensor product:

$$\sigma_i^1 = \sigma_i \otimes \sigma_0 \quad (\text{Atom1}) \quad (5.3)$$

$$\sigma_i^2 = \sigma_0 \otimes \sigma_i \quad (\text{Atom2}) \quad (5.4)$$

In our case, we have changed the basis for representing the effective Hamiltonian from the $\sigma_1, \sigma_2, \sigma_3$ to the $\sigma_+, \sigma_-, \sigma_3$ basis which along with the identity matrix forms a complete basis for the space of 2×2 matrices. The change of basis basically reduces the number of differential equations that is obtained from the GSKL master equation and makes them simpler to solve.

In the transformed basis σ_+ and σ_- are defined as: follows:

$$\sigma_+ = \frac{1}{2}(\sigma_1 + i\sigma_2) = \begin{pmatrix} 0 & 1 \\ 0 & 0 \end{pmatrix}, \quad (5.5)$$

$$\sigma_- = \frac{1}{2}(\sigma_1 - i\sigma_2) = \begin{pmatrix} 0 & 0 \\ 1 & 0 \end{pmatrix}. \quad (5.6)$$

Therefore the operators σ_+^1 , and σ_-^1 for **Atom 1** is defined as:

$$\sigma_+^1 = (\sigma_+ \otimes \sigma_0) = \begin{pmatrix} 0 & \sigma_0 \\ 0 & 0 \end{pmatrix} \quad (5.7)$$

$$\sigma_-^1 = (\sigma_- \otimes \sigma_0) = \begin{pmatrix} 0 & 0 \\ \sigma_0 & 0 \end{pmatrix} \quad (5.8)$$

Similarly, the operators σ_+^2 , and σ_-^2 for **Atom 2** is defined in a similar way as:

$$\sigma_+^2 = (\sigma_0 \otimes \sigma_+) = \begin{pmatrix} \sigma_+ & 0 \\ 0 & \sigma_+ \end{pmatrix} \quad (5.9)$$

$$\sigma_-^2 = (\sigma_0 \otimes \sigma_-) = \begin{pmatrix} \sigma_- & 0 \\ 0 & \sigma_- \end{pmatrix} \quad (5.10)$$

Now we transform the Hamiltonian in the new basis which is equivalent to diagonalising the $n_i^\alpha \sigma_i^\beta$ term, and basically reduces it to the σ_3 model. Hence the terms of H_{System} in the diagonalized basis respectively becomes:

$$\text{Atom 1 : } H_1 = \frac{\omega}{2} n_i^1 \sigma_i^1 = \frac{\omega}{2} n_i (\sigma_i \otimes \sigma_0) \implies \frac{\omega'}{2} \sigma_3 \otimes \sigma_0 \quad (5.11)$$

$$\text{Atom 2 : } H_2 = \frac{\omega}{2} n_i^2 \sigma_i^2 = \frac{\omega}{2} n_i (\sigma_0 \otimes \sigma_i) \implies \frac{\omega'}{2} \sigma_0 \otimes \sigma_3 \quad (5.12)$$

where ω' is the modified frequency. When the term $n_i \sigma_i$ is diagonalized in the new basis, a factor of $\sqrt{n_3^2 + n_+ n_-}$ arises, which can be incorporated in the frequency as the modification factor. Thus the frequency gets modified by this process and is given by:

$$\omega' = \omega \sqrt{n_3^2 + n_+ n_-}. \quad (5.13)$$

Here, n_3 , n_+ and n_- are the normal unit vectors of the two atoms in the new basis defined as:

$$n_+ = \frac{1}{2}(n_1 + in_2) = \frac{1}{2}(\cos \alpha_1 + i \cos \alpha_2) \quad (5.14)$$

$$n_- = \frac{1}{2}(n_1 - in_2) = \frac{1}{2}(\cos \alpha_1 - i \cos \alpha_2) \quad (5.15)$$

Similarly the $H_{\text{Lamb Shift}}$ term reduces to the following form:

$$H_{\text{Lamb Shift}} = -\frac{i}{2} \sum_{\alpha, \beta=1}^2 \sum_{i, j=1}^3 H_{ij}^{\alpha\beta} (n_i^\alpha \sigma_i^\alpha) (n_j^\beta \sigma_j^\beta) \quad (5.16)$$

Again in the new diagonalized basis (already mentioned earlier) the above mentioned *Lamb Shift* Hamiltonian part reduces to the following simplified form:

$$H_{\text{Lamb Shift}} = -\frac{i}{2} \sum_{\alpha, \beta=1}^2 \sum_{i, j=\pm}^3 H_{ij}^{\alpha\beta} \sigma_i^\alpha \sigma_j^\beta \quad (5.17)$$

In this context, the effective Hamiltonian matrix elements, $H_{ij}^{\alpha\beta}$, is given by:

$$H_{ij}^{\alpha\beta} = A^{\alpha\beta} \delta_{ij} - iB^{\alpha\beta} \epsilon_{ijk} \delta_{3j} - A^{\alpha\beta} \delta_{3i} \delta_{3j} \quad (5.18)$$

where $A^{\alpha\beta}$ and $B^{\alpha\beta}$ for the two atomic system are defined as :

$$A^{\alpha\beta} = \frac{\mu^2}{4}[K^{\alpha\beta}(\omega_0) + K^{\alpha\beta}(-\omega_0)] = \frac{\mu^2 P}{4\pi i} \int_{-\infty}^{\infty} d\omega \left[\frac{\mathcal{G}^{\alpha\beta}(\omega)}{\omega + \omega_0} + \frac{\mathcal{G}^{\alpha\beta}(-\omega)}{\omega - \omega_0} \right] \\ = \frac{\mu^2 P}{4\pi i} \int_{-\infty}^{\infty} d\omega \int_{-\infty}^{\infty} d\Delta\tau G^{\alpha\beta}(\Delta\tau) \left[\frac{e^{i\omega\Delta\tau}}{\omega + \omega_0} + \frac{e^{-i\omega\Delta\tau}}{\omega - \omega_0} \right], \quad (5.19)$$

$$B^{\alpha\beta} = \frac{\mu^2}{4}[K^{\alpha\beta}(\omega_0) - K^{\alpha\beta}(-\omega_0)] = \frac{\mu^2 P}{4\pi i} \int_{-\infty}^{\infty} d\omega \left[\frac{\mathcal{G}^{\alpha\beta}(\omega)}{\omega + \omega_0} - \frac{\mathcal{G}^{\alpha\beta}(-\omega)}{\omega - \omega_0} \right] \\ = \frac{\mu^2 P}{4\pi i} \int_{-\infty}^{\infty} d\omega \int_{-\infty}^{\infty} d\Delta\tau G^{\alpha\beta}(\Delta\tau) \left[\frac{e^{i\omega\Delta\tau}}{\omega + \omega_0} - \frac{e^{-i\omega\Delta\tau}}{\omega - \omega_0} \right], \quad (5.20)$$

where $K^{\alpha\beta}$ is basically the *Hilbert Transform* of the **Wightman function** (two point correlator) computed from the probe massless scalar field placed at the bath and is given by the following expression:

$$K^{\alpha\beta}(\pm\omega_0) = \frac{P}{\pi i} \int_{-\infty}^{\infty} d\omega \frac{\mathcal{G}^{\alpha\beta}(\pm\omega)}{\omega \pm \omega_0} = \frac{P}{\pi i} \int_{-\infty}^{\infty} d\omega \frac{1}{\omega \pm \omega_0} \int_{-\infty}^{\infty} d\Delta\tau e^{\pm i\omega\Delta\tau} G^{\alpha\beta}(\Delta\tau) \quad (5.21)$$

where P is the principal value of the integral. Here $\mathcal{G}^{\alpha\beta}$ is the *Fourier transform* of the of the **Wightman function** in the frequency (ω) space and can be expressed as:

$$\mathcal{G}^{\alpha\beta}(\pm\omega_0) = \int_{-\infty}^{\infty} d\Delta\tau e^{\pm i\omega\Delta\tau} G^{\alpha\beta}(\Delta\tau), \quad (5.22)$$

where ω_0 is the energy difference between the ground and excited states of the atoms and $G^{\alpha\beta}$ is the forward two atomic Wightman Function which is defined as ⁴:

$$G^{\alpha\beta}(\Delta\tau = \tau - \tau') = \langle \Phi(x_\alpha, \tau) \Phi(x_\beta, \tau') \rangle. \quad (5.23)$$

In the above equations μ the coupling parameter, represents the interaction strength between the system and the external thermal bath (i.e the gravitationally coupled scalar) field degrees of freedom. The structure of the elements of the coefficient matrix $H_{ij}^{\alpha\beta}$ can be computed in terms of the Wightman function of the external free probe massless scalar field in static De-Sitter background, which finally fix the structure of the effective Hamiltonian in the present scenario.

6 Quantum Dissipator or Lindbladian Construction

The concept of fluctuation and dissipation in the context of OQS is introduced into the system by the additional contribution of the Lindbladian operator in the time evolution

⁴For more details on the computation of the two atomic Wightman function of the probe massless scalar field in the static De Sitter background geometry, its Fourier transform and its Hilbert transform see the Appendix F, Appendix G and Appendix H.

equation of the reduced subsystem density matrix. The second term in the *Gorini Kossakowski Sudarshan Lindblad Master (GSKL)* equation is actually characterised as the *Lindbladian* or *Quantum Dissipator* which in our present context can be written as:

$$\mathcal{L}[\rho_{\text{System}}(\tau)] = \frac{1}{2} \sum_{i,j=1}^3 \sum_{\alpha,\beta=1}^2 C_{ij}^{\alpha\beta} \left[2(n_j^\beta \cdot \sigma_j^\beta) \rho_{\text{System}}(\tau) (n_i^\alpha \cdot \sigma_i^\alpha) - \left\{ (n_i^\alpha \cdot \sigma_i^\alpha) (n_j^\beta \cdot \sigma_j^\beta), \rho_{\text{System}}(\tau) \right\} \right], \quad (6.1)$$

where ρ_{System} is the reduced subsystem density matrix of the two entangled atomic system obtained after partially tracing over the external bath scalar field degrees of freedom. The coefficient matrix $C_{ij}^{\alpha\beta}$ is known as the *Gorini Kossakowski Sudarshan Lindblad (GSKL)* matrix, which is constructed under the weak coupling limiting approximation on the coupling parameter μ as appeared in the interaction Hamiltonian. In the context of OQS, the *Lindbladian* captures the effect of dissipation.

In the transformed basis in which the $(\mathbf{n} \cdot \sigma)$ term reduces to the σ_3 model, the *Lindbladian* can be re-expressed as:

$$\mathcal{L}[\rho_{\text{System}}(\tau)] = \frac{1}{2} \sum_{i,j=\pm}^3 \sum_{\alpha,\beta=1}^2 C_{ij}^{\alpha\beta} \left[2\sigma_j^\beta \rho_{\text{System}}(\tau) \sigma_i^\alpha - \left\{ \sigma_i^\alpha \sigma_j^\beta, \rho_{\text{System}}(\tau) \right\} \right]. \quad (6.2)$$

The matrix GSKL matrix $C_{ij}^{\alpha\beta}$ is given by the following expression:

$$C_{ij}^{\alpha\beta} = \tilde{A}^{\alpha\beta} \delta_{ij} - i \tilde{B}^{\alpha\beta} \epsilon_{ijk} \delta_{3k} - \tilde{A}^{\alpha\beta} \delta_{3k} \delta_{3j} \quad (6.3)$$

where the quantities $\tilde{A}^{\alpha\beta}$ and $\tilde{B}^{\alpha\beta}$ for the two atomic system is defined as:

$$\tilde{A}^{\alpha\beta} = \frac{\mu^2}{4} [\mathcal{G}^{\alpha\beta}(\omega_0) + \mathcal{G}^{\alpha\beta}(-\omega_0)] = \frac{\mu^2}{4} \int_{-\infty}^{\infty} G^{\alpha\beta}(\Delta\tau) [e^{i\omega_0\Delta\tau} + e^{-i\omega_0\Delta\tau}] \quad (6.4)$$

$$\tilde{B}^{\alpha\beta} = \frac{\mu^2}{4} [\mathcal{G}^{\alpha\beta}(\omega_0) - \mathcal{G}^{\alpha\beta}(-\omega_0)] = \frac{\mu^2}{4} \int_{-\infty}^{\infty} G^{\alpha\beta}(\Delta\tau) [e^{i\omega_0\Delta\tau} - e^{-i\omega_0\Delta\tau}] \quad (6.5)$$

The components of $C_{ij}^{\alpha\beta}$ matrix are given in the **Appendix G**.

7 Bloch Sphere representation of density matrix

In this section we discuss about the Bloch sphere representation of density matrix. We know that a qubit is a quantum state in a two dimensional Hilbert space $\mathcal{H} = \mathcal{C}^2$ and is spanned by, $\{|0\rangle, |1\rangle\}$, which forms a complete orthonormal basis for the two dimensional Hilbert space. The density operator for any state in this space can be represented by a 2×2 matrix of the following general form:

$$\rho = \begin{pmatrix} a & b \\ c & d \end{pmatrix} \quad (7.1)$$

However the *unit trace* and *hermiticity* condition of the density matrix reduces the matrix which is characterised by only two variables. The first condition of unit trace gives,

$$d = 1 - a, \quad (7.2)$$

and the hermiticity condition reduces to the condition

$$c = b^*. \quad (7.3)$$

This parametrizes the density matrix by the complex number b and the real number a . Thus the matrix finally takes the form

$$\rho = \begin{pmatrix} a & b \\ b^* & 1 - a \end{pmatrix} \quad (7.4)$$

Now using the positivity condition one can further write:

$$|\rho - \lambda I| = 0 \implies \lambda^2 - (\text{Tr}\rho)\lambda + |\rho| = 0. \quad (7.5)$$

To consider only the contribution from the non negative eigenvalues we further use the normalization condition as given by:

$$\text{Tr}(\rho) = 1. \quad (7.6)$$

Using this constraint condition we can determine the two possible solutions for the eigen values:

$$\lambda_{\pm} = \frac{1}{2}(1 \pm \sqrt{1 - 4|\rho|}) \geq 0. \quad (7.7)$$

This parametrization requires only three variables and thus it can be embedded in three space time dimensions. Thus it is useful to represent the reduced subsystem density matrix in a more useful basis. Recalling that the Pauli matrices together with the identity matrix forms a complete set of orthonormal basis for the space of 2×2 matrices, any qubit density matrix can therefore be written in terms of the identity matrix and the Pauli matrices and is represented by the following expression ⁵:

$$\rho(\tau) = \frac{1}{2} \left(I + \sum_{i=1}^3 v_i(\tau) \sigma_i \right) = \frac{1}{2} [I + \mathbf{v}(\tau) \cdot \boldsymbol{\sigma}] \quad (7.8)$$

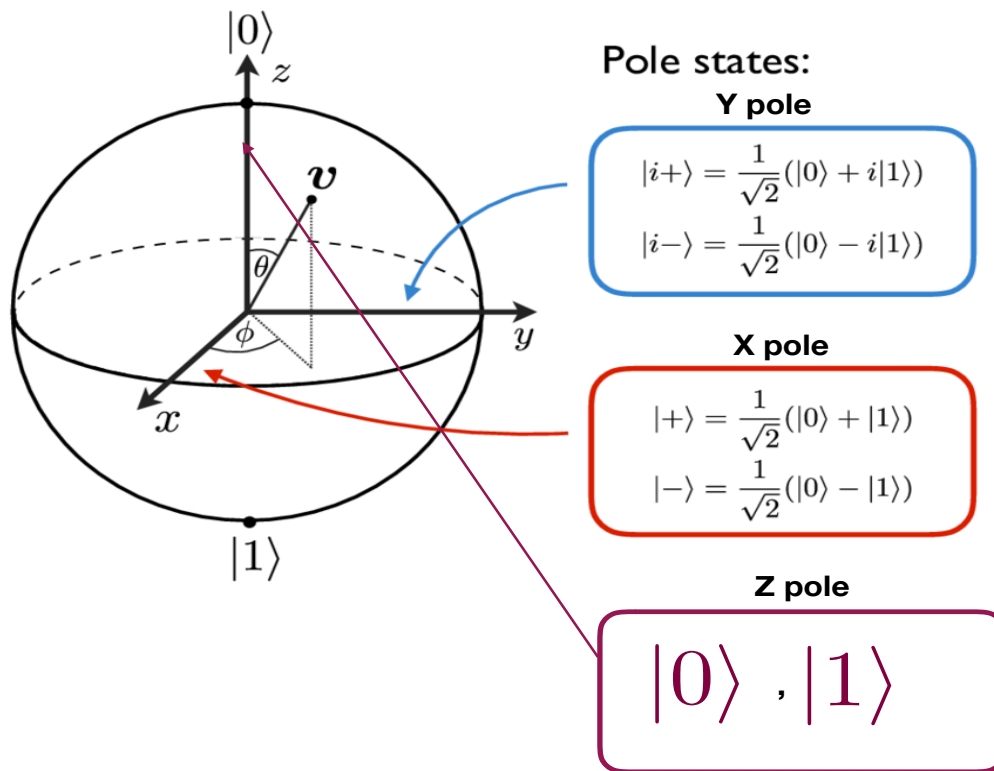
where \mathbf{v} is called the **Bloch vector**. The above representation of the density matrix ensures unit trace or the appearance of positive eigen values. In this context, the positivity criteria can be explicitly observed by the following expression:

$$|\rho| = \frac{1}{4}(1 - \|\mathbf{v}\|^2) \quad (7.9)$$

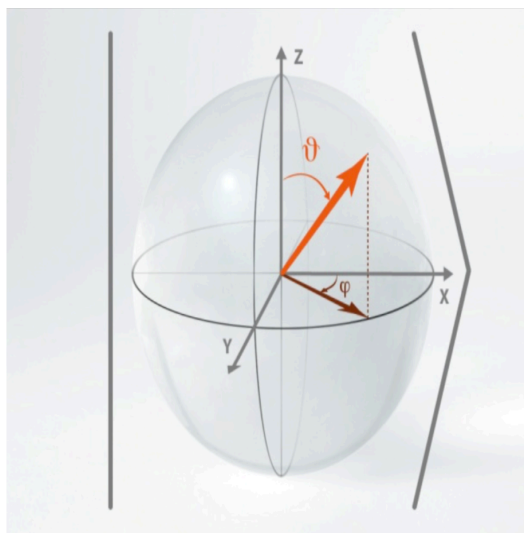
which gives the following eigenvalues:

$$\lambda_{\pm} = \frac{1}{2}(1 \pm \sqrt{\|\mathbf{v}\|^2}) = \frac{1}{2}(1 \pm \|\mathbf{v}\|) \geq 0. \quad (7.10)$$

Bloch Sphere Representation of Density Matrix



(a) Bloch sphere representation of density matrix.



(b) Bloch sphere representation of a quantum state pointing in any arbitrary direction.

$$|\psi\rangle = \cos\left(\frac{\theta}{2}\right) \left| \begin{matrix} \uparrow \\ \downarrow \end{matrix} \right\rangle + \sin\left(\frac{\theta}{2}\right) \left| \begin{matrix} \downarrow \\ \uparrow \end{matrix} \right\rangle$$

$$|\psi\rangle = \frac{1}{\sqrt{2}} \left| \begin{matrix} \uparrow \\ \downarrow \end{matrix} \right\rangle + \frac{1}{\sqrt{2}} \left| \begin{matrix} \downarrow \\ \uparrow \end{matrix} \right\rangle$$

(c) Bloch sphere representation of a quantum state in terms of linear combination of two states pointed along particular direction.

Figure 3. Bloch sphere representation of an arbitrary quantum state and density matrix.

Here $\|\mathbf{v}\|$ represents the norm of the **Bloch vector**, \mathbf{v} . To find a condition on the lengths of the *Bloch vectors* to yield finally pure or mixed states we need to actually calculate ρ^2 which is given by the following expression:

$$\rho^2(\tau) = \frac{1}{4} [I + 2\mathbf{v}(\tau) \cdot \boldsymbol{\sigma} + (\mathbf{v}(\tau) \cdot \boldsymbol{\sigma})^2]. \quad (7.11)$$

Now further taking the trace of the square of the density matrix, yields:

$$\text{Tr} [\rho^2(\tau)] = \frac{1}{2} (1 + \|\mathbf{v}\|^2) \geq 0. \quad (7.12)$$

From the above equation it is clear that unit Bloch vector will makes the trace of the square of the density matrix is equal to unity which is the condition for getting a *pure state* from this calculation. Bloch vectors of length less than unity will yield *mixed states* from this calculation.

Figure 3(a), represents a Bloch sphere, which is basically a geometric collection of all **Bloch vectors** which describes valid qubit density operators. It means that the sphere is of radius unity. Any vector touching the surface of the sphere represents a **pure state** and any vector lying in the interior of the sphere represents a **mixed state**. It is also shown in the figure that the *Z*-pole is written in terms of the basis vectors $Z \equiv \{|0\rangle, |1\rangle\}$ which forms a complete basis for the two dimensional Hilbert space. Any vector lying on the *X*-pole and the *Y* pole can be expressed in terms of the $X \equiv \{|+\rangle, |-\rangle\}$ and $Y \equiv \{|i+\rangle, |i-\rangle\}$ basis vectors, which are clearly written in the figure 3(a).

In figure 3(b), we have depicted schematically a quantum mechanical state pointing in any arbitrary direction in terms of the *Bloch sphere*. In figure 3(c), we have actually expressed two different quantum states as a linear combination of two other state vectors pointed along particular direction.

8 Time evolution of the reduced subsystem density matrix

The density matrices for **Atom 1** and **Atom 2** are given by following expressions in the *Bloch sphere* representation:

$$\text{Atom 1 :} \quad \rho_1(\tau) = \frac{1}{2} \left(I + \sum_{i=1}^3 a_i(\tau) \sigma_i \right) = \frac{1}{2} [I + \mathbf{a}(\tau) \cdot \boldsymbol{\sigma}]. \quad (8.1)$$

$$\text{Atom 2 :} \quad \rho_2(\tau) = \frac{1}{2} \left(I + \sum_{j=1}^3 b_j(\tau) \sigma_j \right) = \frac{1}{2} [I + \mathbf{b}(\tau) \cdot \boldsymbol{\sigma}]. \quad (8.2)$$

⁵In the context of two atomic OQS density matrix of the each atom can be represented by this expression. However, instead of choosing the $\sigma_i \forall i = 1, 2, 3$ we actually choose the transformed basis, $\sigma_j \forall j = +, -, 3$. This is very useful in the present computation as it reduces the number as well as the complicated structures of all the coupled differential equations arising from the GSKL master equation.

Since the two atoms are initially not entangled, the density matrix for the system can be written as the direct product of the two individual density matrices i.e.

$$\begin{aligned}
\rho_{\text{System}}(\tau) &= \rho_1(\tau) \otimes \rho_2(\tau) \\
&= \frac{1}{2} \left(I + \sum_{i=1}^3 a_i(\tau) \sigma_i \right) \otimes \frac{1}{2} \left(I + \sum_{j=1}^3 b_j(\tau) \sigma_j \right) \\
&= \frac{1}{4} \left[\sigma_0 \otimes \sigma_0 + \sum_{j=1}^3 b_j(\tau) \sigma_0 \otimes \sigma_j + \sum_{i=1}^3 a_i(\tau) \sigma_i \otimes \sigma_0 + \sum_{i,j=1}^3 a_i(\tau) b_j(\tau) \sigma_i \otimes \sigma_j \right]. \quad (8.3)
\end{aligned}$$

Note that in the above equation the identity matrix is denoted by σ_0 . Now we define:

$$a_i(\tau) \equiv a_{i0}(\tau) \quad \forall \quad i = 1, 2, 3, \quad (8.4)$$

$$b_j(\tau) \equiv a_{0j}(\tau) \quad \forall \quad j = 1, 2, 3, \quad (8.5)$$

$$a_i(\tau) b_j(\tau) \equiv a_{ij}(\tau) \quad \forall \quad i, j = 1, 2, 3. \quad (8.6)$$

Using these definitions the density matrix $\rho_{\text{System}}(\tau)$ for the reduced subsystem can be re-expressed as:

$$\rho_{\text{System}}(\tau) = \frac{1}{4} \left[\sigma_0 \otimes \sigma_0 + \sum_{i=1}^3 a_{0i}(\tau) (\sigma_0 \otimes \sigma_i) + \sum_{i=1}^3 a_{i0}(\tau) (\sigma_i \otimes \sigma_0) + \sum_{i,j=1}^3 a_{ij}(\tau) (\sigma_i \otimes \sigma_j) \right] \quad (8.7)$$

In the new transformed basis i.e in terms of σ_+ , σ_- and σ_3 basis $\rho_{\text{System}}(\tau)$ can be written as:

$$\begin{aligned}
\rho_{\text{System}}(\tau) &= \frac{1}{4} \left[\sigma_0 \otimes \sigma_0 + \sum_{m=+,-}^3 a_{0m}(\tau) (\sigma_0 \otimes \sigma_m) \right. \\
&\quad \left. + \sum_{m=+,-}^3 a_{m0}(\tau) (\sigma_m \otimes \sigma_0) + \sum_{m,n=+,-}^3 a_{mn}(\tau) (\sigma_m \otimes \sigma_n) \right]. \quad (8.8)
\end{aligned}$$

In this new basis the reduced subsystem density matrix, in terms of the *Bloch vectors* can be explicitly written as:

$$\rho_{\text{System}}(\tau) = \frac{1}{4} \begin{pmatrix} 1 + a_{03} + a_{30} + a_{33} & 0 & 0 & a_{++} \\ 0 & 1 - a_{03} + a_{30} - a_{33} & a_{+-} & 0 \\ 0 & a_{-+} & 1 + a_{03} - a_{30} - a_{33} & 0 \\ a_{--} & 0 & 0 & 1 - a_{03} - a_{30} + a_{33} \end{pmatrix}, \quad (8.9)$$

where the Hermiticity and $\text{Tr}(\rho_{\text{System}}(\tau)) = 1$ property of the density matrix has been used to find the matrix elements explicitly.

8.1 Large Scale time dependent solution

Solving the master equation in the new basis i.e. σ_+ , σ_- and σ_3 basis in the large time limit ($\tau = \infty$) we get the following solution for the components of the density matrix as given by:

$$a_{03}(\infty) = a_{30}(\infty) = -\tanh(\pi k\omega), \quad (8.10)$$

$$a_{33}(\infty) = \tanh^2(\pi k\omega), \quad (8.11)$$

$$a_{++}(\infty) = a_{--}(\infty) = 0, \quad (8.12)$$

$$a_{+-}(\infty) = a_{-+}(\infty) = 0, \quad (8.13)$$

where all other *Bloch vector* components are zero.

We can get the large time reduced density matrix from the above solution, which can be expressed as

$$\begin{aligned} \rho_{\text{System}}(\infty) &= \frac{1}{4} [\sigma_0 \otimes \sigma_0 + a_{03}(\infty)(\sigma_0 \otimes \sigma_3) + a_{30}(\infty)(\sigma_3 \otimes \sigma_0) + a_{33}(\infty)(\sigma_3 \otimes \sigma_3)] \\ &= \frac{1}{4} \begin{pmatrix} 1 + 2a_{03}(\infty) + a_{33}(\infty) & 0 & 0 & 0 \\ 0 & 1 - a_{33}(\infty) & 0 & 0 \\ 0 & 0 & 1 - a_{33}(\infty) & 0 \\ 0 & 0 & 0 & 1 - 2a_{03}(\infty) + a_{33}(\infty) \end{pmatrix}. \end{aligned} \quad (8.14)$$

The large time behaviour basically demonstrates the equilibrium behaviour of the system. Hence the solution of the *Bloch vectors* obtained in the large time scale is applicable in any basis. These solutions can therefore be used as the boundary conditions for obtaining the finite time solution of the density matrix. Writing the density matrix in terms of the solutions of the *Bloch vectors* as,

$$\rho_{\text{System}}(\infty) = \frac{1}{4} \begin{pmatrix} (1 - \tanh(\pi k\omega))^2 & 0 & 0 & 0 \\ 0 & 1 - \tanh^2(\pi k\omega) & 0 & 0 \\ 0 & 0 & 1 - \tanh^2(\pi k\omega) & 0 \\ 0 & 0 & 0 & (1 + \tanh(\pi k\omega))^2 \end{pmatrix}. \quad (8.15)$$

On the other hand, from quantum statistical mechanics one can compute the expression for the density matrix at finite temperature and large time limit, which is given by the following

expression:

$$\begin{aligned} \rho_{\text{System}}(\infty) &= \frac{e^{-\beta H_{\text{System}}}}{\text{Tr}(e^{-\beta H_{\text{System}}})} \\ &= \frac{1}{4} \begin{pmatrix} (1 - \tanh(\frac{\beta\omega}{2}))^2 & 0 & 0 & 0 \\ 0 & 1 - \tanh^2(\frac{\beta\omega}{2}) & 0 & 0 \\ 0 & 0 & 1 - \tanh^2(\frac{\beta\omega}{2}) & 0 \\ 0 & 0 & 0 & (1 + \tanh(\frac{\beta\omega}{2}))^2 \end{pmatrix}. \end{aligned} \quad (8.16)$$

Comparing Eq (8.57) and Eq (8.16), we obtain the following result:

$$T = \frac{1}{\beta} = \frac{1}{2\pi k} = \frac{1}{2\pi\sqrt{\alpha^2 - r^2}}, \quad \text{where } \alpha = \sqrt{\frac{3}{\Lambda}} > 0. \quad (8.17)$$

which physically represents the equilibrium temperature of the thermal bath at large time scale.

In ref. [27] we have explicitly shown that the temperature of the thermal bath can be computed in terms of the *Gibbons Hawking* temperature and *Unruh* temperature, which can be expressed as:

$$T = \sqrt{T_{\text{GH}}^2 + T_{\text{Unruh}}^2} = \frac{1}{2\pi\alpha} \sqrt{1 + \frac{r^2}{\alpha^2 - r^2}}, \quad \text{where } \alpha = \sqrt{\frac{3}{\Lambda}} > 0. \quad (8.18)$$

Here *Gibbons Hawking* and *Unruh* temperature is defined in the present context as:

$$T_{\text{GH}} = \frac{1}{2\pi\alpha}, \quad (8.19)$$

$$T_{\text{Unruh}} = \frac{a}{2\pi} = T_{\text{GH}} \frac{r}{\sqrt{\alpha^2 - r^2}}. \quad (8.20)$$

Here a is the acceleration, which is defined as:

$$a = 2\pi T_{\text{GH}} \frac{r}{\sqrt{\alpha^2 - r^2}} = \frac{1}{\alpha} \frac{r}{\sqrt{\alpha^2 - r^2}}. \quad (8.21)$$

Now, we know that in static patch of the De Sitter space[28, 29] the curvature is determined by the following expression for the Ricci scalar:

$$R = \frac{12}{\alpha^2} > 0, \quad \text{where } \alpha = \sqrt{\frac{3}{\Lambda}} > 0. \quad (8.22)$$

Consequently, the equilibrium temperature of the thermal bath can be re-expressed in terms of the curvature of the static patch of the De Sitter space as:

$$T = \frac{1}{\beta} = \frac{1}{2\pi k} = \frac{1}{2\pi\sqrt{(\frac{12}{R}) - r^2}} = \frac{\sqrt{R}}{2\pi} \frac{1}{\sqrt{12 - Rr^2}}. \quad (8.23)$$

Similarly, the *Gibbons Hawking* and *Unruh* temperature can be re-expressed in terms of the curvature of the static patch of the De Sitter space as:

$$T_{\text{GH}} = \frac{\sqrt{R}}{4\sqrt{3}\pi}, \quad (8.24)$$

$$T_{\text{Unruh}} = \frac{a}{2\pi} = T_{\text{GH}} \frac{\sqrt{R}r}{\sqrt{12 - Rr^2}}. \quad (8.25)$$

In this context, one can consider the following limiting situations:

1. **Flat space limit:**

Flat space limit is characterised by the following condition:

$$R \rightarrow 0, \implies \alpha \rightarrow \infty, \implies T_{\text{GH}}, T_{\text{Unruh}} \rightarrow 0, \implies T \rightarrow 0, \implies k \rightarrow \infty \implies k \gg L. \quad (8.26)$$

Here L represents the Euclidean distance between the two atoms. In this case, we will get back the result obtained in the Minkowski flat space inertial case where $k \gg L$.

2. **Zero acceleration limit:**

The zero acceleration limit is characterised by the following condition:

$$a \rightarrow 0, \implies r \rightarrow 0, \implies T_{\text{GH}} \neq 0, T_{\text{Unruh}} \rightarrow 0, \implies T \rightarrow T_{\text{GH}}, \implies k \ll L. \quad (8.27)$$

In this case, we will get back the result obtained in the limiting case where $k \ll L$.

8.2 Arbitrary time dependent solution

To obtain the finite time solution of the *Bloch vector* components we use the σ_+ , σ_- and σ_3 basis. Substituting the components of the density matrix in the *GSKL master equation* in this new basis, we obtain the following sets of *evolution equations* for the Bloch vectors:

$$\begin{aligned} \dot{a}_{03}(\tau) = & \frac{1}{4}(A^{12} + A^{21})(a_{++} - a_{--}) + \frac{1}{2}(\tilde{A}^{21} - \tilde{A}^{12})(a_{++} - a_{--}) \\ & + \frac{i}{2}(\tilde{B}^{12} + \tilde{B}^{21})(a_{+-} + a_{-+}) + 4i\tilde{B}^{22} \end{aligned} \quad (8.28)$$

$$\begin{aligned} \dot{a}_{03}(\tau) = & \frac{1}{4}(A^{12} + A^{21})(a_{++} - a_{--}) + \frac{1}{2}(\tilde{A}^{21} + \tilde{A}^{12})(a_{++} - a_{--}) \\ & + \frac{i}{2}(\tilde{B}^{12} + \tilde{B}^{21})(a_{+-} + a_{-+}) + 4i\tilde{B}^{11} \end{aligned} \quad (8.29)$$

$$\begin{aligned} \dot{a}_{++}(\tau) = & (A^{12} + A^{21})(a_{03} + a_{30}) + ia_{++}(B^{11} + B^{22}) + 2\omega a_{++} + 2\tilde{A}^{22}a_{+-} + 2\tilde{A}^{11}a_{-+} \\ & + 2\tilde{A}^{21}(a_{03} - a_{30} - 2a_{33}) + 2\tilde{A}^{12}(-a_{03} + a_{30} - 2a_{33}) \end{aligned} \quad (8.30)$$

$$\begin{aligned} \dot{a}_{+-}(\tau) = & i(-B^{12} + B^{21})(a_{30} - a_{03}) + ia_{12}(B^{11} - B^{22}) + 2i\tilde{B}^{21}(a_{03} - a_{30} + 2a_{33}) \\ & - 2i\tilde{B}^{12}(a_{03} - a_{30} + 2a_{33}) + 2\tilde{A}^{11}a_{--} + 2\tilde{A}^{22}a_{++} \end{aligned} \quad (8.31)$$

$$\begin{aligned} \dot{a}_{-+}(\tau) = & i(B^{12} - B^{21})(a_{03} - a_{30}) + ia_{21}(-B^{11} + B^{22}) - 2i\tilde{B}^{21}(a_{03} + a_{30} + 2a_{33}) \\ & - 2i\tilde{B}^{12}(-a_{03} - a_{30} + 2a_{33}) + 2\tilde{A}^{11}a_{++} + 2\tilde{A}^{22}a_{--} \end{aligned} \quad (8.32)$$

$$\begin{aligned} \dot{a}_{--}(\tau) = & (A^{12} + A^{21})(-a_{03} - a_{30}) + ia_{--}(B^{11} + B^{22}) + 2\omega a_{--} + 2\tilde{A}^{22}a_{-+} + 2\tilde{A}^{11}a_{+-} \\ & + 2\tilde{A}^{21}(a_{03} - a_{30} - 2a_{33}) + 2\tilde{A}^{12}(-a_{03} + a_{30} - 2a_{33}) \end{aligned} \quad (8.33)$$

$$\dot{a}_{33}(\tau) = -(\tilde{A}^{12} + \tilde{A}^{21})a_{++} - (\tilde{A}^{21} + \tilde{A}^{12})a_{--} + 4i\tilde{B}^{11}a_{03} + 4i\tilde{B}^{22}a_{30} \quad (8.34)$$

In this paper, the above evolution equations have been solved in the limit $2\pi\kappa\omega \gg 1$, along with an additional condition on the natural frequency of the two identical atoms i.e restricting ω_o to take values such that $\coth(\pi\kappa\omega_o)=0$. The first condition ensures that the factor $(1 - e^{-2\pi\kappa\omega})^{-1}$ appearing in $\tilde{A}^{\alpha\beta}$ and $\tilde{B}^{\alpha\beta}$ term of the *GKSL* matrix $C_{ij}^{\alpha\beta}$ reduces to unity. Similarly, in the above limit, the spectroscopic integrals representing the components H_{ij}^{11} and H_{ij}^{22} of the coefficient matrix becomes zero. For more details see **Appendix H**.

For the explicit functional form of $\tilde{A}^{\alpha\beta}$ and $\tilde{B}^{\alpha\beta}$ and the integral representation of A_1 and B_1 please refer to the **Appendix G.1** and **G.2**. In the above mentioned limit, the evolution equations of the Bloch vectors reduces to the following sets of equations:

$$\dot{a}_{03}(\tau) = 4B_1 + A_1a_{++} + B_2a_{+-} + B_2a_{-+} - A_1a_{--} \quad (8.35)$$

$$\dot{a}_{30}(\tau) = 4B_1 + A_1a_{++} + B_2a_{+-} + B_2a_{-+} - A_1a_{--} \quad (8.36)$$

$$\dot{a}_{++}(\tau) = 4A_1a_{03} + 4A_1a_{30} + 2\omega a_{11} \quad (8.37)$$

$$\dot{a}_{+-}(\tau) = D_2a_{03} - D_2a_{30} - 4B_2a_{30} \quad (8.38)$$

$$\dot{a}_{-+}(\tau) = D_2a_{03} - D_2a_{30} - 4B_2a_{03} - 4B_2a_{30} \quad (8.39)$$

$$\dot{a}_{--}(\tau) = -4A_1a_{03} - 4A_1a_{30} + 2\omega a_{--} \quad (8.40)$$

$$\dot{a}_{33}(\tau) = 4B_1a_{03} + 4B_2a_{30} \quad (8.41)$$

where in the above sets of equations the following notations have been used:

$$A_1(\omega) = \frac{1}{4}(A^{12} + A^{21}) \quad (8.42)$$

$$D_2(\omega) = i(B^{12} - B^{21}) \quad (8.43)$$

$$B_2(\omega) = i\tilde{B}^{12} = i\tilde{B}^{21} \quad (8.44)$$

$$B_1(\omega) = i\tilde{B}^{11} = i\tilde{B}^{22} \quad (8.45)$$

8.3 Solution of the evolution equations

The following sets of equations are the finite time dependent solution of the Bloch vector components:

$$a_{03}(\tau) = C_1 e^{f_1(\omega)\tau} \frac{f_1(\omega)}{4(B_1 + B_2)} + C_2 e^{f_2(\omega)\tau} \frac{f_2(\omega)}{4(B_1 + B_2)} + C_3 e^{f_3(\omega)\tau} \frac{f_3(\omega)}{4(B_1 + B_2)} \quad (8.46)$$

$$a_{30}(\tau) = C_1 e^{f_1(\omega)\tau} \frac{f_1(\omega)}{4(B_1 + B_2)} + C_2 e^{f_2(\omega)\tau} \frac{f_2(\omega)}{4(B_1 + B_2)} + C_3 e^{f_3(\omega)\tau} \frac{f_3(\omega)}{4(B_1 + B_2)} \quad (8.47)$$

$$\begin{aligned} a_{++}(\tau) = & C_4 e^{2\omega\tau} + C_1 e^{f_1(\omega)\tau} \left(\frac{-2f_1(\omega)A_1}{(-2\omega + f_1)(B_1 + B_2)} + \frac{(f_1^2(\omega) + 12B_2^2)}{4A_1(B_1 + B_2)} \right) \\ & + e^{f_2(\omega)\tau} \left(\frac{-2f_2(\omega)A_1}{(-2\omega + f_2)(B_1 + B_2)} + \frac{(f_2^2(\omega) + 12B_2^2)}{4A_1(B_1 + B_2)} \right) \\ & + e^{f_3(\omega)\tau} \left(\frac{-2f_3(\omega)A_1}{(-2\omega + f_3)(B_1 + B_2)} + \frac{(f_3^2(\omega) + 12B_2^2)}{4A_1(B_1 + B_2)} \right) \end{aligned} \quad (8.48)$$

$$a_{+-}(\tau) = -C_5 - \left(\frac{B_2}{B_1 + B_2} \right) (C_1 e^{f_1(\omega)\tau} + C_2 e^{f_2(\omega)\tau} + C_3 e^{f_3(\omega)\tau}) \quad (8.49)$$

$$a_{-+}(\tau) = C_5 - \left(\frac{2B_2}{B_1 + B_2} \right) (C_1 e^{f_1(\omega)\tau} + C_2 e^{f_2(\omega)\tau} + C_3 e^{f_3(\omega)\tau}) \quad (8.50)$$

$$a_{--}(\tau) = C_4 e^{2\omega\tau} - \frac{2A_1}{B_1 + B_2} \left(\frac{C_1 f_1(\omega) e^{f_1(\omega)\tau}}{-2\omega + f_1} + \frac{C_2 f_2(\omega) e^{f_2(\omega)\tau}}{-2\omega + f_2} + \frac{C_3 f_3(\omega) e^{f_3(\omega)\tau}}{-2\omega + f_3} \right) \quad (8.51)$$

$$a_{33}(\tau) = (C_6 + C_1 e^{f_1(\omega)\tau} + C_2 e^{f_2(\omega)\tau} + C_3 e^{f_3(\omega)\tau}) \quad (8.52)$$

where $C_i \forall i = 1, 6$ are arbitrary constants which can be determined from the boundary conditions i.e the equilibrium behaviour of the Bloch vector components already obtained in the previous section.

In the above sets of equations $f_1(\omega)$, $f_2(\omega)$, $f_3(\omega)$ can explicitly be written as:

$$f_1(\omega) = -2\omega(\Delta_1(\omega))^2 + (\Delta_1(\omega))^3 - 24\omega B_2^2 + \Delta_1(\omega)(-16A_1^2(\omega) + 12B_2^2(\omega)) \quad (8.53)$$

$$f_2(\omega) = -2\omega(\Delta_2(\omega))^2 + (\Delta_2(\omega))^3 - 24\omega B_2^2 + \Delta_2(\omega)(-16A_1^2(\omega) + 12B_2^2(\omega)) \quad (8.54)$$

$$f_3(\omega) = -2\omega(\Delta_3(\omega))^2 + (\Delta_1(\omega))^3 - 24\omega B_2^2 + \Delta_3(\omega)(-16A_1^2(\omega) + 12B_2^2(\omega)) \quad (8.55)$$

where $\Delta_1(\omega)$ is real and $\Delta_2(\omega)$, $\Delta_3(\omega)$ are complex whose explicit forms are written in **Appendix J**.

The very basic assumption underlying the derivation of the solution of the evolution equations, is that the two atoms mimicking the role of the Unruh De-Witt detectors are **identical**. This assumption plays a very significant role which can be understood from the density matrices of the individual atoms.

The density matrices of the individual atoms are written below:

$$\text{Atom 1:} \quad \rho_1(\tau) = \frac{1}{2} \begin{pmatrix} 1 + a_{30}(\tau) & 0 \\ 0 & 1 - a_{30}(\tau) \end{pmatrix}. \quad (8.56)$$

$$\text{Atom 2:} \quad \rho_2(\tau) = \frac{1}{2} \begin{pmatrix} 1 + a_{03}(\tau) & 0 \\ 0 & 1 - a_{03}(\tau) \end{pmatrix}. \quad (8.57)$$

A look at Eq. 8.46 and Eq. 8.47, shows that both the solutions are identical which indicates that the density matrix of the individual atoms are equal as it should be to justify the assumption of having identical atoms. If the two atoms are considered to be **non-identical** then these two atomic density matrices would not have been equal and have different structure.

8.4 General solution

In this section the arbitrary constants are determined using the equilibrium behaviour as the boundary conditions which are already mentioned in equation 8.10. From the appearance it might seem that the function $e^{f_l(\omega)\tau}$ diverges as τ tends to infinity but it can be explicitly shown that the function $f_l(\omega) (l = 1, 2, 3) < 0$, taking into account the leading order term in Δ , which is a decaying function. Hence the function, $e^{f_l(\omega)\tau}$ tends to a finite value, which we

denote by $f_i(\omega)\tau'$. Hence the physically acceptable solutions which satisfies the boundary conditions are given by the following simplified expressions:

$$a_{03}(\tau) = - \left[g_1(\omega)e^{-|f_1(\omega)|(\tau-\tau')} \frac{|f_1(\omega)|}{4(B_1 + B_2)} + g_2(\omega)e^{-|f_2(\omega)|(\tau-\tau')} \frac{|f_2(\omega)|}{4(B_1 + B_2)} + g_3(\omega)e^{-|f_3(\omega)|(\tau-\tau')} \frac{|f_3(\omega)|}{4(B_1 + B_2)} \right] \quad (8.58)$$

$$a_{30}(\tau) = - \left[g_1(\omega)e^{-|f_1(\omega)|(\tau-\tau')} \frac{|f_1(\omega)|}{4(B_1 + B_2)} + g_2(\omega)e^{-|f_2(\omega)|(\tau-\tau')} \frac{|f_2(\omega)|}{4(B_1 + B_2)} + g_3(\omega)e^{-|f_3(\omega)|(\tau-\tau')} \frac{|f_3(\omega)|}{4(B_1 + B_2)} \right] \quad (8.59)$$

$$a_{++}(\tau) = g_1(\omega)e^{-|f_1(\omega)|(\tau-\tau')} \left(\frac{2|f_1(\omega)|A_1}{-(2\omega + |f_1|)(B_1 + B_2)} + \frac{f_1^2(\omega) + 12B_2^2}{4A_1(B_1 + B_2)} \right) + g_2(\omega)e^{-|f_2(\omega)|(\tau-\tau')} \left(\frac{2|f_2(\omega)|A_1}{-(2\omega + |f_2|)(B_1 + B_2)} + \frac{f_2^2(\omega) + 12B_2^2}{4A_1(B_1 + B_2)} \right) + g_3(\omega)e^{-|f_3(\omega)|(\tau-\tau')} \left(\frac{2|f_3(\omega)|A_1}{-(2\omega + |f_3|)(B_1 + B_2)} + \frac{f_3^2(\omega) + 12B_2^2}{4A_1(B_1 + B_2)} \right) \quad (8.60)$$

$$a_{+-}(\tau) = -g_5(\omega) - \left(\frac{B_2}{B_1 + B_2} \right) \left(g_1(\omega)e^{-|f_1(\omega)|(\tau-\tau')} + g_2(\omega)e^{-|f_2(\omega)|(\tau-\tau')} + g_3(\omega)e^{-|f_3(\omega)|(\tau-\tau')} \right) \quad (8.61)$$

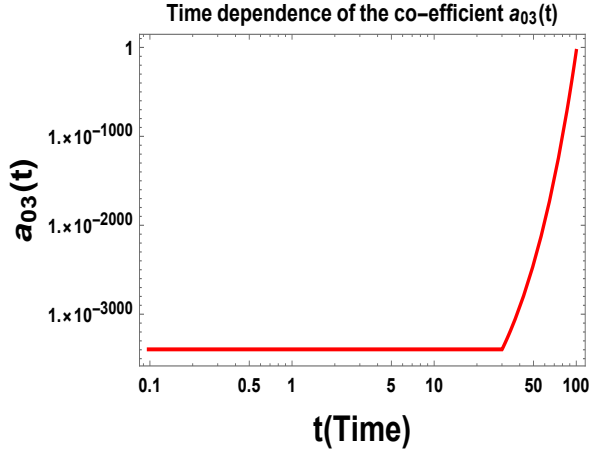
$$a_{-+}(\tau) = g_5(\omega) - \left(\frac{2B_2}{B_1 + B_2} \right) \left(g_1(\omega)e^{-|f_1(\omega)|(\tau-\tau')} + g_2(\omega)e^{-|f_2(\omega)|(\tau-\tau')} + g_3(\omega)e^{-|f_3(\omega)|(\tau-\tau')} \right) \quad (8.62)$$

$$a_{--}(\tau) = -\frac{2A_1}{B_1 + B_2} \left[\frac{g_1(\omega)|f_1(\omega)|e^{-|f_1(\omega)|(\tau-\tau')}}{2\omega + |f_1|} + \frac{g_2(\omega)|f_2(\omega)|e^{-|f_2(\omega)|(\tau-\tau')}}{2\omega + |f_2|} + \frac{g_3(\omega)|f_3(\omega)|e^{-|f_3(\omega)|(\tau-\tau')}}{2\omega + |f_3|} \right] \quad (8.63)$$

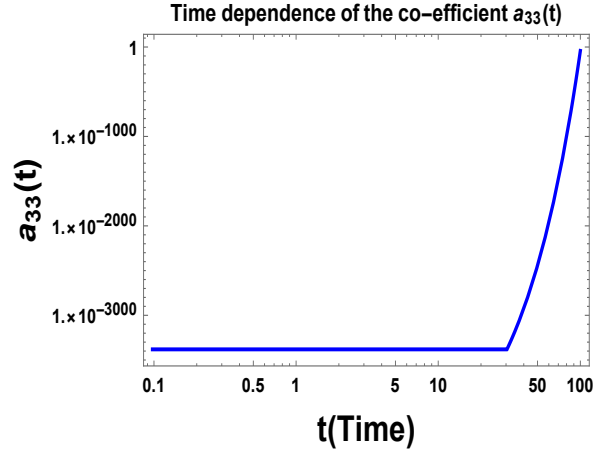
$$a_{33}(\tau) = g_6(\omega) + g_1(\omega)e^{-|f_1(\omega)|(\tau-\tau')} + g_2(\omega)e^{-|f_2(\omega)|(\tau-\tau')} + g_3(\omega)e^{-|f_3(\omega)|(\tau-\tau')} \quad (8.64)$$

where the explicit functional forms of $g_i(\omega) \forall i = 1, \dots, 6$ are given in **Appendix J** and the constant C_4 is zero which is consistent with the given boundary condition. Using these solution the variation of the Bloch vector components with respect to various parameters are plotted in fig. 4, fig. 5, fig. 6 and fig. 7.

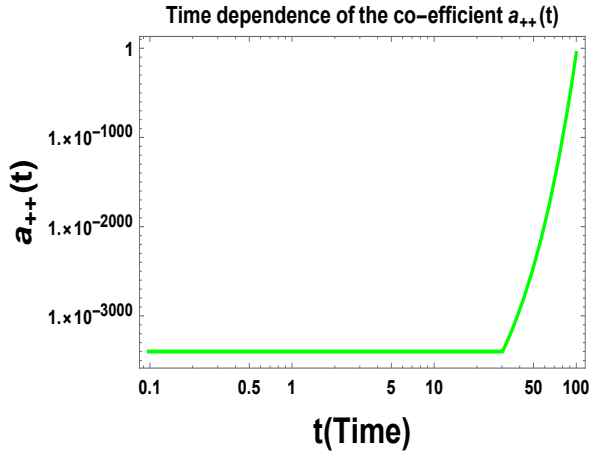
Using these solution our next objective is to compute various entanglement measures from the present OQS set up. The various entanglement measures which are most commonly used nowadays in the context of quantum information theory are listed in the figure 8.4.



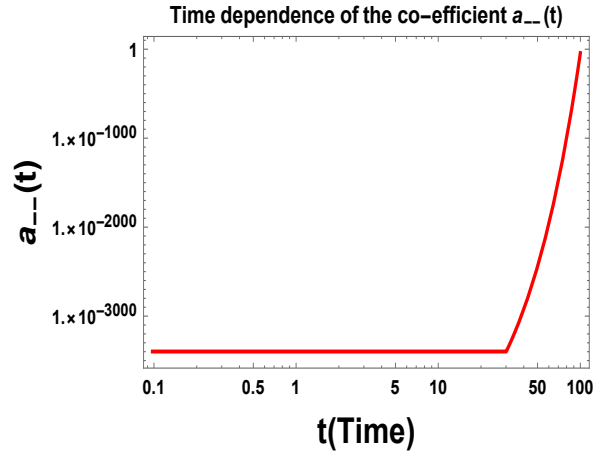
(a) Bloch vector component a_{03} vs Time profile.



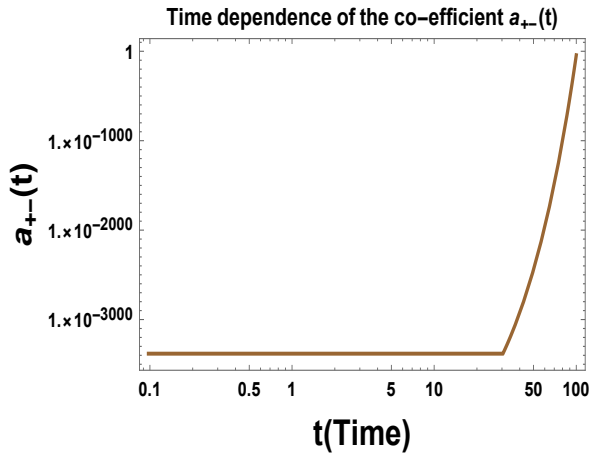
(b) Bloch vector component a_{33} vs Time profile.



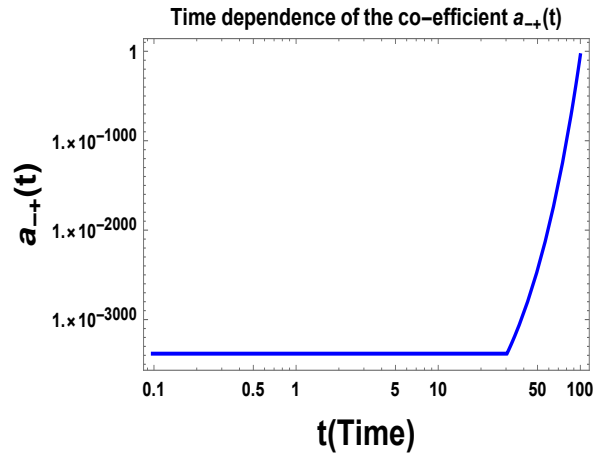
(c) Bloch vector component a_{++} vs Time profile.



(d) Bloch vector component a_{--} vs Time profile.

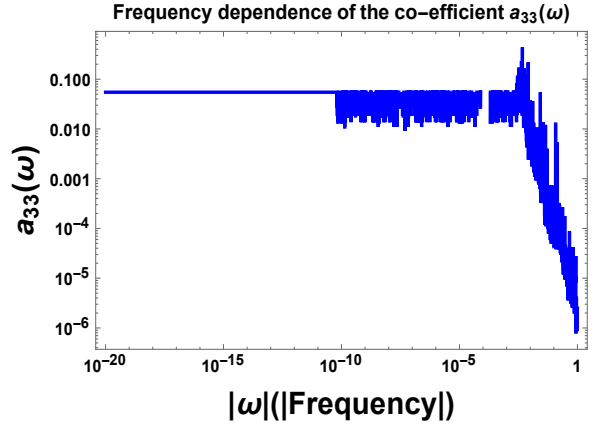
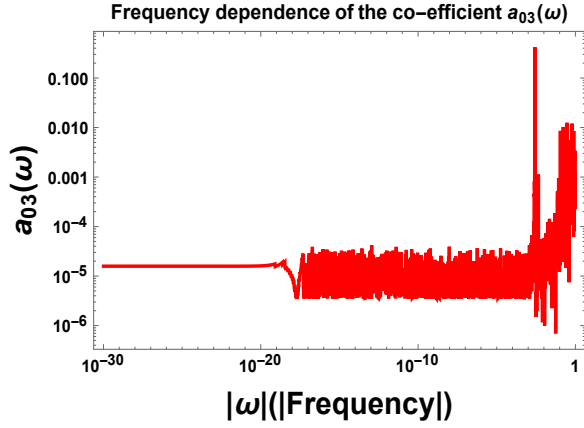


(e) Bloch vector component a_{+-} vs Time profile.

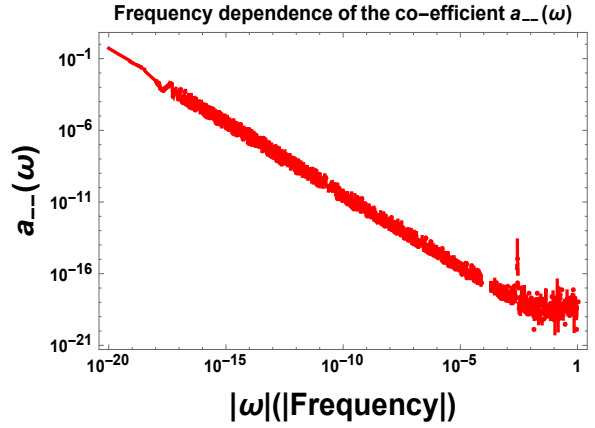
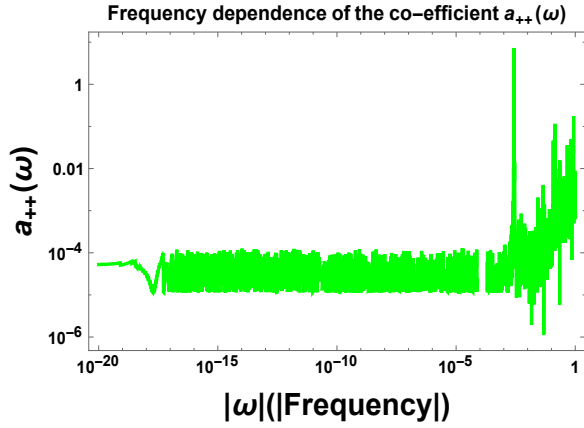


(f) Bloch vector component a_{-+} vs Time profile.

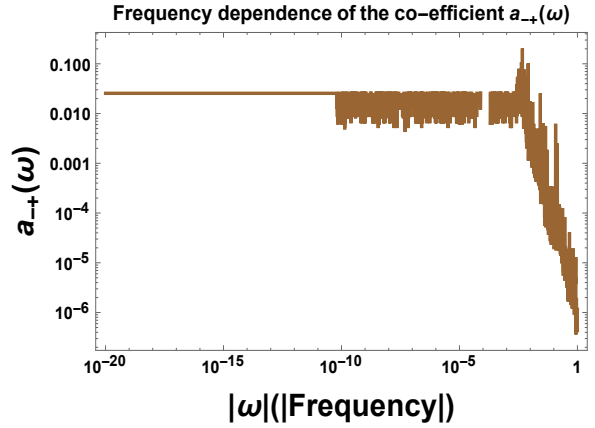
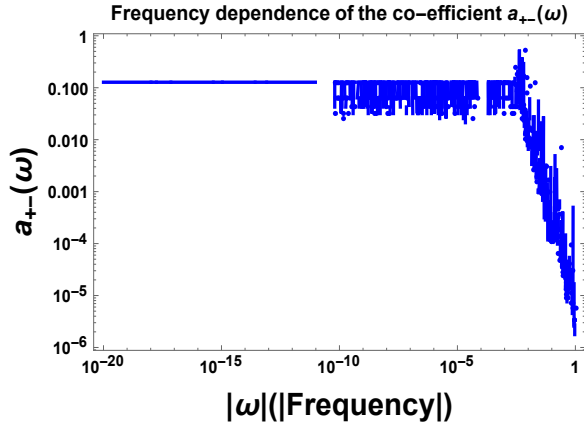
Figure 4. Dependence of the Bloch vector components on Time is shown here



(a) Bloch vector component a_{03} vs Frequency profile. (b) Bloch vector component a_{33} vs Frequency profile.

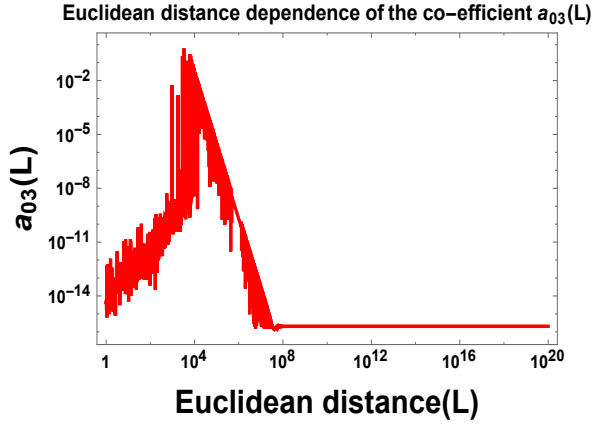


(c) Bloch vector component a_{++} vs Frequency profile. (d) Bloch vector component a_{--} vs Frequency profile.

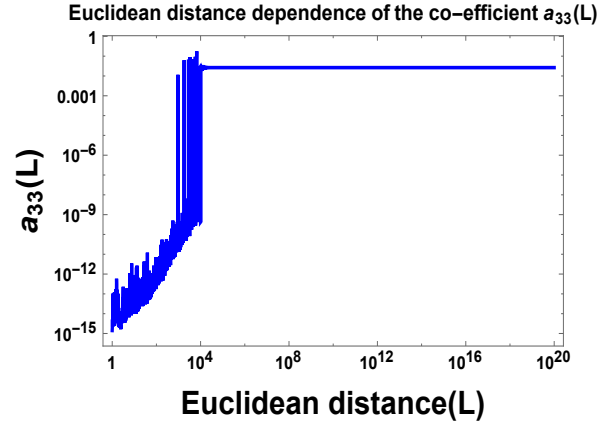


(e) Bloch vector component a_{+-} vs Frequency profile. (f) Bloch vector component a_{-+} vs Frequency profile.

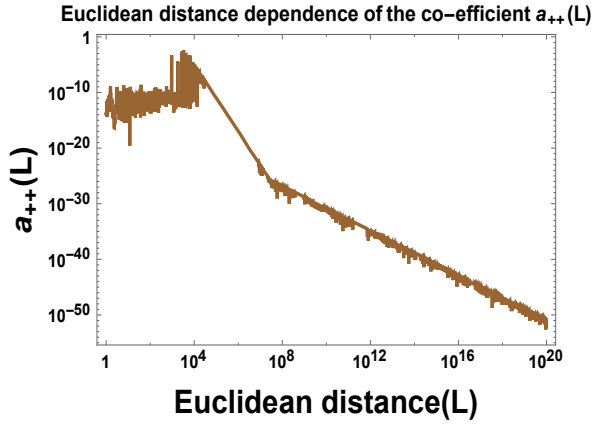
Figure 5. Dependence of the Bloch vector components on frequency is shown here.



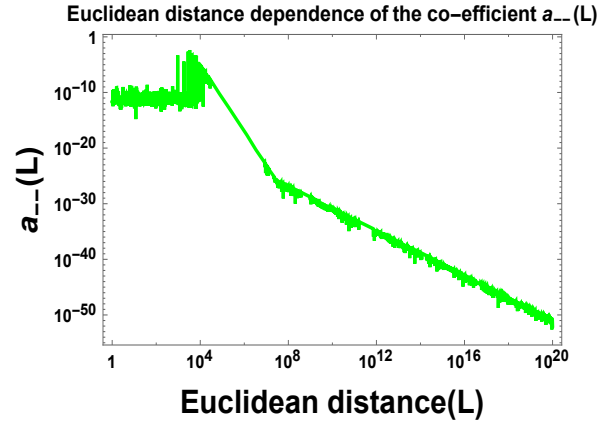
(a) Bloch vector component a_{03} vs Euclidean Distance profile.



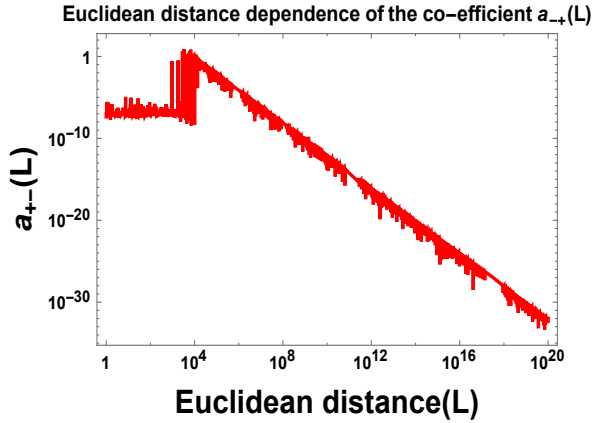
(b) Bloch vector component a_{33} vs Euclidean Distance profile.



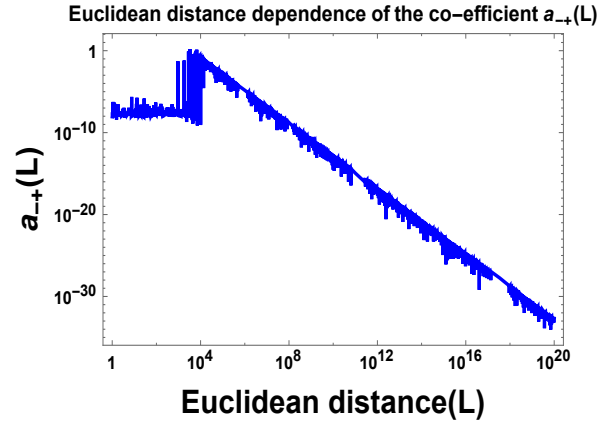
(c) Bloch vector component a_{++} vs Euclidean Distance profile.



(d) Bloch vector component a_{--} vs Euclidean Distance profile.

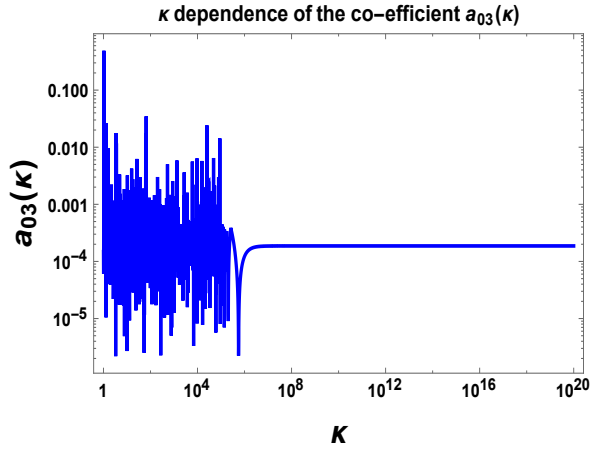


(e) Bloch vector component a_{+-} vs Euclidean Distance profile.

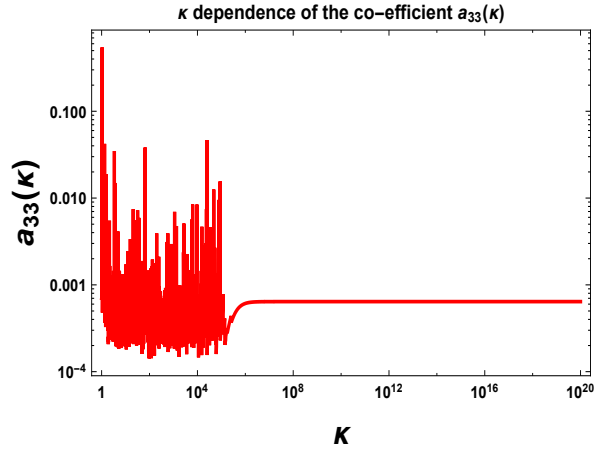


(f) Bloch vector component a_{-+} vs Euclidean Distance profile.

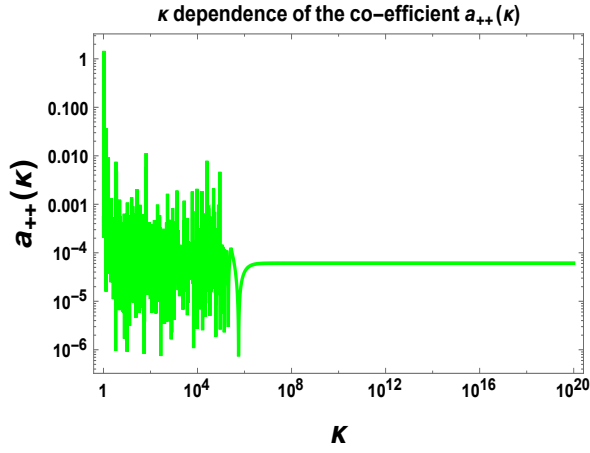
Figure 6. Dependence of the various Bloch vector components on the Euclidean distance is shown here.



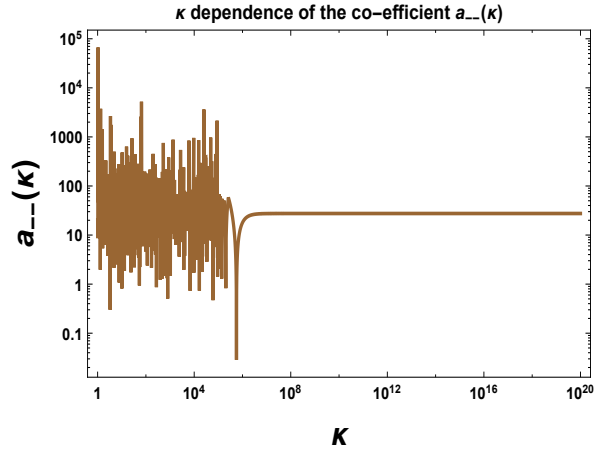
(a) Bloch vector component a_{03} vs κ profile.



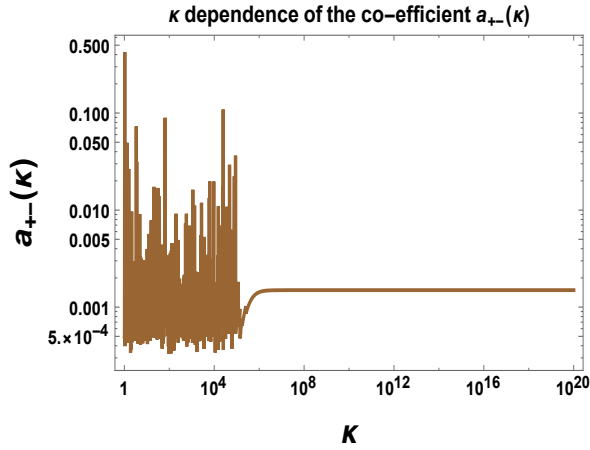
(b) Bloch vector component a_{33} vs κ profile.



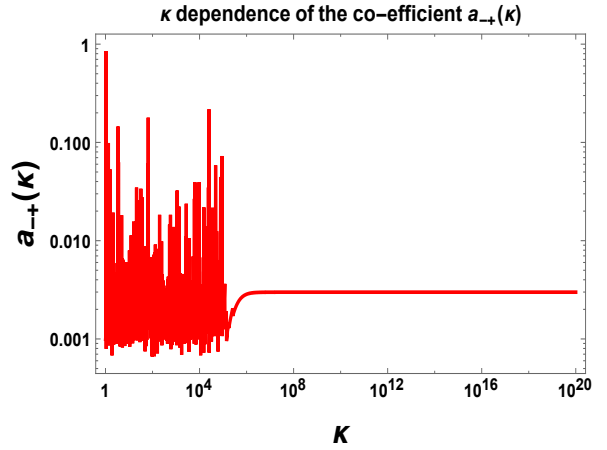
(c) Bloch vector component a_{++} vs κ profile.



(d) Bloch vector component a_{--} vs κ profile.



(e) Bloch vector component a_{+-} vs κ profile.



(f) Bloch vector component a_{-+} vs κ profile.

Figure 7. Dependence of the Bloch vector components on κ is shown here

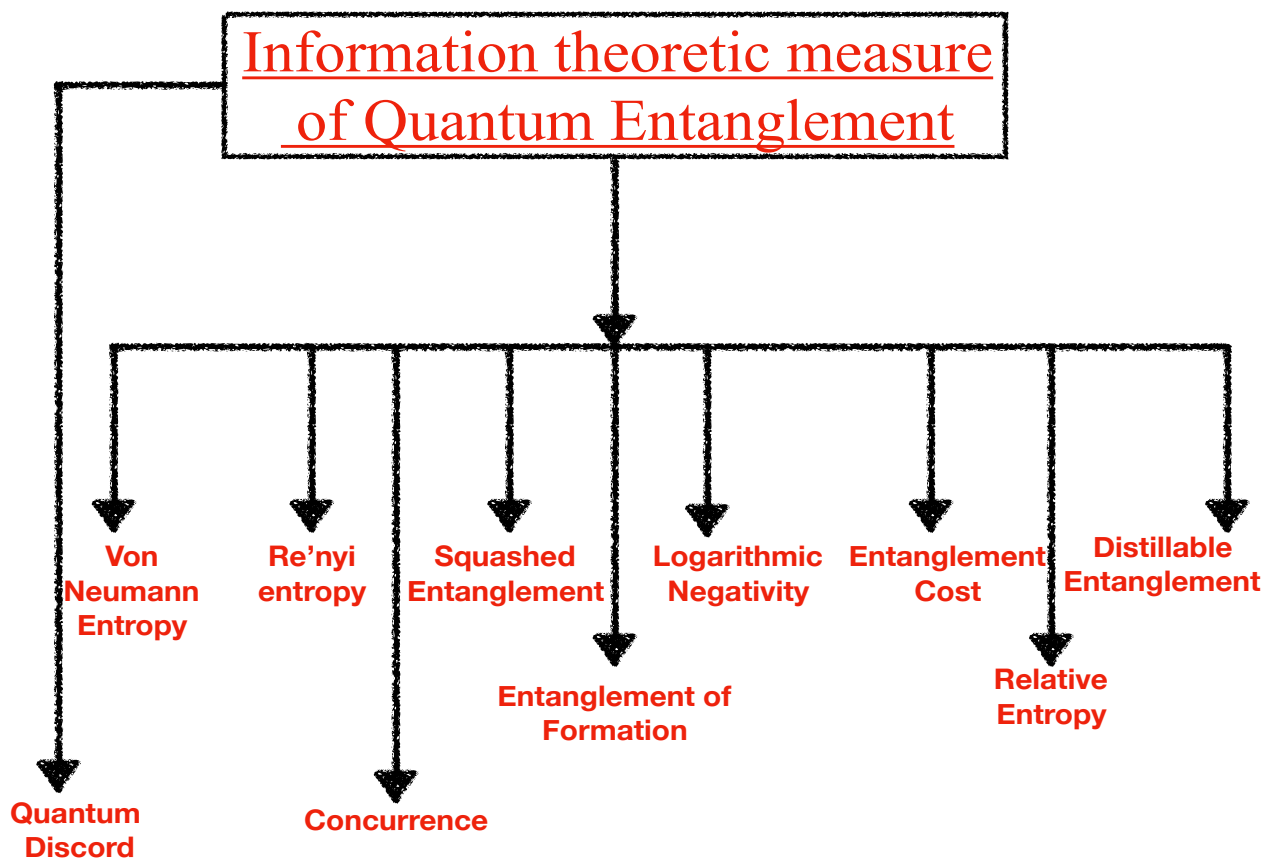


Figure 8. Chart showing various entanglement measures used in the context of quantum information theory.

9 Von Neumann Entanglement Entropy

In the context of quantum statistical mechanics and quantum information theory *Von Neumann entropy* plays the role of extended version of classical *Gibbs entropy*. It actually measures the amount of quantum entanglement for a subsystem or reduced system of a bipartite quantum system.

In the present context, for the two atomic subsystem, which we have obtained after partially tracing over the bath degrees of freedom the *Von Neumann entanglement entropy* is defined in terms of the reduced density matrix (ρ_{System}) as:

$$S(\rho_{\text{System}}) = -\text{Tr} [\rho_{\text{System}} \ln (\rho_{\text{System}})] . \quad (9.1)$$

For the OQS under consideration, the *Von Neumann entanglement entropy* satisfies the following criteria, which are very useful to know about the underlying physics of the OQS under consideration:

1. It is expected from our present OQS set up that the measure of *Von Neumann entanglement entropy* is non zero because our subsystem, which we have obtained by

partially tracing over bath degrees of freedom, is described by mixed states. We know from quantum statistical mechanics that for a mixed state, the Von Neumann measure of entanglement entropy is non zero, which is true for our set up as well. Conversely, if the subsystem can be characterised by pure quantum mechanical states, in such a situation the entanglement measure is zero. Since in our set up we are dealing with pure quantum mechanical states as we have assumed no correlation initially, we get zero entanglement measure from our computation. But during time evolution of the subsystem it becomes more correlated and consequently pure state transforms to a mixed state, for which we get a saturation but non-zero value of the *Von Neumann entanglement entropy*.

2. In the context of OQS, one can construct a unitary operator \mathcal{U} such that the Von Neumann measure of entanglement entropy is invariant under a unitary similarity transformation on the subsystem reduced density matrix, which technically implies:

$$\rho_{\text{System}} \longrightarrow \mathcal{U}\rho_{\text{System}}\mathcal{U}^\dagger = \rho'_{\text{System}}. \quad (9.2)$$

Consequently the Von Neumann measure of entanglement entropy transforms under the above mentioned unitary similarity transformation as:

$$\begin{aligned} S(\rho'_{\text{System}}) &= -\text{Tr}(\rho'_{\text{System}} \ln \rho'_{\text{System}}) \\ &= -\text{Tr}(\mathcal{U}\rho_{\text{System}}\mathcal{U}^\dagger \ln(\mathcal{U}\rho_{\text{System}}\mathcal{U}^\dagger)) \\ &= -\text{Tr}(\rho_{\text{System}} \ln \rho_{\text{System}}) \\ &= S(\rho_{\text{System}}) \end{aligned} \quad (9.3)$$

3. In our prescribed OQS setup the reduced subsystem density matrix can be written in terms of the tensor products of two atoms. Consequently, the *Von Neumann entanglement* measure for the reduced subsystem can be expressed as a sum of the contributions from the two independent and identical atoms. Technically this statement can be expressed as:

$$\rho_{\text{System}} = \rho_1 \otimes \rho_2 \quad (9.4)$$

where ρ_1 and ρ_2 are the density matrix for **Atom 1** and **Atom 2** respectively. Consequently, for our set up one can explicitly show that:

$$S(\rho_{\text{System}}) = S(\rho_1 \otimes \rho_2) = S(\rho_1) + S(\rho_2) \quad (9.5)$$

4. In quantum information theory, *Von Neumann entanglement* measure is treated as the quantum generalized version of *Shannon entropy*. In classical measurement, the *Shannon entropy* is treated as a natural measure of our ignorance about the properties of a subsystem under consideration, whose physical existence is actually independent of measurement on that system. In general, one can use the concept of *Borel functional calculus* to compute a non polynomial function such as $\ln(\rho_{\text{System}})$, which is explicitly appearing in the expression for the *Von Neumann entanglement* measure. Now, if the non-negative reduced density operator ρ_{System} acts on a finite dimensional Hilbert space, which has eigenvalues $\lambda_i \forall i = 1 \dots n$ (Here n represents the finite dimension of the Hilbert space), in that case $\ln(\rho_{\text{system}})$ can be expressed as an operator which has

the same eigenvectors but the eigenvalues will be modified as, $\ln(\lambda_i) \forall i = 1 \dots n$. In this situation, the generalization of *Quantum Shannon entropy* or the *Von Neumann entanglement* measure can be written as:

$$S(\rho_{\text{System}}) = -\text{Tr} [\rho_{\text{System}} \ln (\rho_{\text{System}})] = - \sum_i \lambda_i \ln(\lambda_i) \quad (9.6)$$

This idea can be extended for the infinite dimensional Hilbert space as well. In that case, the reduced density matrix for the subsystem can be expressed in terms of spectral resolution, which is defined as:

$$\rho_{\text{System}} = \int_0^\infty \lambda dP_\lambda, \quad (9.7)$$

where dP_λ represents the Haar measure of the eigen values. Consequently, the *Von Neumann entanglement* measure for an infinite dimensional Hilbert space can be expressed in terms of spectral resolution as:

$$S(\rho_{\text{System}}) = -\text{Tr}(\rho_{\text{System}} \ln \rho_{\text{System}}) \equiv - \int_0^\infty \lambda \ln \lambda dP_\lambda. \quad (9.8)$$

5. Additionally, it is important to note that, for mixed states the *Von Neumann entanglement* measure computed from the reduced density matrix for the subsystem is not the only reasonable measure of quantum entanglement. For this reason, in this paper we study the role of other quantum entanglement measures, which are commonly used in the context of *quantum information theory*. For more technical details see the next subsections.

9.1 Bloch sphere representation of Von Neumann Entropy

In terms of Bloch vectors it can be explicitly shown that the Von Neumann Entropy takes the following simplified form:

$$S = \frac{1}{4} [8 \ln 2 - (\alpha - \beta) \ln(\alpha - \beta) - (\alpha + \beta) \ln(\alpha + \beta) - (\eta - \gamma) \ln(\eta - \gamma) - (\eta + \gamma) \ln(\eta + \gamma)], \quad (9.9)$$

where in the above expression the symbols α , β , γ , η have been used to represent the following terms:

$$\alpha = 1 - a_{33}(\tau) \quad (9.10)$$

$$\eta = 1 + a_{33}(\tau) \quad (9.11)$$

$$\beta = \sqrt{a_{03}^2(\tau) - 2a_{03}(\tau)a_{30}(\tau) + a_{30}^2(\tau) + a_{-+}(\tau)a_{+-}(\tau)} \quad (9.12)$$

$$\gamma = \sqrt{a_{03}^2(\tau) + 2a_{03}(\tau)a_{30}(\tau) + a_{30}^2(\tau) + a_{--}(\tau)a_{++}(\tau)} \quad (9.13)$$

9.2 Von Neumann entropy from OQS of two entangled atoms

In the context of two entangled atoms relevant to our OQS it can be seen from the solution of the Bloch vector components that $a_{03}(\tau)$ and $a_{30}(\tau)$ has the same form i.e. $a_{03}(\tau) = a_{30}(\tau)$. So in that case the *Von Neumann entropy* can be written as:

$$S = \frac{1}{4} \left[8 \ln 2 - (\alpha - \tilde{\beta}) \ln(\alpha - \tilde{\beta}) - (\alpha + \tilde{\beta}) \ln(\alpha + \tilde{\beta}) - (\eta - \tilde{\gamma}) \ln(\eta - \tilde{\gamma}) - (\eta + \tilde{\gamma}) \ln(\eta + \tilde{\gamma}) \right], \quad (9.14)$$

where we have introduced two new functions, $\tilde{\beta}$ and $\tilde{\gamma}$, which are defined as:

$$\tilde{\beta} = \beta_{\text{Two atom}} = \sqrt{a_{-+}(\tau)a_{+-}(\tau)}, \quad (9.15)$$

$$\tilde{\gamma} = \gamma_{\text{Two atom}} = \sqrt{4a_{03}^2(\tau) + a_{--}(\tau)a_{++}(\tau)}. \quad (9.16)$$

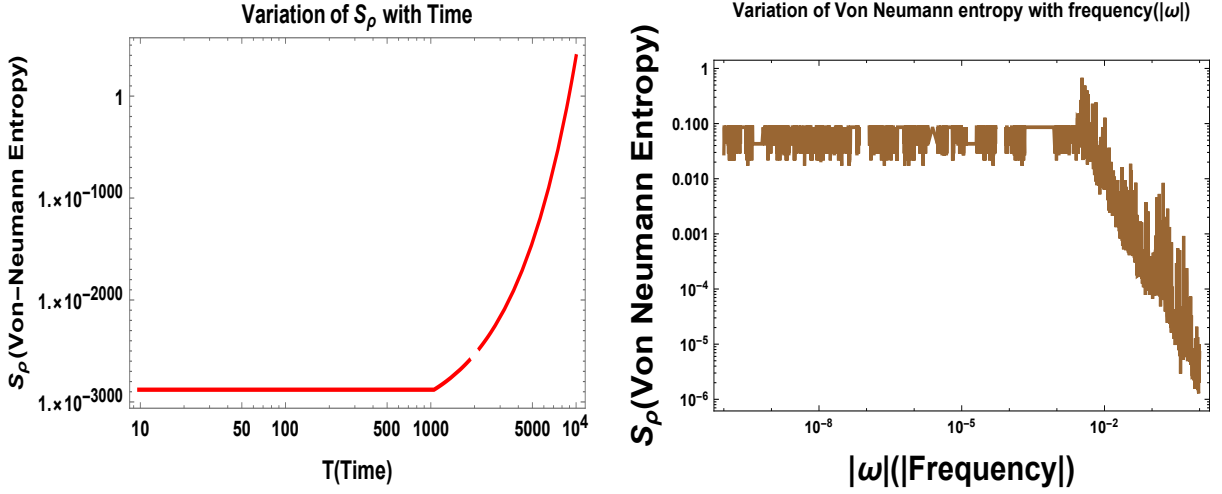
Here all of these time dependent coefficients $a_{03}(\tau)$, $a_{-+}(\tau)$, $a_{+-}(\tau)$, $a_{--}(\tau)$, $a_{++}(\tau)$ and $a_{33}(\tau)$ have explicitly been computed for the two atomic OQS in the previous section.

To physically analyse this result we have plotted the behaviour of the *Von Neumann entropy* from the present two atomic OQS set up with respect to different useful parameters present in the theory.

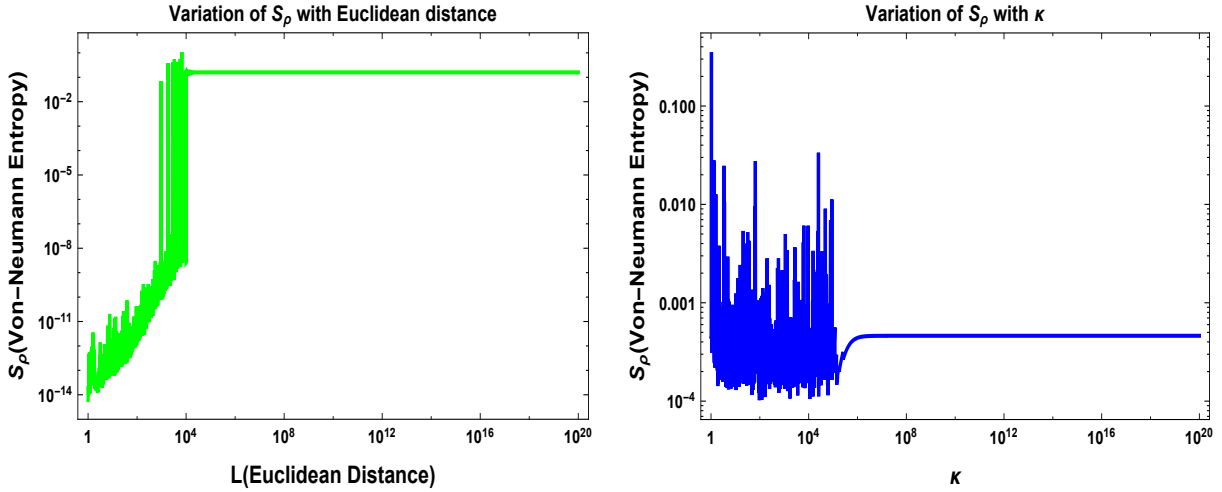
In Fig. 9(a), we have explicitly shown the behaviour of *Von-Neumann entropy* of our two atomic OQS set up in De Sitter space with respect to rescaled time T by keeping all other parameters fixed. Here T is defined as the time difference, $T = \tau - \tau'$, which is very useful for further analysis. Here τ is the usual time scale and τ' is the time scale where the equilibrium boundary condition is imposed. We have normalized the entropy with the result obtained from $T = 10^4$ i.e. we always compute $S(T)/S(T = 10^4)$. We consider both small and large time scale limiting situations to understand the underlying physics. It is clearly observed that initially the value of entropy is almost zero implying that our two atomic OQS set up do not show any signature of quantum entanglement. This is consistent with our assumption that initially there is no correlation and the quantum states being represented by pure states only. As time goes on, the sub-system gets more and more entangled due to more correlation and at a late time scale, it almost saturates to unity after normalization, which is the maximum value of the entropy for our system. The late time scale behaviour is also consistent with the prediction from the present system i.e. as time goes on the system is represented by mixed quantum states due to getting more quantum correlation.

In Fig. 9(b), we have explicitly shown the behaviour of *Von-Neumann entropy* of our two atomic OQS set up in De Sitter space with respect to frequency $|\omega|$ by keeping all other parameters fixed. We have normalized the entropy with the result obtained from $|\omega| = 5 \times 10^{-2}$ i.e. we always compute $S(\omega)/S(\omega = 5 \times 10^{-2})$. We consider both small and large frequency scale limiting situations for our analysis. It is clearly observed that initially for a finite frequency scale, the value of entropy is almost constant showing entanglement due to the appearance of mixed quantum states. As frequency is further increased the value of entropy decreases implying reduction in entanglement and when it gets close to $|\omega_0|$ the value of entropy is almost zero indicating that the joint density matrix of our subsystem becomes separable as in that case it is described by pure quantum mechanical states.

In Fig. 9(c), we have explicitly shown the behaviour of *Von-Neumann entropy* of our two atomic OQS set up in De Sitter space with respect to Euclidean distance L by keeping



(a) Normalized Von Neumann Entanglement entropy vs Time profile. (b) Normalized Von Neumann Entanglement entropy vs $|Frequency|$ profile.



(c) Normalized Von Neumann Entanglement entropy vs Euclidean Distance profile. (d) Normalized Von Neumann Entanglement entropy vs κ profile.

Figure 9. Normalized Von Neumann Entanglement entropy variation with various parameters is shown here.

all other parameters fixed. We have normalized the entropy with the result obtained from $L = 10^4$ i.e. we always compute $S(L)/S(L = 10^4)$. We consider both small and large length scale limiting situations for our analysis. It is clearly observed that initially there are some fluctuations with increase in entropy for small length scale. However, the maximum value of the fluctuation implies the maximum value of the entangled entropy one can obtain once we want to analyse the behaviour with respect to the Euclidean distance L . This is because at small L value the quantum states are dominated by pure states and there is no corresponding quantum correlation. But as the distance between the two atoms increases, the subsystem gets entangled to a maximum value close to 1. With further increase in distance, there is no change in entropy implying that the correlation between the atoms in our OQS set up is maximum and the corresponding quantum state is dominated by mostly

mixed states.

Further in Fig. 9(d), we have explicitly shown the behaviour of *Von-Neumann entropy* of our two atomic OQS set up in De Sitter space with respect to the parameter κ by keeping all other parameters fixed. We have normalized the entropy with the result obtained from κ i.e. we always compute $S(\kappa)/S(\kappa = 1)$. We consider both small and large κ scale limiting situations. We know that the curvature of static patch of the De Sitter space can be expressed in terms of the parameter κ as:

$$R = \frac{12}{\alpha^2} = \frac{12}{\kappa^2 + r^2} \approx \frac{12}{\kappa^2} \quad \text{for } \kappa = \sqrt{\alpha^2 - r^2} \approx \alpha \gg r, \quad (9.17)$$

which implies we actually have considered both flat and static De Sitter space by varying the parameter κ . It is clearly observed that initially there are fluctuations in entanglement entropy with increase in the value of κ . However, the maximum value the fluctuation implies the maximum value of the entangled entropy one can obtain once we want to analyse the behaviour with respect to the parameter κ . This is because at small κ or non-zero effect of curvature value the quantum states are dominated by mixed states and the corresponding quantum correlation is non zero. With further increase in the value of the parameter κ , the entanglement entropy remains constant and very very small implying almost getting no quantum correlation and described by the pure quantum states for the large values of κ , which corresponds to the flat space time situation.

10 Rényi Entropy

Rényi entropy is a generalisation of various information theoretic measure which quantify randomness of a quantum mechanical system. The Rényi entropy can be expressed in terms of Hartley function as:

$$S_q(\rho_{\text{System}}) = \frac{1}{1-q} \ln \text{Tr}[(\rho_{\text{System}})^q] \equiv \mathcal{H}_q(\rho_{\text{System}}), \quad q \geq 0, q \neq 1 \quad (10.1)$$

where q is known as the Rényi Index.

In general, the Hartley function of order q satisfy the following characteristics:

1. If we consider the limiting situation at $q \rightarrow 1$, then Hartley function or the corresponding Rényi entropy can be written in terms of the Von Neumann entanglement as given by:

$$\begin{aligned} \lim_{q \rightarrow 1} S_q(\rho_{\text{System}}) &\equiv \lim_{q \rightarrow 1} \mathcal{H}_q(\rho_{\text{System}}) = \lim_{q \rightarrow 1} \frac{1}{1-q} \ln \text{Tr}[(\rho_{\text{System}})^q] \\ &= -\text{Tr}(\rho_{\text{System}} \ln \rho_{\text{System}}) = S(\rho_{\text{System}}). \end{aligned} \quad (10.2)$$

2. For $q = 0$ the Rényi entropy can be interpreted as the Hartley entropy of the quantum system as:

$$S_0(\rho_{\text{System}}) = \ln \text{Tr}[\mathbf{I}] \equiv \mathcal{H}_0(\rho_{\text{System}}), \quad (10.3)$$

3. For $q = 2$ the Rényi entropy can be interpreted as the Collision entropy of the quantum system as:

$$S_2(\rho_{\text{System}}) = -\ln(\text{Tr}[(\rho_{\text{System}}^2)]) \equiv \mathcal{H}_2(\rho_{\text{System}}), \quad (10.4)$$

4. If we consider the limiting situation $q \rightarrow \infty$, the Re'nyi entropy can be interpreted as the Minimum entropy of the quantum system which is expressed as:

$$\lim_{q \rightarrow \infty} S_q(\rho_{\text{System}}) = \lim_{q \rightarrow \infty} \frac{1}{1-q} \ln \text{Tr}[(\rho_{\text{System}})^q] = \lim_{q \rightarrow \infty} \mathcal{H}_q(\rho_{\text{System}}) \quad (10.5)$$

5. If all the Hartley functions are individually computed for all positive Re'nyi indices then it can be shown that the following inequality holds:

$$\mathcal{H}_0(\rho_{\text{System}}) > \mathcal{H}_1(\rho_{\text{System}}) > \mathcal{H}_2(\rho_{\text{System}}) > \mathcal{H}_\infty(\rho_{\text{System}}) \quad (10.6)$$

Re'nyi entropy is a more general concept which contains the total spectrum of the reduced density matrix of the subsystem under consideration. However, using this concept the underlying connection between the fundamental aspects of quantum field theory and bulk holographic space time have not been understood well. It is a very well known fact that, in the context of quantum field theory, the Re'nyi entropy can be computed by considering the Euclidean time scale instead of using Lorentzian time, which can be obtained by Wick rotation and inserting a conical type of defect around the entangling surface $\Sigma = \partial\mathcal{A}$. In such a physical situation, the Re'nyi entropy can be explicitly expressed in terms of the Euclidean partition function, Z_q of the geometry under consideration during entanglement with a conical excess of the order of $2\pi(q-1)$ across the entangling surface $\Sigma = \partial\mathcal{A}$:

$$S_q = \frac{1}{1-q} [\ln Z_q - q \ln Z_1]. \quad (10.7)$$

Here q is the Re'nyi index, which physically represents the number of replicas considered in the present context. To interpret this result more clearly here one can consider a specific example, where the thermal partition function is computed on $\mathcal{H}_q^D = S^1 \times \mathbb{H}^{D-1}$ which is described by the following metric:

$$ds_{\mathcal{H}_q^D}^2 = d\tau^2 + du^2 + \sinh^2 u d\Omega_{D-2}^2, \quad \text{with } \tau \sim \tau + 2\pi q. \quad (10.8)$$

Here we have considered the compactification around Euclidean time τ . In this situation, the partition function can be written as:

$$Z_q = \text{Tr} (e^{-2\pi q H_\tau}), \quad (10.9)$$

where H_τ is the Hamiltonian that can generate the translation along S^1 and is identified as the *Modular Hamiltonian* in the present context. In particular, we get the following result for the Re'nyi entropy from this computation:

$$S_q = \frac{1}{1-q} [\ln (\text{Tr} (e^{-2\pi q H_\tau})) - q \ln (\text{Tr} (e^{-2\pi H_\tau}))], \quad (10.10)$$

where H_τ can be computed from the following expression:

$$H_\tau = \int_{\mathbb{H}^{D-1}} d^{D-1}x \sqrt{-g} T_{\tau\tau}. \quad (10.11)$$

Here $T_{\tau\tau}$ is the stress tensor at the boundary. Then it can be shown that around $q = 1$ one can expand the Re'nyi entropy S_q as given by the following expression:

$$S_q = \langle H_\tau \rangle_1 + \ln Z_1 + 2\pi \sum_{n=1}^{\infty} \frac{(-1)^n (2\pi)^n (q-1)^n}{(n+1)!} \underbrace{\langle H_\tau H_\tau H_\tau \cdots H_\tau \rangle_{q=1}}_{(n+1) \text{ connected correlations}}, \quad (10.12)$$

which means that derivatives of S_q with respect to the Re'nyi index q can generate all connected correlation functions of the *Modular Hamiltonian* H_τ in this case. However computation of the *Modular Hamiltonian* H_τ for our problem is very complicated and also we don't have proper understanding on that in OQS set up.

On the other hand, insertion of conical singularity introduces UV divergence, which one can regulate by introducing a lattice cut-off ϵ_Δ and finally get back a finite result which is far from the singularity. After introducing the cut-off one can compute the following general result from the quantum field theory, as given by:

$$S_q = \frac{c_{D-2}(q)}{\epsilon_\Delta^{D-2}} + \frac{c_{D-4}(q)}{\epsilon_\Delta^{D-4}} + \cdots + c_{\text{even}}(q) \ln \epsilon_\Delta + c_0(q) + \cdots, \quad (10.13)$$

where the logarithmic term is only appearing in the even dimensions. Here by considering the analogy with the entanglement entropy one can interpret in the even dimensions, the *universal* contribution in the Re'nyi entropy is the $\ln \epsilon_\Delta$ containing term, which is characterized by the coefficient $c_{\text{even}}(q)$. On the other hand, in the odd dimensions the *universal* contribution in the expression for the Re'nyi entropy is given by the constant $c_0(q)$.

But in practical purposes for a given quantum field theory it is very difficult to compute all of these coefficients appearing in the above expression. However, using the concept of *Re'nyi perturbation theory* one can consider deformation in the reduced density matrix, which can be applicable to any general quantum field theory prescription. This can be shown explicitly that computations of correlation functions of the deformed quantum field theory operators in the canonical space time can serve our purpose. See ref. [40] for more details on this issue.

10.1 Bloch sphere representation of Re'nyi Entropy

In terms of the components of the *Bloch vectors* the Re'nyi entropy can be represented as:

$$S_q(\rho_{\text{System}}) = \frac{1}{1-q} \ln \left[4^{-q} ((\alpha - \beta)^q + (\alpha + \beta)^q + (\eta - \gamma)^q + (\eta + \gamma)^q) \right] \quad (10.14)$$

where the symbols used has already been defined in the earlier section.

10.2 Re'nyi entropy from OQS of two entangled atoms

In case of our two atomic OQS set up the expression for the Re'nyi entropy reduces to the following simplified form:

$$S_q(\rho_{\text{System}}) = \frac{1}{1-q} \ln \left[4^{-q} \left((\alpha - \tilde{\beta})^q + (\alpha + \tilde{\beta})^q + (\eta - \tilde{\gamma})^q + (\eta + \tilde{\gamma})^q \right) \right], \quad (10.15)$$

where the symbols used has already been defined in the previous section. It can be very easily verified that in this context relevant to our OQS the Re'nyi entropy reduces to the *Von Neumann entropy* in the limit $q \rightarrow 1$.

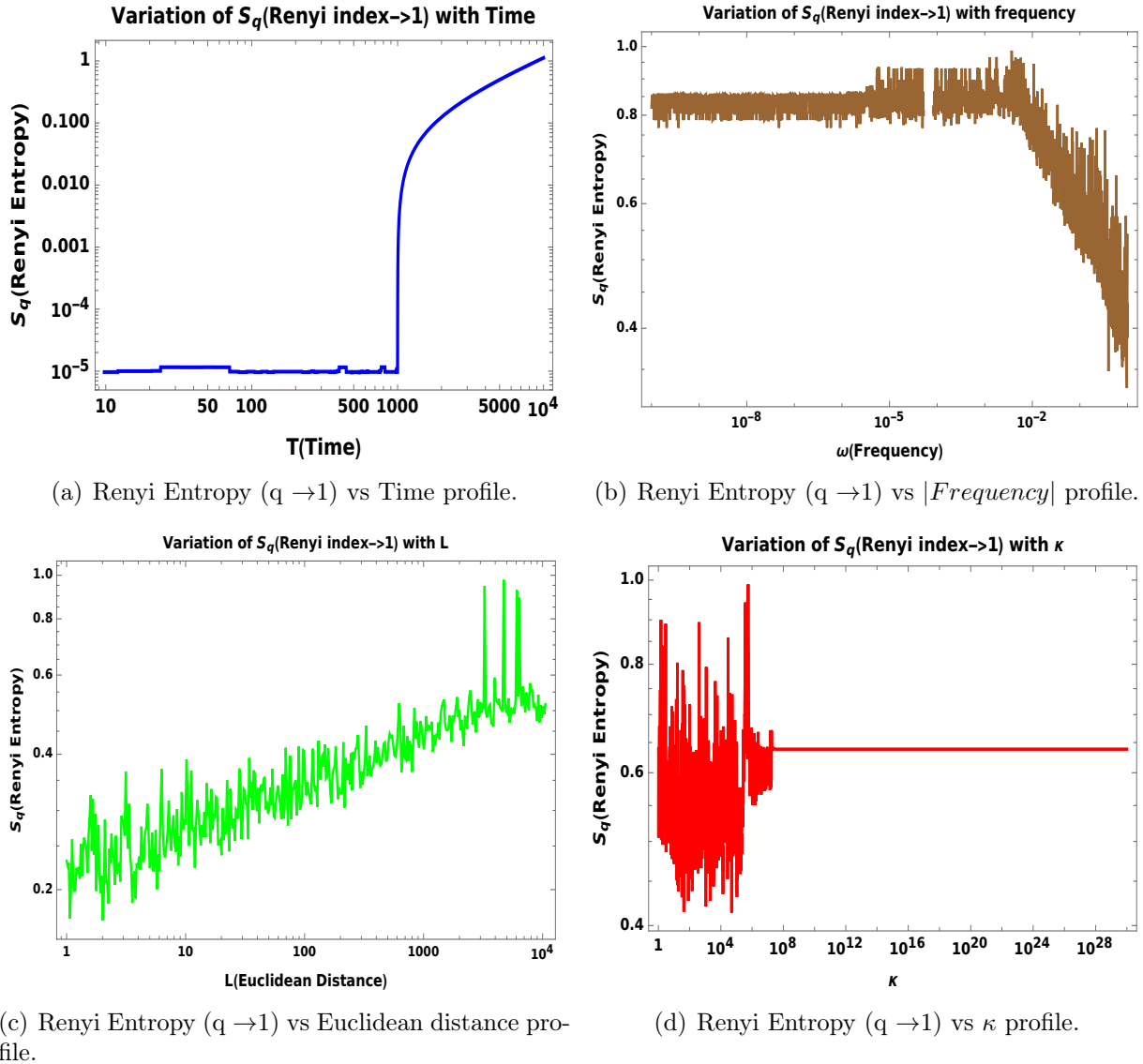


Figure 10. Renyi Entropy ($q \rightarrow 1$) variation with various parameters are shown here.

In Fig. 10(a), we have explicitly shown the behaviour of Renyi entropy ($q \rightarrow 1$) of our two atomic OQS set up in De Sitter space with respect to rescaled time T , which is already defined in the earlier section. We have normalized the entropy with the result obtained from $T = 10^4$ i.e. here we have analysed $S_{q \rightarrow 1}(T)/S_{q \rightarrow 1}(T = 10^4)$ which is nothing but the normalised *Von Neumann entropy* computed from our system. This also verifies the fact that the result obtained for the Renyi entropy from our two atomic OQS set up is perfectly correct as in the $q \rightarrow 1$ limit it is able to produce the result obtained for *Von Neumann entropy* in the previous section. We consider both small and large time scale limiting situations. It is clearly observed that initially the value of entropy is almost zero implying that our two atomic OQS set up do not show any signature of quantum entanglement. As time goes on, the sub-system gets more and more entangled and at a late time scale, it saturates to unity, which is the maximum value of the measure.

In Fig. 10(b), we have explicitly shown the behaviour of Renyi entropy ($q \rightarrow 1$) of our two atomic OQS set up in the static patch of De Sitter space with respect to frequency ω . We have normalized the entropy with the result obtained from $\omega = 5 \times 10^{-2}$. It is clearly observed that initially for a finite frequency scale, the value of entropy is almost constant showing entanglement. As frequency is further increased the value of entropy decreases implying reduction in entanglement and when it gets close to ω_0 the value of entropy is almost zero indicating that the joint density matrix of our subsystem becomes separable.

In Fig. 10(c), we have explicitly shown the behaviour of Renyi entropy ($q \rightarrow 1$) of our two atomic OQS set up in the static patch of De Sitter space with respect to Euclidean distance between two atoms L . We have normalized the entropy with the result obtained from $L=5000$. It is clearly observed that initially there is some fluctuation with increase in entropy for small length scale. But as the distance between the two atoms increases, the subsystem gets entangled to a maximum value.

Further in Fig. 10(d), we have explicitly shown the behaviour of Renyi entropy ($q \rightarrow 1$) of our two atomic OQS set up in the static patch of De Sitter space with respect to the parameter κ . We have normalized the entropy with the result obtained from $\kappa = 5 \times 10^4$. It is clearly observed that initially there are fluctuations in entropy with increase in κ . With further increase in κ , the entropy remains constant to negligibly small value implying zero quantum entanglement.

In Fig. 11(a), we have explicitly shown the behaviour of Collision entropy of our two atomic OQS set up in the static patch of De Sitter space with respect to the rescaled time scale T . We have normalized the entropy with the result obtained from $T=100000$. It is clearly observed that initially the value of entropy is almost zero implying that our two atomic OQS set up do not show any signature of quantum entanglement. As time goes on, the sub-system gets more and more entangled and at a late time scale, it saturates to unity, which is the maximum value of the measure.

In Fig. 11(b), we have explicitly shown the behaviour of Collision entropy of our two atomic OQS set up in the static patch of De Sitter space with respect to the frequency ω . We have normalized the entropy with the result obtained from $\omega = 5 \times 10^{-2}$. It is clearly observed that initially for a finite frequency scale, the value of entropy is almost constant showing quantum entanglement. As frequency is further increased the value of entropy decreases implying reduction in entanglement and when it gets close to ω_0 the value of entropy is almost zero indicating that the joint density matrix of our subsystem becomes separable.

In Fig. 11(c), we have explicitly shown the behaviour of Collision entropy of our two atomic OQS set up in the static patch of De Sitter space with respect to the Euclidean distance between two atoms L . We have normalized the entropy with the result obtained from $L = 10^4$. It is clearly observed that initially there is some fluctuation with increase in entropy for small length scale. But as the distance between the two atoms increases, the subsystem gets entangled to a maximum value. With further increase in distance, there is no change in entropy implying that the quantum correlation between the atoms in our OQS set up is maximum.

Finally in Fig. 11(d), we have explicitly shown the behaviour of Collision entropy of our two atomic OQS set up in the static patch of De Sitter space with respect to κ . We have normalized the entropy with the result obtained from $\kappa = 1$. It is clearly observed that initially there are fluctuations in entropy with increase in κ . With further increase in κ , the

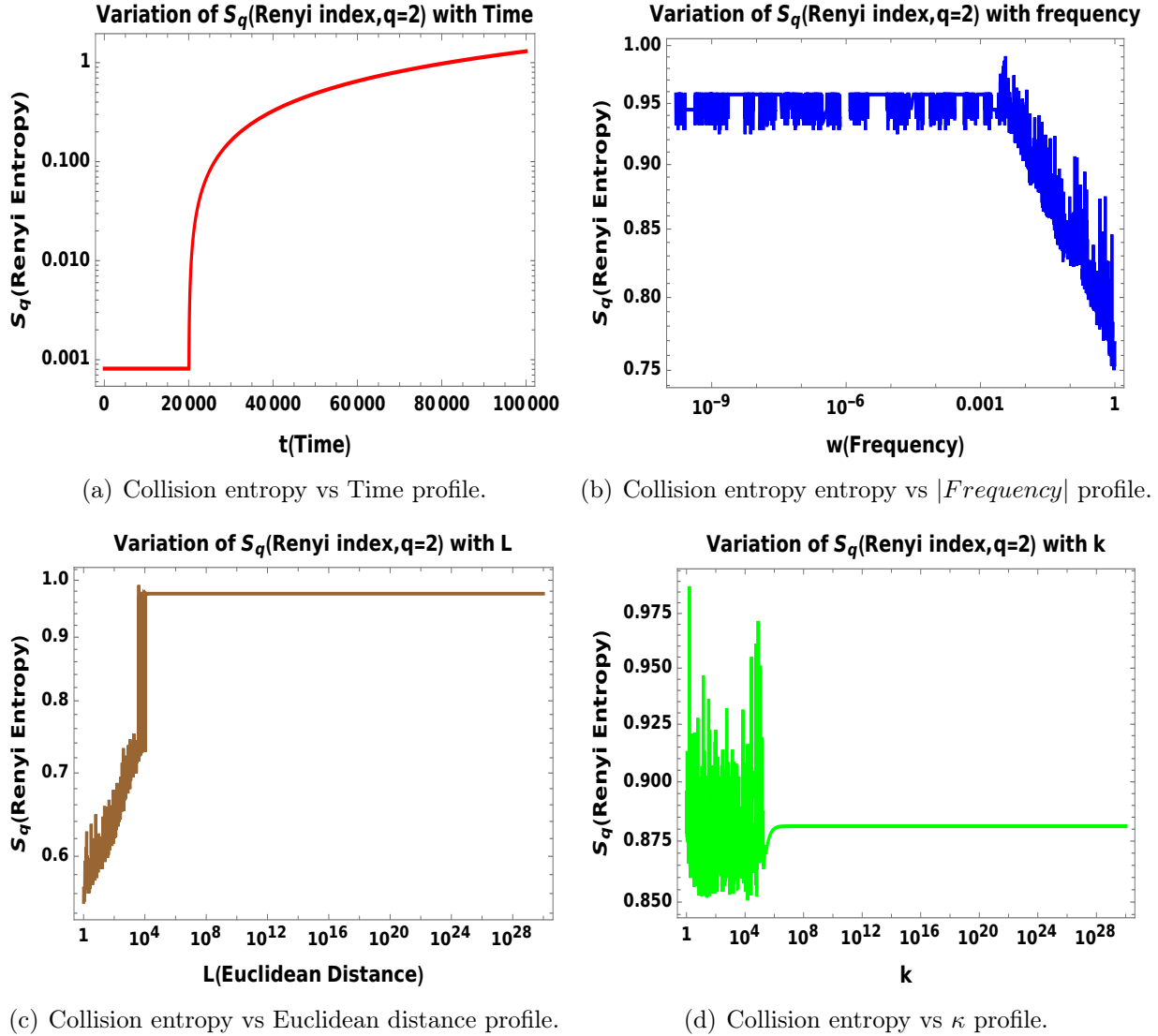


Figure 11. Collision entropy variation with various parameters are shown here.

entropy remains constant to negligibly small value implying zero quantum entanglement.

In Fig. 12(a), we have explicitly shown the behaviour of Min Entanglement entropy of our two atomic OQS set up in the static patch of De Sitter space with respect to the rescaled time scale T . We have normalized the entropy with the result obtained from $T = 10^4$. We consider both small and large time scale limiting situations. It is clearly observed that initially the value of entropy is almost zero implying that our two atomic OQS setup do not show any signature of quantum entanglement. As time goes on, the sub-system gets more and more entangled and at a late time scale, it saturates to unity.

In Fig. 12(b), we have explicitly shown the behaviour of Min Entanglement entropy of our two atomic OQS set up in the static patch of De Sitter space with respect to frequency ω . We have normalized the entropy with the result obtained from $\omega = 5 \times 10^{-2}$. It is clearly observed that initially for a finite frequency scale, the value of entropy is almost constant showing entanglement. As frequency is further increased the value of entropy decreases

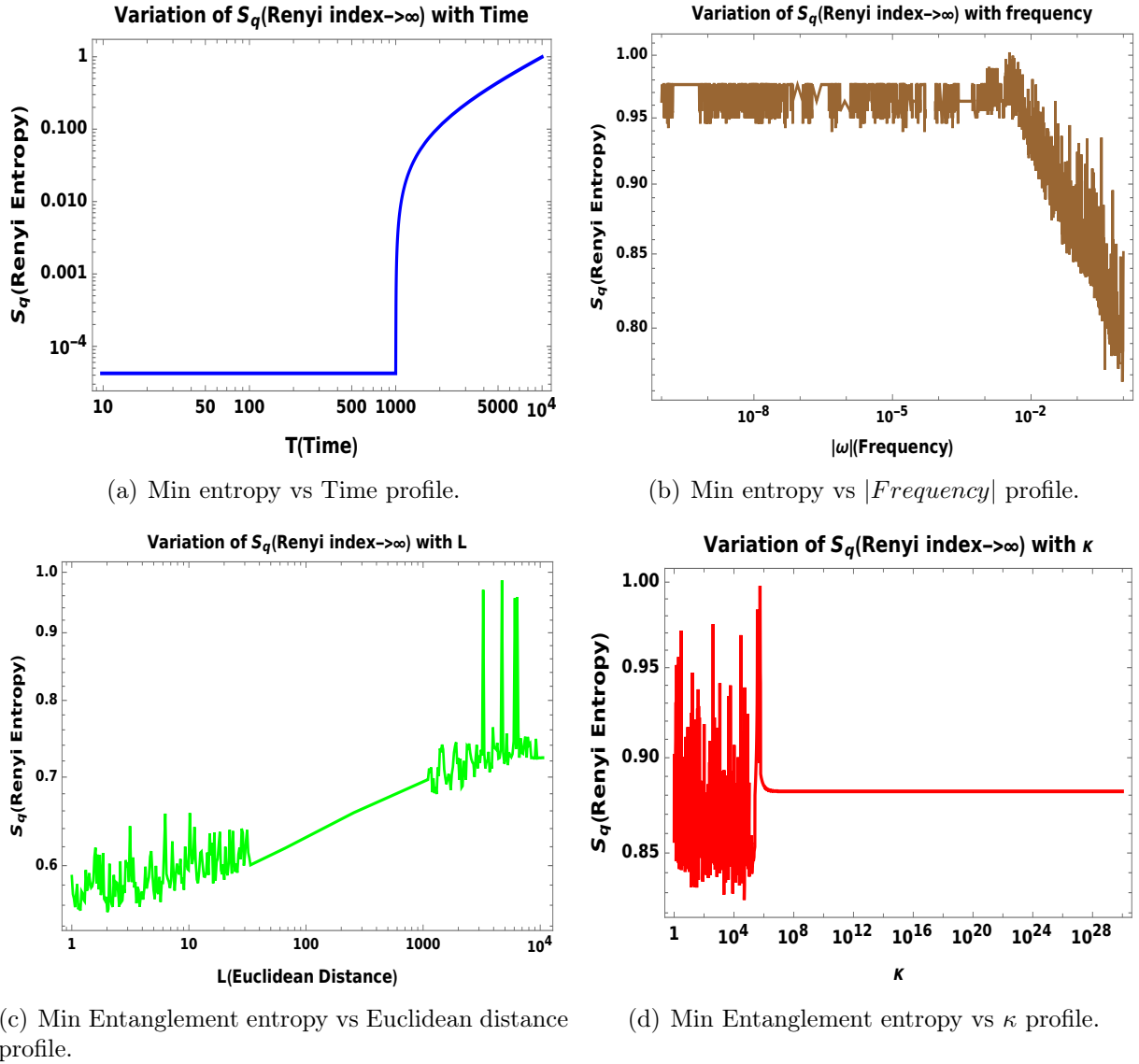


Figure 12. Min entropy variation with various parameters are shown here.

implying reduction in entanglement and when it gets close to ω_0 the value of entropy is almost zero indicating that the joint density matrix of our subsystem becomes separable.

In Fig. 12(c), we have explicitly shown the behaviour of Min Entanglement entropy of our two atomic OQS set up in the static patch of De Sitter space with respect to the Euclidean distance between two atoms L . We have normalized the entropy with the result obtained from $L = 5 \times 10^3$. It is clearly observed that initially there is some fluctuation with increase in entropy for small length scale. But as the distance between the two atoms increases, the subsystem gets entangled to a maximum value.

Further In Fig. 12(d), we have explicitly shown the behaviour of Min Entanglement entropy of our two atomic OQS set up in the static patch of De Sitter space with respect to κ . We have normalized the entropy with the result obtained from $\kappa = 5 \times 10^4$. It is clearly observed that initially there are fluctuations in entropy with increase in κ . With further

increase in κ , the entropy remains negligibly small implying no quantum entanglement.

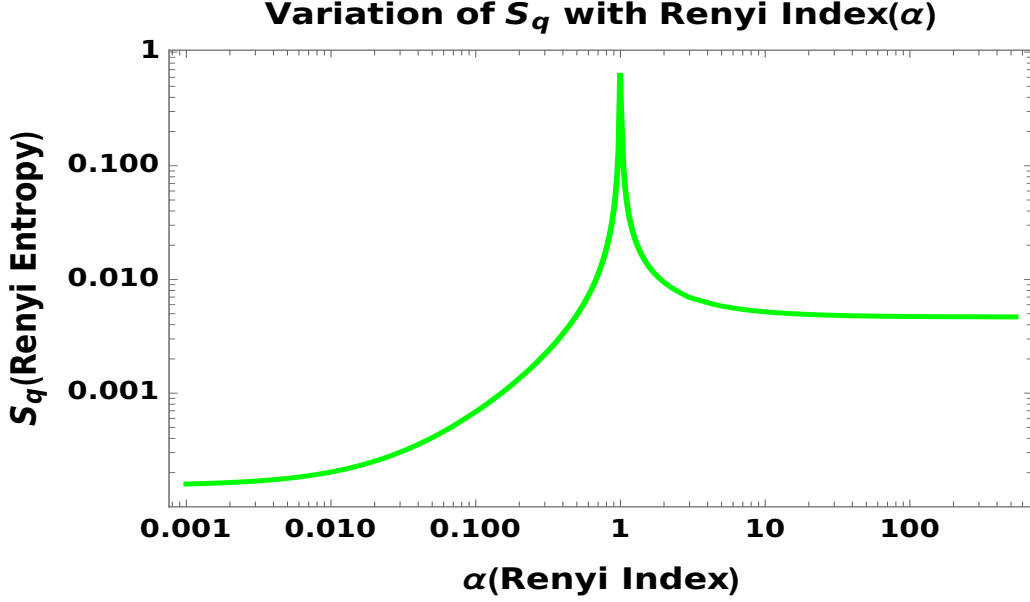


Figure 13. Renyi Entropy variation with Renyi Index is shown here.

11 Logarithmic Negativity

Let us start with *Peres-Horodeski criterion* which is the necessary condition for the joint density matrix of two quantum mechanical system A and B, to be separable. This is sometimes called *Positive Partial Transpose (PPT) criterion*. This is mainly used to decide the separability of mixed states, where *Schmidt decomposition* does not apply. Using this criteria one can define Logarithmic Negativity which is an entanglement measure as:

$$E_N(\rho_{\text{System}}) = \ln \|\rho^{TA}\|, \quad (11.1)$$

where, $\|\rho_A^T\|$ is the trace norm and is defined as:

$$\|\rho_A^T\| = \text{Tr} \left(\sqrt{(\rho_A^T)^\dagger (\rho_A^T)} \right) = \sum_i |\lambda_i| = \sum_{\lambda_i > 0} \lambda_i + \sum_{\lambda_i < 0} |\lambda_i| = 2 \sum_{\lambda_i < 0} |\lambda_i| + 1 = 2N + 1. \quad (11.2)$$

Then the Logarithmic Negativity can be recast as:

$$E_N(\rho_{\text{System}}) = \ln(2N + 1). \quad (11.3)$$

If we fix $N = 0$ then it represents no entanglement in the quantum system. For this non entangled case one can write the system density matrix as:

$$\rho_{\text{System}} = \sum_i \lambda_i \rho_i^A \otimes \rho_i^B = \rho^{TA}, \quad (11.4)$$

where we define the sub system density matrix as:

$$\rho_i^q = |i\rangle_{qq}\langle i| \quad \forall \quad q = A, B \quad \text{with} \quad \lambda_i \geq 0. \quad (11.5)$$

For $N \neq 0$ which represents the non entangled case the system density matrix can be expressed as:

$$\rho_{\text{System}} = \sum_{i,j,k,l} \mathcal{C}_{ijkl} (|i\rangle_{AA}\langle j|) \otimes (|k\rangle_{AA}\langle l|) = \sum_{i,j,k,l} \mathcal{C}_{ijkl} (|j\rangle_{AA}\langle i|) \otimes (|k\rangle_{AA}\langle l|). \quad (11.6)$$

So from this computation if we get negative eigen values for a quantum mechanical system then we can say that the corresponding quantum states are entangled.

11.1 Bloch sphere representation of Logarithmic negativity

In terms of Bloch vectors it can be explicitly shown that the logarithmic negativity can be written as:

$$\begin{aligned} E_N(\rho) = \ln & \left[\frac{17}{100} \left\{ 2 + 2(\gamma^2 - a_{--}a_{++}) + \frac{1}{2}(\eta - \alpha)(4 + \eta - \alpha) + a_{-+}^2 + a_{+-}^2 \right. \right. \\ & \left. \left. - \sqrt{(4 + 5(\eta - \alpha) + (a_{-+} - a_{+-})^2)(4(\gamma^2 - a_{--}a_{++} + (a_{-+} + a_{+-})^2))} \right\}^{1/2} \right. \\ & + \frac{17}{100} \left\{ 2 + 2(\gamma^2 - a_{--}a_{++}) + \frac{1}{2}(\eta - \alpha)(4 + \eta - \alpha) + a_{-+}^2 + a_{+-}^2 \right. \\ & \left. + \sqrt{(4 + 5(\eta - \alpha) + (a_{-+} - a_{+-})^2)(4(\gamma^2 - a_{--}a_{++} + (a_{-+} + a_{+-})^2))} \right\}^{1/2} \\ & + \frac{17}{100} \left\{ 2 + 2(\beta^2 - a_{-+}a_{+-}) + \frac{1}{2}(\eta - \alpha)(-4 + \eta - \alpha) + a_{--}^2 + a_{++}^2 \right. \\ & \left. - \sqrt{(4 + 3(\eta - \alpha) + (a_{--} - a_{++})^2)(4(\beta^2 - a_{-+}a_{+-} + (a_{--} + a_{++})^2))} \right\}^{1/2} \\ & + \frac{17}{100} \left\{ 2 + 2(\beta^2 - a_{-+}a_{+-}) + \frac{1}{2}(\eta - \alpha)(-4 + \eta - \alpha) + a_{--}^2 + a_{++}^2 \right. \\ & \left. + \sqrt{(4 + 3(\eta - \alpha) + (a_{--} - a_{++})^2)(4(\beta^2 - a_{-+}a_{+-} + (a_{--} + a_{++})^2))} \right\}^{1/2} \Big] (11.7) \end{aligned}$$

where the symbols $\alpha, \beta, \gamma, \eta$ have already been defined earlier.

11.2 Logarithmic negativity from OQS of two entangled atoms

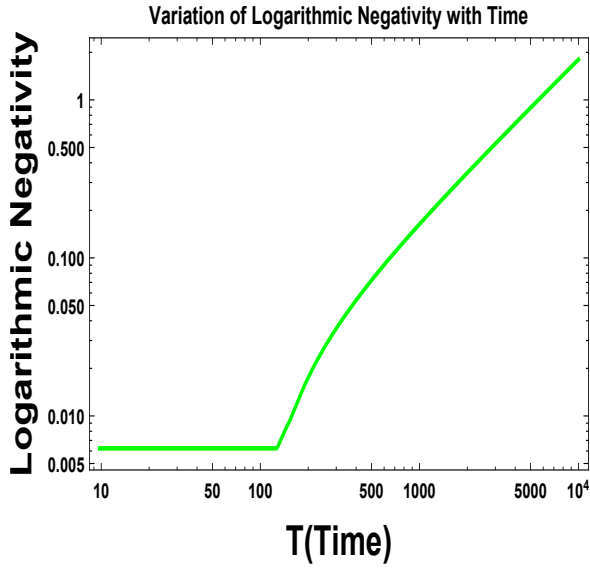
$$\begin{aligned}
E_N(\rho) = \ln & \left[\frac{17}{100} \left\{ 2 + 8a_{03}^2 + a_{33}(4 + 2a_{33}) + a_{-+}^2 + a_{+-}^2 \right. \right. \\
& \left. \left. - \sqrt{(4 + 10a_{33} + (a_{-+} - a_{+-})^2)(16a_{03}^2 + (a_{-+} + a_{+-})^2)} \right\}^{1/2} \right. \\
& + \frac{17}{100} \left\{ 2 + 8^2a_{03} + a_{33}(4 + 2a_{33}) + a_{-+}^2 + a_{+-}^2 \right. \\
& \left. \left. + \sqrt{(4 + 10a_{33} + (a_{-+} - a_{+-})^2)(16a_{03}^2 + (a_{-+} + a_{+-})^2)} \right\}^{1/2} \right. \\
& + \frac{17}{100} \left\{ 2 + a_{33}(-4 + 2a_{33}) + a_{--}^2 + a_{++}^2 \right. \\
& \left. \left. - \sqrt{(4 + 6a_{33} + (a_{--} - a_{++})^2)((a_{--} + a_{++})^2)} \right\}^{1/2} \right. \\
& + \frac{17}{100} \left\{ 2 + a_{33}(-4 + 2a_{33}) + a_{--}^2 + a_{++}^2 \right. \\
& \left. \left. + \sqrt{(4 + 6a_{33} + (a_{--} - a_{++})^2)(4(\beta^2 - a_{-+}a_{+-} + (a_{--} + a_{++})^2))} \right\}^{1/2} \right] \quad (11.8)
\end{aligned}$$

In Fig. 14(a), we have depicted the behaviour of Logarithmic Negativity of our two atomic OQS set up in the static patch of De Sitter space with respect to the rescaled time T . We have normalized the plot with the result obtained from $T = 10^4$. It is clearly observed that initially the value of logarithmic negativity is almost zero implying that the joint density matrix of our subsystem is separable and hence do not show any signature of quantum entanglement. As time goes on, the sub-system gets more and more entangled and at a very late time scale, it almost saturates to unity and show maximum entanglement.

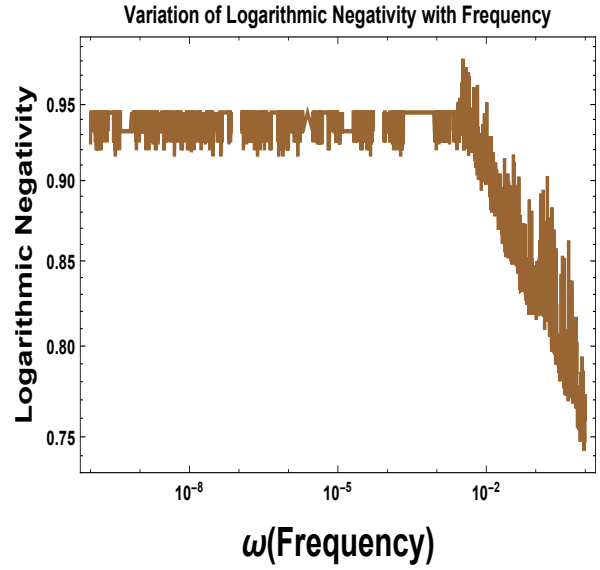
In Fig. 14(b), we have depicted the behaviour of Logarithmic Negativity of our two atomic OQS set up in the static patch of De Sitter space with respect to frequency ω . We have normalized the plot with the result obtained from $\omega = 5 \times 10^{-2}$. It is clearly observed that initially for a finite frequency scale, the value of log negativity is almost constant showing entanglement. As frequency is further increased the value decreases implying reduction in entanglement and when it gets close to ω_0 the value of log negativity is almost zero indicating that the joint density matrix of our subsystem becomes separable.

In Fig. 14(c), we have explicitly shown the behaviour of Logarithmic Negativity of our two atomic OQS set up in the static patch of De Sitter space with respect to the Euclidean distance L . We have normalized the values with the result obtained from $L = 10^4$. It is clearly observed that initially there is some fluctuation with increase in log negativity for small length scale. But as the distance between the two atoms increase, the value almost remains constant and thus the subsystem gets entangled. With further increase in distance, there is no change implying that the quantum entanglement is maximum.

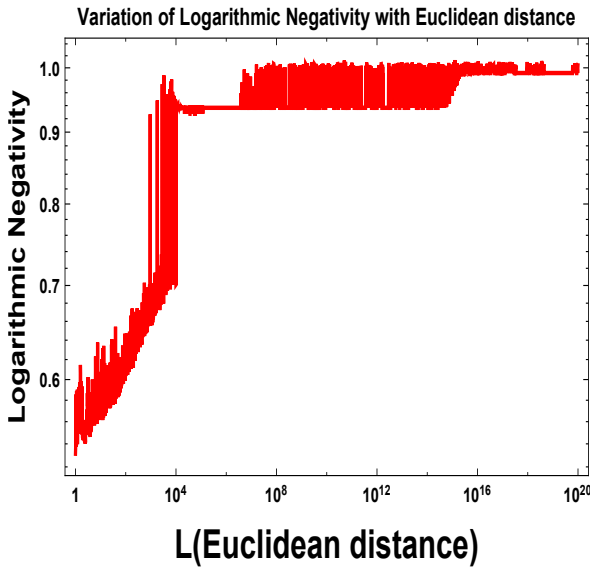
Finally, in Fig. 14(d), we have explicitly shown the behaviour of Logarithmic Negativity of our two atomic OQS set up in the static patch of De Sitter space with respect to the parameter κ . We have normalized the values with the result obtained from $\kappa = 1$. We consider both small and large κ scale limiting situations. It is clearly observed that initially there are fluctuations in log negativity with increase in κ . With further increase in κ , the value remains negligibly small implying no quantum entanglement.



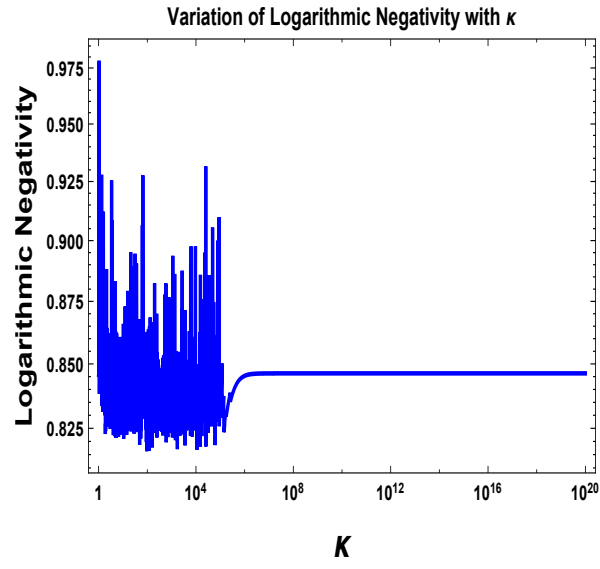
(a) Log Negativity vs Time profile.



(b) Log Negativity vs |Frequency| profile..



(c) Log Negativity vs Euclidean Distance profile.



(d) [Log Negativity vs κ profile.

Figure 14. Log Negativity variation with various parameters are shown here.

12 Entanglement of formation and Concurrence

Both of the measures studied in this section are used to quantify the resources needed to create a given entangled state. Each of them are used as a entanglement measure for bipartite quantum state in quantum information theory. The entanglement of formation for

pure and mixed states takes the following form:

$$E_f(\rho) = \begin{cases} -\text{Tr}(\rho_A \ln \rho_A) = -\text{Tr}(\rho_B \ln \rho_B) & \text{for pure state} \\ \inf \left(\sum_j p_j E_f(\Phi_j) \right) & \text{for mixed state} \end{cases} \quad (12.1)$$

For mixed states the **infimum** is taken over all possible decompositions of the density matrix ρ into pure states. The quantities used in the above equation are defined below:

$$\rho_A = \text{Tr}_B \rho, \quad \rho_B = \text{Tr}_A \rho, \quad \rho_{\text{System}} = |\Phi\rangle\langle\Phi| \quad \text{for pure state} \quad (12.2)$$

$$E_f(\Phi_j) = -\text{Tr}(\Phi_j \ln \Phi_j), \quad \rho_{\text{System}} = \sum_j p_j |\Phi_j\rangle\langle\Phi_j| \quad \text{for mixed state} \quad (12.3)$$

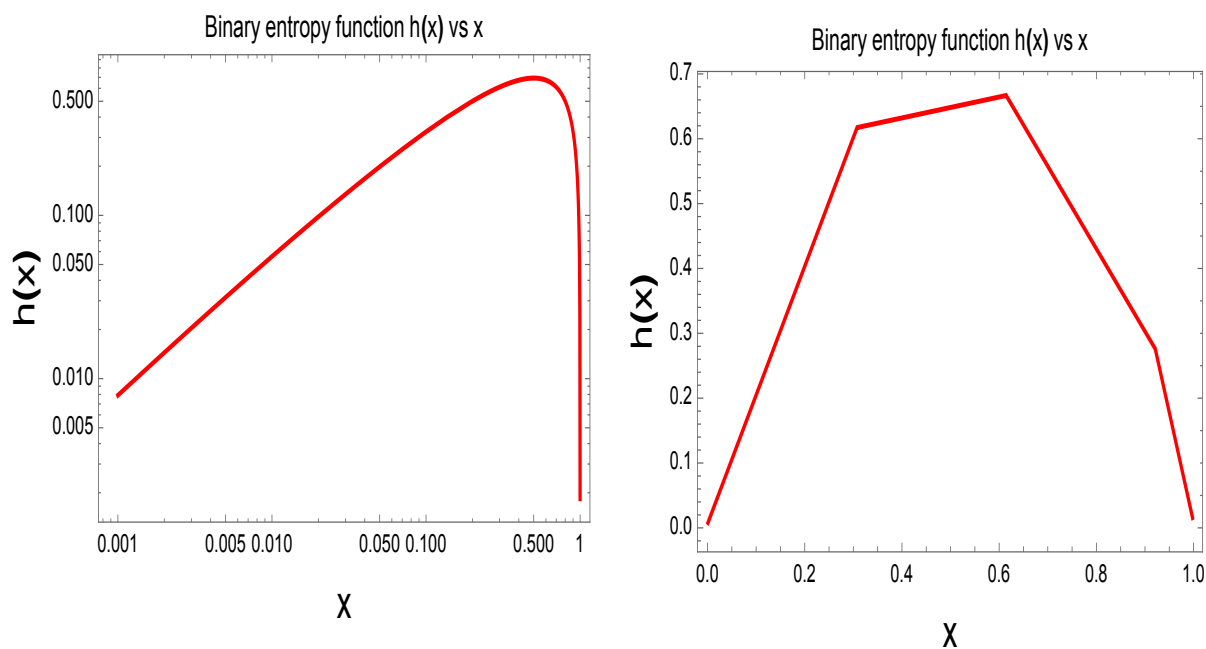
Relation between entanglement of formation and Concurrence can be written as:

$$E_f(\rho_{\text{System}}) = \mathcal{E}(C(\rho_{\text{System}})) = h \left(\frac{1 + \sqrt{1 - C^2(\rho_{\text{System}})}}{2} \right) \quad (12.4)$$

Where $h(x)$ is known as the **Binary Entropy function** which is defined as:

$$h(x) = -x \ln x - (1 - x) \ln(1 - x) \quad (12.5)$$

Concurrence which is also an entanglement measure is studied here in the context of two



(a) Binary entropy function $h(x)$ vs x

(b) Binary entropy function $h(x)$ vs x

Figure 15. Variation of the binary entropy function $h(x)$ with x is shown here.

entangled atoms from the perspective of OQS. For X type states it is defined analytically by the following expression:

$$C(\rho_{\text{System}}) = \max[0, \lambda_1 - \lambda_2 - \lambda_3 - \lambda_4] \quad (12.6)$$

where the λ_i 's are the square roots of the eigenvalues of the matrix:

$$\mathcal{R} \equiv \begin{cases} \sqrt{\sqrt{\rho_{\text{System}}} \tilde{\rho}_{\text{System}} \sqrt{\rho_{\text{System}}}} & \text{for Hermitian} \\ \sqrt{\rho_{\text{System}} \tilde{\rho}_{\text{System}}} & \text{for Non Hermitian} \end{cases} \quad (12.7)$$

where $\tilde{\rho}_{\text{System}}$ is the *spin flip (Werner type) quantum states* [44] given by ⁶:

$$\tilde{\rho}_{\text{System}} = (\sigma_2 \otimes \sigma_2) \rho^* (\sigma_2 \otimes \sigma_2) \quad (12.9)$$

$$= [((\sigma_- - \sigma_+) \otimes (\sigma_- - \sigma_+)) \rho^* ((\sigma_- - \sigma_+) \otimes (\sigma_- - \sigma_+))] \quad (12.10)$$

and ρ_{System}^* in the above expression indicates complex conjugate of ρ_{System} .

The eigenvalues λ 's follow the following sequence:

$$\lambda_1 > \lambda_2 > \lambda_3 > \lambda_4 \quad (12.11)$$

and satisfy the following condition:

$$\lambda_1 - \lambda_2 - \lambda_3 - \lambda_4 > 0 \quad (12.12)$$

12.1 Bloch sphere representation of Concurrence

In terms of Bloch vectors, the eigenvalues ($\lambda_i \forall i=1,4$) of the matrix $\tilde{\rho}$ mentioned in equation 12.9 can be explicitly written as:

$$\lambda_1 = \frac{1}{4} \sqrt{\mathcal{M} - 2\mathcal{N}} \quad (12.13)$$

$$\lambda_2 = \frac{1}{4} \sqrt{\mathcal{M} + 2\mathcal{N}} \quad (12.14)$$

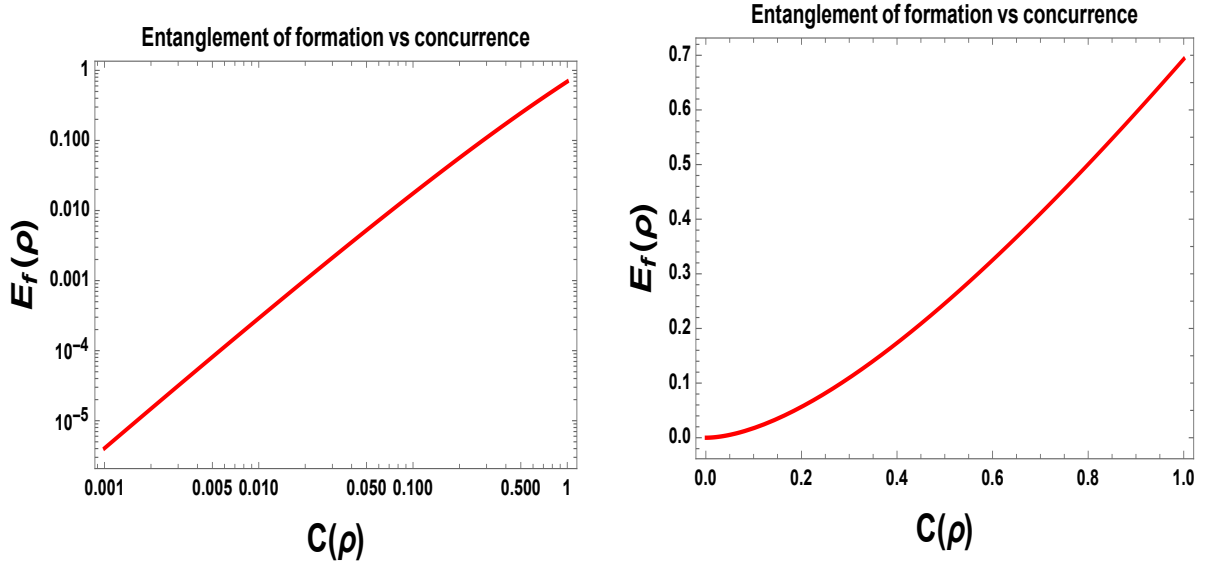
$$\lambda_3 = \frac{1}{4} \sqrt{\mathcal{U} - 2\mathcal{V}} \quad (12.15)$$

$$\lambda_4 = \frac{1}{4} \sqrt{\mathcal{U} + 2\mathcal{V}} \quad (12.16)$$

⁶**Werner State:** A Werner state is a $d \times d$ dimensional bipartite quantum state density matrix that is invariant under all unitary operators of the form $(U \otimes U)$. That is, it is a bipartite quantum state that satisfies the following condition:

$$\rho_{AB} = (U \otimes U) \rho_{AB} (U^\dagger \otimes U^\dagger), \quad (12.8)$$

where for all unitary operators U acting on d -dimensional Hilbert space.



(a) Entanglement of formation vs Concurrence (b) Entanglement of formation vs Concurrence

Figure 16. Relation between the entanglement of formation and concurrence is shown here.

where we define \mathcal{M} , \mathcal{N} , \mathcal{U} and \mathcal{V} as:

$$\mathcal{M} = 1 - a_{03}^2 + 2a_{03}a_{30} - a_{30}^2 - 2a_{33} + a_{33}^2 + a_{-+}a_{+-} \quad (12.17)$$

$$\begin{aligned} \mathcal{N} = a_{-+}a_{+-} - a_{03}^2a_{-+}a_{+-} + 2a_{03}a_{30}a_{-+}a_{+-} - a_{30}^2a_{-+}a_{+-} \\ - 2a_{33}a_{-+}a_{+-} + a_{33}^2a_{-+}a_{+-} \end{aligned} \quad (12.18)$$

$$\mathcal{U} = 1 - a_{03}^2 - 2a_{03}a_{30} - a_{30}^2 + 2a_{33} + a_{33}^2 + a_{--}a_{++} \quad (12.19)$$

$$\begin{aligned} \mathcal{V} = a_{--}a_{++} - a_{03}^2a_{--}a_{++} - 2a_{03}a_{30}a_{--}a_{++} - a_{30}^2a_{--}a_{++} \\ + 2a_{33}a_{--}a_{++} + a_{33}^2a_{--}a_{++} \end{aligned} \quad (12.20)$$

12.2 Concurrence from OQS of two entangled atoms

For the case of two entangled atoms relevant to our system the solutions of the Bloch vector components a_{30} and a_{03} obtained are identical. Thus the eigenvalues λ_1 , λ_2 , λ_3 and λ_4 are given by the following expressions:

$$\lambda_1 = \frac{1}{4}\sqrt{\mathcal{S} - 2\mathcal{F}} \quad (12.21)$$

$$\lambda_2 = \frac{1}{4}\sqrt{\mathcal{S} + 2\mathcal{F}} \quad (12.22)$$

$$\lambda_3 = \frac{1}{4}\sqrt{\mathcal{X} - 2\mathcal{U}} \quad (12.23)$$

$$\lambda_4 = \frac{1}{4}\sqrt{\mathcal{X} + 2\mathcal{U}} \quad (12.24)$$

where we define \mathcal{S} , \mathcal{X} , \mathcal{F} and \mathcal{U} as:

$$\mathcal{S} = 1 - 2a_{33} + a_{33}^2 + a_{-+}a_{+-}, \quad (12.25)$$

$$\mathcal{X} = 1 - 4a_{03}^2 + 2a_{33} + a_{33}^2 + a_{--}a_{++}, \quad (12.26)$$

$$\mathcal{F} = \sqrt{a_{-+}a_{+-} - 2a_{33}a_{-+}a_{+-} + a_{33}^2a_{-+}a_{+-}}, \quad (12.27)$$

$$\mathcal{U} = \sqrt{a_{--}a_{++} - 4a_{03}^2a_{--}a_{++} + 2a_{33}a_{--}a_{++} + a_{33}^2a_{--}a_{++}}. \quad (12.28)$$

Therefore, using equation 12.6 the concurrence for two entangled atoms relevant to our system can be calculated as:

$$C(\rho_{\text{System}}) = \max \left[0, \frac{1}{4} \left(\sqrt{\mathcal{S} - 2\mathcal{F}} - \sqrt{\mathcal{S} + 2\mathcal{F}} - \sqrt{\mathcal{X} - 2\mathcal{U}} - \sqrt{\mathcal{X} + 2\mathcal{U}} \right) \right]. \quad (12.29)$$

In Fig. 17(a), we have explicitly shown the behaviour of Concurrence of our two atomic OQS set up in the static patch of De Sitter space with respect to rescaled time scale T . We have normalized the plot with the result obtained from $T = 10000$. It is clearly observed that initially the value of concurrence is almost zero implying that the joint density matrix our two atomic OQS set up is separable and shows no signature of quantum entanglement. As time goes on, the sub-system gets more and more entangled and at a late time scale, it almost saturates to unity which is obviously the maximum normalized value of the corresponding entangled measure.

In Fig. 17(b), we have plotted the behaviour of Concurrence of our two atomic OQS set up in the static patch of De Sitter space with respect to the frequency scale ω . We have normalized the values with the result obtained from $\omega = 5 \times 10^{-2}$. It is clearly observed that initially for a finite frequency scale, the value of concurrence is almost constant showing the signature of quantum entanglement. As frequency is further increased the value decreases implying reduction in the amount of quantum entanglement and when it gets close to ω_0 the value of concurrence is almost 0 indicating that the joint density matrix of our subsystem becomes separable.

In Fig. 17(c), we have plotted the behaviour of Concurrence of our two atomic OQS set up in the static patch of De Sitter space with respect to the Euclidean distance scale L . We have normalized the values with the result obtained from $L = 10^4$. It is clearly observed that initially there is some fluctuation with increase in concurrence for small length scale L . But as the Euclidean distance between the two atoms increase, the subsystem gets quantum mechanically entangled. With further increase in the Euclidean distance, there is no change in value implying that the entanglement between the atoms in our OQS set up is maximum.

Finally, in Fig.17(d), we have depicted the behaviour of Concurrence of our two atomic OQS set up in the static patch of De Sitter space with respect to the parameter κ which is basically proportional to the inverse of the curvature of the background space time. We have normalized the values with the result obtained from $\kappa = 1$. It is clearly observed that initially there are fluctuations in concurrence with increase in κ . With further increase in κ , the value remains constant implying approximately zero quantum entanglement.

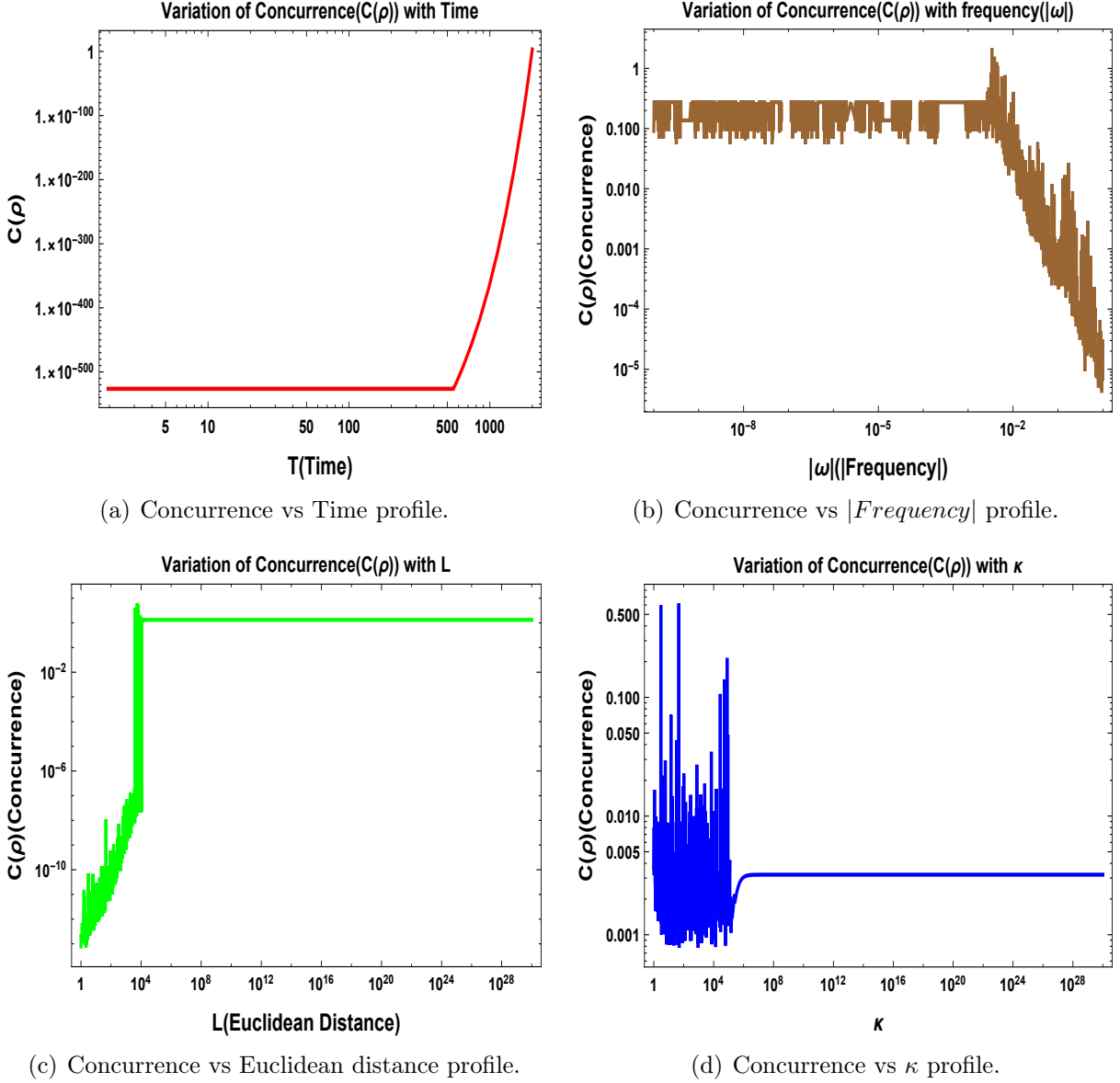


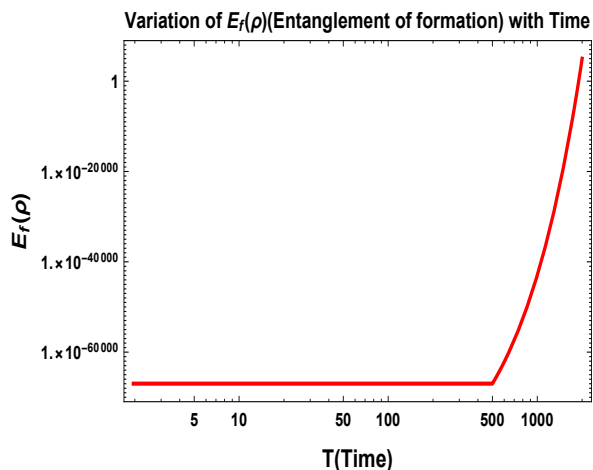
Figure 17. Variation of Concurrence with various parameters is shown here.

12.3 Entanglement of formation from OQS of two entangled atoms

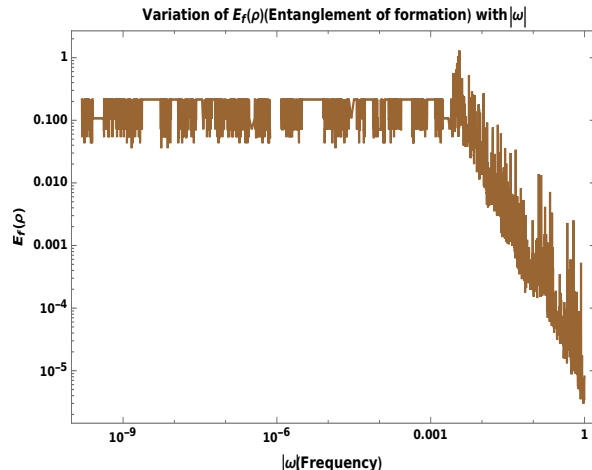
The explicit expression for the entanglement of formation in the context of two entangled atoms relevant to our system the entanglement of formation is given by the following expression:

$$\begin{aligned}
 E_f(\rho) = & \frac{1}{2} \left(-1 - \sqrt{1 - (C(\rho))^2} \right) \log \left[\frac{1}{2} \left(1 + \sqrt{1 - C(\rho)} \right) \right] \\
 & - \left(1 + \frac{1}{2} \left(-1 - \sqrt{1 - C(\rho)} \right) \right) \log \left[1 + \frac{1}{2} \left(-1 - \sqrt{1 - C(\rho)} \right) \right] \quad (12.30)
 \end{aligned}$$

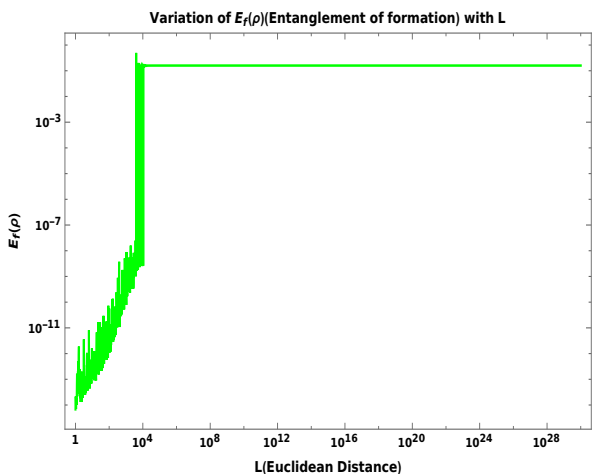
The following section shows various plots of entanglement of formation calculated from concurrence from our model.



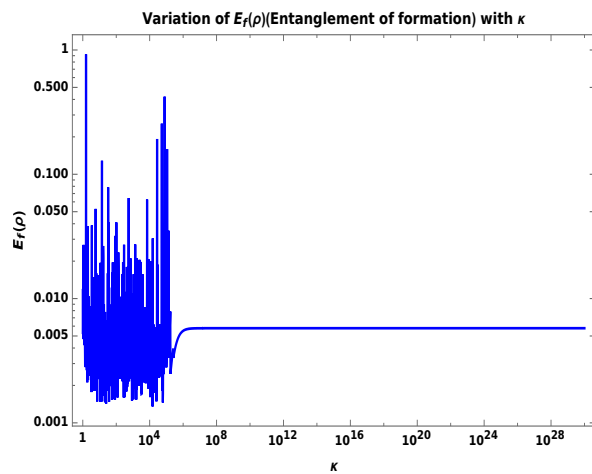
(a) Entanglement of formation vs Time profile.



(b) Entanglement of formation vs $|Frequency|$ profile.



(c) Entanglement of formation vs vs Euclidean distance profile.



(d) Entanglement of formation vs κ profile.

Figure 18. Variation of Entanglement of formation with various parameters is shown here.

In Fig. 18(a), we have explicitly shown the behaviour of Entanglement of formation of our two atomic OQS set up in the static patch of De Sitter space with respect to the time scale T , which we have defined earlier. We have normalized the values with the result obtained from $T = 10000$. It is clearly observed that initially the value of entanglement of formation is almost zero implying that our two atomic OQS set up do not show any signature of quantum entanglement at initial time scale. As time goes on, the sub-system gets more and more entangled and at a late time scale, it almost saturates to unity.

In Fig. 18(b), we have plotted the behaviour of Entanglement of formation of our two atomic OQS set up in the static patch of De Sitter space with respect to the frequency ω . We have normalized the values with the result obtained from $\omega = 5 \times 10^{-2}$. It is clearly observed that initially for a finite frequency scale, the value of entanglement of formation is almost constant. As frequency is further increased the value decreases implying reduction in entanglement and when it gets close to ω_0 the value of entanglement of formation is almost

zero indicating that the joint density matrix of our subsystem becomes separable.

In Fig. 18(c), we have plotted the behaviour of Entanglement of formation of our two atomic OQS set up in the static patch of De Sitter space with respect to the Euclidean distance L . We have normalized the plot with the result obtained from $L = 10^4$ to explore the underlying physics. It is clearly observed that initially there is some fluctuation with increase in entanglement of formation for small length scale. But as the distance between the two atoms increase, the subsystem gets entangled to a maximum value. With further increase in distance, there is no change in the value implying that the quantum correlation between the atoms in our OQS set up is non-local due to the existence of non-zero entanglement.

Finally in Fig. 18(d), we have explicitly shown the behaviour of Entanglement of formation of our two atomic OQS set up in the static patch De Sitter space with respect to parameter κ which is inversely proportional to the curvature of the background space time. We have normalized the plot with the result obtained from $\kappa = 1$. It is clearly observed that initially there are fluctuations in entanglement of formation with increase in κ . With further increase in κ , the value remains constant with very small value implying negligibly small quantum correlation.

13 Quantum Discord

It is a measure of non classical correlations between two subsystems of a quantum system. It includes correlations that are due to quantum physical effects, but do not necessarily involve the concept of quantum entanglement. Sometimes it is also identified as measure of quantumness of correlation functions. If the two quantum states are separable then it does not imply the quantum correlations. It is defined as

$$\mathcal{D}_A(\rho_{\mathbf{System}}) = \mathcal{I}(\rho_{\mathbf{System}}) - \mathbf{max}_{\Pi_j^A} \mathcal{T}_{\Pi_j^A}(\rho_{\mathbf{System}}) \quad (13.1)$$

where mutual information $\mathcal{I}(\rho_{\mathbf{System}})$ is defined as:

$$\mathcal{I}(\rho_{\mathbf{System}}) = S(\rho_A) + S(\rho_B) - S(\rho_{\mathbf{System}}), \quad (13.2)$$

where $S(\rho_A)$, $S(\rho_B)$ and $S(\rho_{\mathbf{System}})$ represent the Von Neumann entropy of system A (**Atom 1**), B (**Atom 2**) and the combined system respectively.

On the other hand, the part of the correlation that can be attributed to the classical correlation, which is represented by, $\Pi_j^A \mathcal{T}_{\Pi_j^A}(\rho_{\mathbf{System}})$, is defined as:

$$\Pi_j^A \mathcal{T}_{\Pi_j^A}(\rho_{\mathbf{System}}) = S(\rho_B) - \Pi_j^A S(\rho_B | \Pi_j^A) \quad (13.3)$$

Now we know that for any two qubit state the density matrix is given by the following expression:

$$\rho = \frac{1}{4} \left(I^a \otimes I^b + \sum_{i=1}^3 (a_i \sigma_i \otimes I^b + I^a \otimes b_i \sigma_i) + \sum_{i,j=1}^3 T_{ij} \sigma_i \otimes \sigma_j \right). \quad (13.4)$$

Then the geometric measure of quantum discord is evaluated as:

$$\mathcal{D}(\rho) = \frac{1}{4} (\|a\|^2 + \|T\|^2 - \lambda_{max}) \quad (13.5)$$

where a is the column vector, which is defined as:

$$a = (a_1 + a_2 + a_3)^t. \quad (13.6)$$

Also, the trace norm square is defined as:

$$\|a\|^2 = \sum_i a_i^2. \quad (13.7)$$

Here $T = (t_{ij})$ is a matrix which one can compute for a specific quantum system and λ_{max} is the largest eigenvalue of the matrix $(aa^t + TT^t)$. Here the superscript t denotes the transpose of the vectors or matrices.

13.1 Bloch sphere representation of Quantum Discord

The matrix T relevant to our system is given by:

$$T = \begin{pmatrix} a_{++} & a_{+-} & 0 \\ a_{-+} & a_{--} & 0 \\ 0 & 0 & a_{33} \end{pmatrix} \quad (13.8)$$

whereas the column vector a is given by:

$$a = \begin{pmatrix} 0 \\ 0 \\ a_{30} \end{pmatrix} \quad (13.9)$$

The norm of any matrix T is given by:

$$\|M\| = \sqrt{\text{Tr}(M^\dagger M)} \quad (13.10)$$

Using the above definition, the square of the norm of the matrix T and the column vector a relevant to the system studied is given by:

$$\|T\|^2 = a_{33}^2 + a_{--}^2 + a_{-+}^2 + a_{+-}^2 + a_{++}^2 \quad (13.11)$$

$$\|a\|^2 = a_{30}^2. \quad (13.12)$$

The matrix $(aa^t + TT^t)$ for our case is given by:

$$T = \begin{pmatrix} a_{+-}^2 + a_{++}^2 & a_{--}a_{+-} + a_{-+} + a_{++} & 0 \\ a_{--}a_{+-} + a_{-+} + a_{++} & a_{--}^2 + a_{-+}^2 & 0 \\ 0 & 0 & a_{33}^2 + a_{30}^2 \end{pmatrix} \quad (13.13)$$

whose eigenvalues can be evaluated as

$$\lambda_1 = a_{33}^2 + a_{03}^2 \quad (13.14)$$

$$\lambda_2 = \frac{1}{2}(\mathcal{P} - \mathcal{Q}) \quad (13.15)$$

$$\lambda_3 = \frac{1}{2}(\mathcal{P} + \mathcal{Q}) \quad (13.16)$$

where \mathcal{P} and \mathcal{Q} is defined as:

$$\mathcal{P} = a_{--}^2 + a_{-+}^2 + a_{+-}^2 + a_{++}^2, \quad (13.17)$$

$$\mathcal{Q} = \sqrt{(-a_{--}^2 - a_{-+}^2 - a_{+-}^2 - a_{++}^2)^2 - 4(a_{-+}^2 a_{+-}^2 - 2a_{--} a_{-+} a_{+-} a_{++} + a_{--}^2 a_{++}^2)}. \quad (13.18)$$

13.2 Quantum Discord from OQS of two entangled atoms

It has already been mentioned in the earlier sections that the solution of the Bloch vector components a_{30} and a_{03} are identical.

Thus the quantum discord for the two entangled atoms relevant to our system calculated using equation 13.5 is therefore given by the following expression:

$$\mathcal{D}(\rho) = \frac{1}{4} [a_{03}^2 + a_{33}^2 + \mathcal{Q}] - \max \left[a_{03}^2 + a_{33}^2, \frac{1}{2}(\mathcal{Q} - \sqrt{\mathcal{Q}^2 - 4\mathcal{W}}), \frac{1}{2}(\mathcal{Q} + \sqrt{\mathcal{Q}^2 - 4\mathcal{W}}) \right] \quad (13.19)$$

where the symbols \mathcal{Q} and \mathcal{W} are defined by the following expressions:

$$\mathcal{Q} = a_{--}^2 + a_{-+}^2 + a_{+-}^2 + a_{++}^2 \quad (13.20)$$

$$\mathcal{W} = a_{-+}^2 a_{+-}^2 - 2a_{--} a_{-+} a_{+-} a_{++} + a_{--}^2 a_{++}^2. \quad (13.21)$$

For a given set of parameters the maximum eigenvalue is calculated and the following set of plots is obtained by varying various parameters appearing in our model.

In Fig. 19(a), we have explicitly shown the behaviour of quantum discord of our two atomic OQS set up in static patch of De Sitter space with respect to rescaled time T . We have normalized the values with the result obtained from $T = 10000$ for properly interpret the obtained result from our model. We consider both small and large time scale limiting situations in this context. It is clearly observed that initially the value of quantum discord is almost zero implying that our two atomic OQS set up do not show any signature of quantum correlations at initial time scale. As time goes on, the sub-system gets more and more quantum mechanically correlated and at a very late time scale, it almost saturates to unity, which implies the maximum measure one can obtain from our model to get quantum correlation. Now as we have passed the test for Von Neumann entropy for our model i.e. that this measure is non-zero then one can surely say that non-zero value of quantum discord and Von Neumann entropy together imply the existence of quantum entanglement in the context of our present model of discussion.

In Fig. 19(b), we have explicitly shown the behaviour of quantum discord of our two atomic OQS set up in static patch of De Sitter space with respect to frequency ω by keeping all other parameters of the model are fixed. We have normalized the values with the result obtained from $\omega = 5 \times 10^{-2}$ to physically interpret the obtained result from this model more

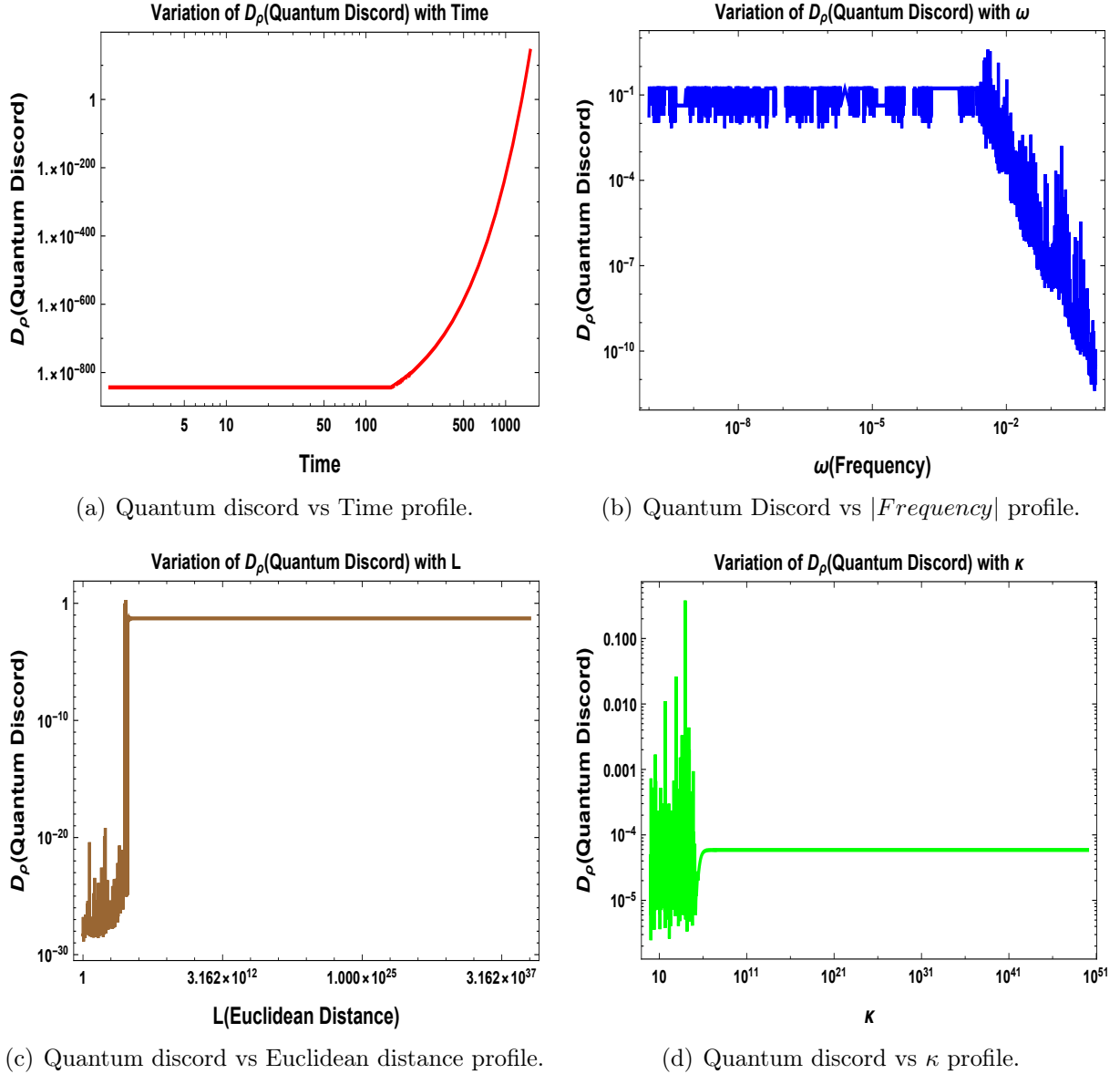


Figure 19. Variation of the geometric measure of Quantum discord with various parameters is shown here.

correctly and comprehensive manner. For better understanding the underlying physics we consider both small and large frequency scale limiting situations. It is clearly observed that initially for a finite frequency scale, the value of quantum discord is almost constant showing maximum measure of quantum correlations obtained from quantum discord. From this figure it is easily observed that, as frequency is further increased the obtained measure of quantum discord decreases for our system implying reduction in quantum correlations and when it gets close to ω_0 the value of quantum discord is almost approximately zero indicating no quantum correlation in our system.

In Fig. 19(c), we have shown the behaviour of quantum discord of our two atomic OQS set up in the static patch of De Sitter space with respect to the Euclidean distance L . Again

like previous plots we have normalized the values with the result obtained from $L = 10^4$ to explain the underlying physics from this system. We consider both small and large length scale limiting situations. It is clearly observed that initially there is some fluctuation with increase in quantum discord for small length scale. But as the Euclidean distance between the two atoms increase, the subsystem becomes quantum correlated to a maximum saturated value. With further increase in Euclidean distance between the two atoms, there is no change in value implying that the quantum correlation between the atoms in our OQS set up is reaches its maximum value.

Last but not the least, in Fig. 19(d), we have shown the behaviour of quantum discord of our two atomic OQS set up in the static patch of De Sitter space with respect to the parameter κ , which is basically proportional to the curvature scalar or the Ricci scalar of the static patch of De Sitter space. Like previous plots here also we have normalized the obtained value of quantum discord with the result obtained from $\kappa = 10^4$. Similarly like previously mentioned all the plots we consider both small and large values of the κ scale limiting situations to interpret the obtained result from our OQS set up . It is clearly observed that initially there are fluctuations in quantum spectrum discord with increase in the parameter κ . With further increase in the value of κ , the value remains constant implying no change in quantum correlations which reaches its accessible stable very small value. This further implies that the effect of quantum correlation is extremely small for the large value of the parameter κ .

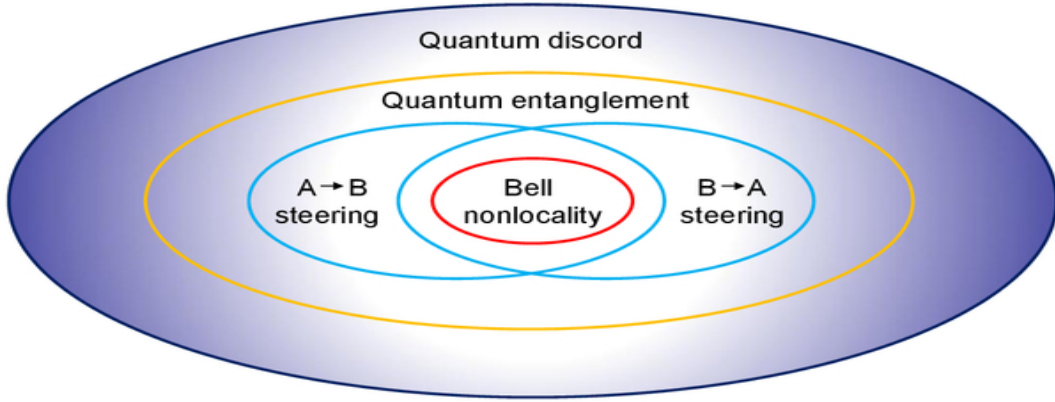
14 Non Locality from Bell CHSH inequality in De Sitter space

14.1 Non-locality in Quantum Mechanics

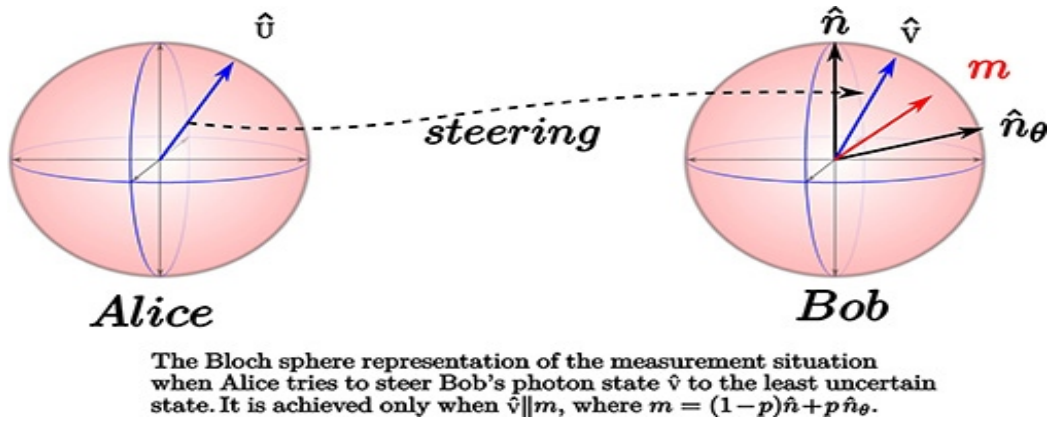
In this section, we describe the concept of non-locality which has wide applications in the context of Quantum Mechanics. A physical theory is said to be non-local if observers can produce instantaneous effects over systems which are far from each other. Non-local theories depend on two basic effects: local uncertainty relations and steering of physical states at a distance. In quantum mechanics, the former one dominates the other in a well-known class of non-local games known as XOR games. In fig.(20(a)) and fig. (20(b)), we have depicted the schematic process of the non-locality and steering and presented both of them as very special aspects of quantum mechanics compared to the quantum entanglement and quantum discord.

In particular, optimal quantum strategies for XOR games are completely determined by the uncertainty principle alone. This breakthrough result has yielded the fundamental open question whether optimal quantum strategies are always restricted by local uncertainty principles, with entanglement-based steering playing no role. In ref. [45–49], the authors provide a negative answer to the question, showing that both steering and uncertainty relations play a fundamental role in determining optimal quantum strategies for non-local games. This particular theoretical findings are confirmed by an experimental implementation with entangled photons.

Quantum non-locality, precisely the lack of a local realistic description of nature, can be understood as the advantage that a set of parties have when executing common tasks (Bell's Inequalities) and using resources from quantum mechanics instead of classical mechanics. It has been recently proven that the optimal strategies for any non-local task are a consequence



(a) Schematic diagram showing Bell's non-locality compared to quantum entanglement and quantum discord.



(b) Bloch sphere representation of steering process from Alice to Bob.

Figure 20. Schematic diagram representing Bell's CHSH non-locality in the static patch of De Sitter space with Open Quantum System.

of two effects: the ability of parties to steer quantum states at a distance and the strength of local uncertainty relations. Quite surprisingly, the complete dominance of the uncertainty relation in determining the optimal strategy has been observed for a large class of non-local tasks.

Also in ref. [45–49] the authors have addressed a fundamental question whether the

two foundational pillars of quantum mechanics, namely its non-local correlations and local uncertainty principle, are always in such inextricable quantitative correspondence with each other. This work particularly provide - both theoretically and experimentally - an answer to this very significant question. Here explicitly a non-local task is shown, for which the full dominance of the uncertainty relation in determining the optimal quantum strategy would lead to the violation of the Einstein rule of no superluminal signaling. It has been proved that this task has the so called self-testing property (a unique quantum state and measurements up to unitaries are necessary for its optimal violation) which allows us to test the claim experimentally. The corresponding quantum optical experiment performed using entangled quantum photons rules out the uncertainty relation supremacy in determining the optimal quantum strategy for the task.

The respective discussions regarding non-locality in Quantum Mechanics are appended below point-wise:

1. Non-locality provides a description of the apparent ability of objects to instantaneously know about each other's state, even when separated by large distances (potentially even billions of light years), almost as if the universe at large instantaneously arranges its particles in anticipation of future events.
2. Non-locality suggests that the universe is in fact profoundly different from our habitual understanding of it, and that the "separate" parts of the universe are actually potentially connected in an intimate and immediate way. In fact, Einstein was so upset by the conclusions on non-locality at one point that he declared that the whole of quantum theory must be wrong, and he never accepted the idea of non-locality up till his dying day.
3. Quantum non-locality is often portrayed as being equivalent to entanglement. Though for a pure bipartite quantum state to produce non local correlations entanglement is necessary, the existence of some entangled (mixed) states, which do not produce such correlations and some non-entangled (namely, separable) states that do produce some type of non-local behavior, can be shown. For the former, a well-known example is constituted by a subset of Werner states that are entangled but whose correlations can always be described using local hidden variables. On the other hand, reasonably simple examples of Bell inequalities have been found for which the quantum state giving the largest violation is never a maximally entangled state, showing that entanglement is, in some sense, not even proportional to non-locality.
4. In short, entanglement of a two-party state is necessary but not sufficient for that state to be nonlocal. It is important to recognise that entanglement is more commonly viewed as an algebraic concept, noted for being a precedent to nonlocality as well as quantum teleportation and superdense coding, whereas nonlocality is interpreted according to experimental statistics and is much more involved with the foundations and interpretations of quantum mechanics.

14.2 Bell's CHSH inequality violation in De-Sitter Space

To establish the concept of non-locality in De Sitter space let us start with a quantum mechanical Bell CHSH operator, which can be defined in the following form:

$$\mathcal{B}_{\text{CHSH}} = [(\mathbf{a} \cdot \sigma) \otimes \{(\mathbf{b} + \mathbf{b}') \cdot \sigma\} + (\mathbf{a}' \cdot \sigma) \otimes \{(\mathbf{b} - \mathbf{b}') \cdot \sigma\}] \quad (14.1)$$

where \mathbf{a} , \mathbf{b} , \mathbf{a}' and \mathbf{b}' are real unit vectors which play significant role to establish non-locality in the present context.

Now the Bell CHSH inequality states that ⁷

$$|\langle B_{\text{CHSH}} \rangle| \leq 2 \quad (14.2)$$

To establish the non-locality we necessarily have to violate CHSH inequality in De Sitter, which is of course not a trivial task to do. The main problem in De Sitter space to generate the effect of long range quantum correlation at late time scale from a non-local Bell's inequality violating set up. However, in ref. [45–49] we and other authors have explicitly shown that in case of axion one can construct such a Bell's inequality violating set up, where the axion effective potential is generated from string theory. In the present set up instead of choosing axion as a Bell's inequality violating candidate to establish non-locality in quantum mechanics we establish this in a more general and model independent way. We use the density matrix formalism from quantum statistical mechanics where the general density matrix for a quantum system can be parametrized as:

$$\rho = \frac{1}{4} \left[I \otimes I + \mathbf{a} \cdot \sigma \otimes I + I \otimes \mathbf{b} \cdot \sigma + \sum_{j,k=1}^3 c_{jk} \sigma_j \otimes \sigma_k \right] \quad (14.3)$$

where \mathbf{a} , \mathbf{b} and c_{jk} all are in general time dependent quantities which can be explicitly obtained by solving the GSKL master equation in presence of the *effective Hamiltonian* and the quantum dissipator *Lindbladian* operator. Here, the vectors \mathbf{a} and \mathbf{b} are given by the following general representation in terms of the elements of the density matrix:

$$\mathbf{a} = (0, 0, \rho_{11} + \rho_{22} - \rho_{33} - \rho_{44}) \quad (14.4)$$

$$\mathbf{b} = (0, 0, \rho_{11} + \rho_{33} - \rho_{22} - \rho_{44}) \quad (14.5)$$

and the c_{jk} matrix takes the form

$$c_{jk} = \frac{1}{4} \begin{pmatrix} 2\rho_{23} - 2(\rho_{14}) & 2(\rho_{14})_I & 0 \\ 2(\rho_{14})_I & 2\rho_{23} - 2(\rho_{14}) & 0 \\ 0 & 0 & \rho_{11} + \rho_{44} - \rho_{22} - \rho_{33} \end{pmatrix} \quad (14.6)$$

In the context of OQS described by the two entangled atoms the vectors \mathbf{a} and \mathbf{b} are given by following simplified form:

$$\mathbf{a} = (0, 0, a_{30}) \quad (14.7)$$

$$\mathbf{b} = (0, 0, a_{03}), \quad (14.8)$$

⁷For local hidden variable (LHV) description of correlation CHSH inequality holds. Violation of CHSH inequality indicates existence of non-locality.

and the coefficient matrix c_{jk} can be written as:

$$c_{jk} = \frac{1}{4} \begin{pmatrix} 2a_{+-} - a_{++} - a_{--} & i(a_{--} - a_{++}) & 0 \\ i(a_{--} - a_{++}) & 2a_{+-} + a_{++} + a_{--} & 0 \\ 0 & 0 & a_{33} \end{pmatrix} \quad (14.9)$$

Now, Bell CHSH inequality is violated in OQS if and only if when the sum of the two largest eigenvalues of the following matrix satisfy the following constraint condition:

$$c c^\dagger > 1 \quad (14.10)$$

where the eigenvalues are:

$$\lambda_1 = 4 \left(\rho_{11} + \rho_{44} - \frac{1}{2} \right)^2 = a_{33}^2 \quad (14.11)$$

$$\lambda_{2,3} = 4(|\rho_{14}| \pm \rho_{23})^2 = \frac{1}{4}(|a_{--}| \pm a_{+-})^2 \quad (14.12)$$

For the initial separable state $\rho_0 = |00\rangle\langle 00|$, we cannot expect these eigenvalues to exceed unity after evolution because only non-zero component of the initial state is $\rho_{44} = 1$. However, the Bell CHSH inequality provides only a necessary condition for the LHV(local hidden variable)description and does not guarantee existence of a LHV. For this reason we need to pass each detector through a local filter, which transforms the matrix c and ρ in the following form.

$$c' = (f_A \otimes f_B) c (f_A \otimes f_B) \quad (14.13)$$

$$\rho' = (f_A \otimes f_B) \rho (f_A \otimes f_B) \quad (14.14)$$

where the two local filters f_A and f_B are described by the following square matrix:

$$f_A = f_B = \begin{pmatrix} 1 & 0 \\ 0 & \eta \end{pmatrix} \quad (14.15)$$

acts as the local filter. The matrices ρ' and c' can be represented as

$$\rho' = \frac{1}{\rho_{11} + \eta^2(\rho_{22} + \rho_{33}) + \eta^4\rho_{44}} \begin{pmatrix} \rho_{11} & 0 & 0 & \eta^2\rho_{14} \\ 0 & \eta^2\rho_{22} & \eta^2\rho_{22} & 0 \\ 0 & \eta^2\rho_{23} & \eta^2\rho_{33} & 0 \\ \eta^2\rho_{14}^* & 0 & 0 & \eta^4\rho_{44} \end{pmatrix}, \quad (14.16)$$

$$c' = \frac{2\eta^2}{\rho_{11} + \eta^2(\rho_{22} + \rho_{33}) + \eta^4\rho_{44}} \begin{pmatrix} \rho_{23} - (\rho_{14})_R & (\rho_{14})_R & 0 \\ (\rho_{14})_R & \rho_{23} + (\rho_{14})_R & 0 \\ 0 & 0 & \frac{\rho_{11} - \eta^2(\rho_{22} + \rho_{33}) + \eta^4\rho_{44}}{2\eta^2} \end{pmatrix}. \quad (14.17)$$

The eigenvalues of the new matrix $c'(c')^\dagger$ are appended below:

$$\begin{aligned} \lambda'_1 &= \frac{\rho_{11} - \eta^2(\rho_{22} + \rho_{33}) + \eta^4\rho_{44}}{\rho_{11} + \eta^2(\rho_{22} + \rho_{33}) + \eta^4\rho_{44}} \\ &= \frac{(1 - 2\eta^2) + (1 - \eta^4)(a_{03} + a_{30}) + (1 + \eta^2)^2}{(1 + 2\eta^2) + (1 - \eta^4)(a_{03} + a_{30}) + (1 - \eta^2)^2}, \end{aligned} \quad (14.18)$$

$$\begin{aligned} \lambda'_{2,3} &= \frac{2\eta^2(\rho_{23} \pm |\rho_{14}|)}{\rho_{11} + \eta^2(\rho_{22} + \rho_{33}) + \eta^4\rho_{44}} \\ &= \frac{2\eta^2(a_{+-} + |a_{--}|)}{(1 + 2\eta^2) + (1 - \eta^4)(a_{03} + a_{30}) + (1 - \eta^2)^2}. \end{aligned} \quad (14.19)$$

In Fig. 21(a), we have explicitly shown the behaviour of the two functions appearing in either sides of Bell Inequality of our two atomic OQS setup in de Sitter space with respect to T(Time). We have normalized the values with the result obtained from $T = 10^3$. We consider both small and large time scale limiting situations. It is clearly observed that for all values of T(time) scale, if we restrict the other parameters of the theory within a fixed range then always we achieve that the function represented by green colour is always greater than that of red colour. This establishes Bell-CHSH inequality violation and non-locality in De Sitter space with the present two atomic open quantum set up.

In Fig. 21(b), we have explicitly shown the behaviour of the two functions appearing in either sides of Bell Inequality of our two atomic OQS setup in de Sitter space with respect to $|\omega|$ (Frequency). We have normalized the values with the result obtained from $|\omega| = 5 \times 10^{-2}$. We consider both small and large frequency scale limiting situations. It is clearly observed that for all values of $|\omega|$ (Frequency), if we restrict the other parameters of the theory within a fixed range then always we achieve that the function represented by green colour is always greater than that of red colour. This establishes Bell-CHSH inequality violation and non-locality in De Sitter space with the present two atomic open quantum set up.

In Fig. 21(c), we have explicitly shown the behaviour of the two functions appearing in either sides of Bell Inequality of our two atomic OQS setup in de Sitter space with respect to L(Euclidean Distance). We have normalized the values with the result obtained from $L = 10^1$. We consider both small and large length scale limiting situations. It is clearly observed that for all values of L(Euclidean Distance), if we restrict the other parameters of the theory within a fixed range then always we achieve that the function represented by green colour is always greater than that of red colour. This establishes Bell-CHSH inequality violation and non-locality in De Sitter space with the present two atomic open quantum set up.

In Fig. 21(d), we have explicitly shown the behaviour of the two functions appearing in either sides of Bell Inequality of our two atomic OQS setup in de Sitter space with respect

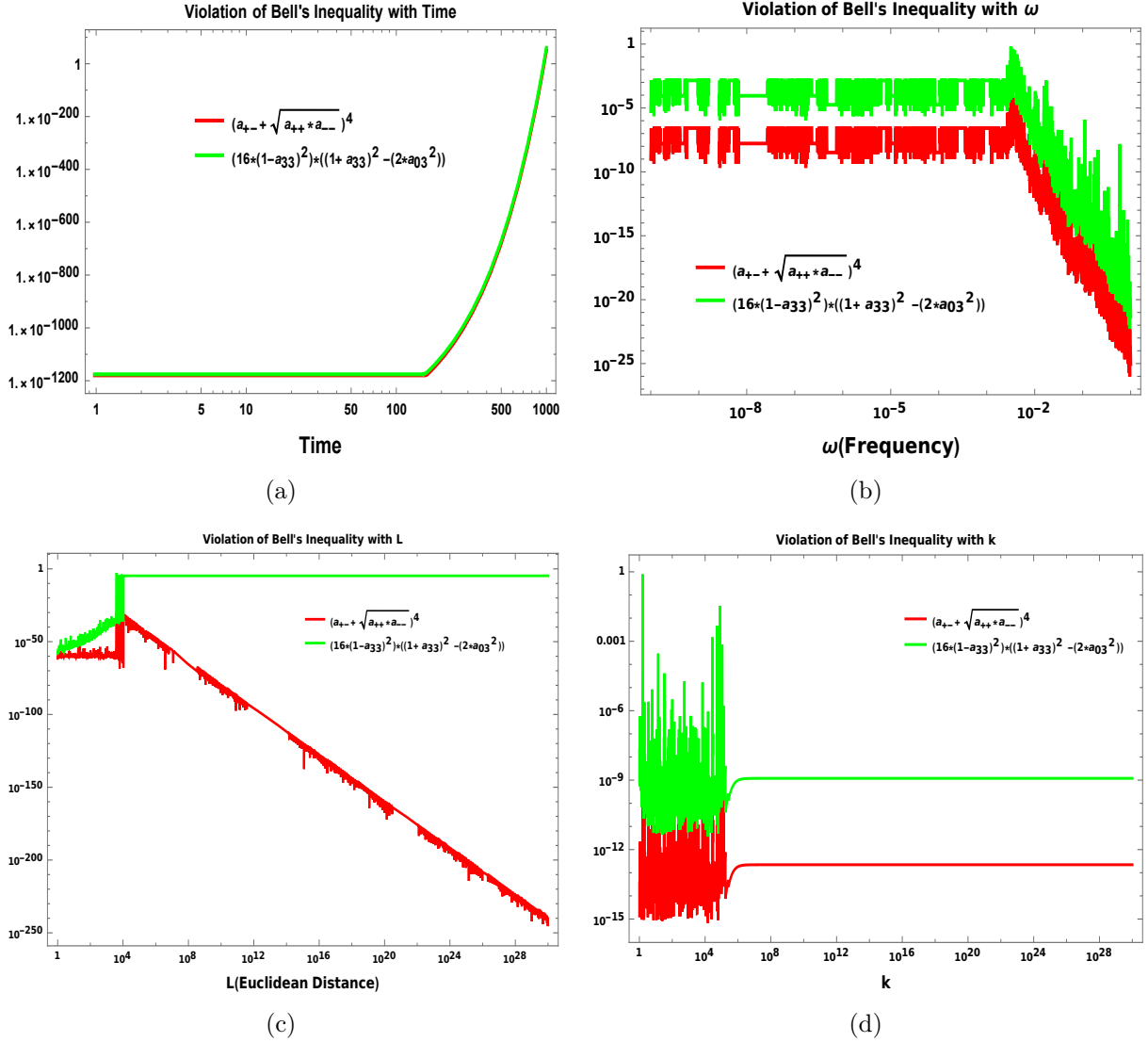


Figure 21. Verification of the Violation of the Bell-CHSH inequality with various parameters is shown here

to κ . We have normalized the values with the result obtained from $\kappa = 1$. We consider both small and large κ scale limiting situations. It is clearly observed that for all values of κ , if we restrict the other parameters of the theory within a fixed range then always we achieve that the function represented by green colour is always greater than that of red colour. This establishes Bell-CHSH inequality violation and non-locality in De Sitter space with the present two atomic open quantum set up.

Now, to implement the violation of the Bell-CHSH inequality in De Sitter now we have follow the following number of steps:

1. **Step 1:**

After passing through the local filter in the new basis we have to satisfy the following necessary constraint condition:

$$c'(c')^\dagger > 1. \quad (14.20)$$

2. **Step 2:**

The above condition directly implies the following inequality:

$$0 > \eta^4 - \frac{(\rho_{23} + |\rho_{14}|)^2}{\rho_{44}(\rho_{22} + \rho_{33})}\eta^2 + \frac{\rho_{11}}{\rho_{44}}, \quad (14.21)$$

where each of the quantities are appearing previously in the density matrix after passing through local filter.

3. **Step 3:**

The above inequality further can be rewritten in the following simplified form:

$$(\rho_{23} + |\rho_{14}|)^4 > 4\rho_{11}\rho_{44}(\rho_{22} + \rho_{33})^2 \quad (14.22)$$

4. **Step 4:**

For real parameter η if we substitute the entries of the local filter transformed density matrix in terms of the time dependent Bloch coefficients in the $(+, -, 3)$ transformed basis is given by the following inequality:

$$(a_{+-} + |a_{--}|)^4 > (1 - a_{33})^2[(1 + a_{33})^2 - (a_{03} + a_{30})^2]. \quad (14.23)$$

5. **Step 5:**

Now here our job is to explicitly verify this inequality for our open quantum system described by two entangled atoms. To serve this purpose we plot the following functions:

$$\mathcal{J}_1(t) = (a_{+-}(t) + |a_{--}(t)|)^4, \quad (14.24)$$

$$\mathcal{J}_2(t) = (1 - a_{33}(t))^2[(1 + a_{33}(t))^2 - (a_{03}(t) + a_{30}(t))^2], \quad (14.25)$$

separately. In the plot we represent $\mathcal{J}_1(t)$ and $\mathcal{J}_2(t)$ with green and red color. We have found out from our analysis that for all values of the time scale if we restrict the other parameters of the theory within a fixed range then always we achieve:

$$\mathcal{J}_1(t) > \mathcal{J}_2(t) \quad \forall t. \quad (14.26)$$

This actually establishes Bell-CHSH inequality violation and non-locality in De Sitter space with the present two atomic open quantum set up.

In 14.2 a comparative study of different entanglement measure is done for our two atomic OQS setup. Various entanglement measures calculated in this context, are compared taking into account various parameters like *rescaled time, Frequency, Euclidean distance, Inverse curvature*. The best entanglement measure is found after studying the entanglement with respect to the respective parameter in the entire chosen range and then the conclusion is given.

In 14.2 a comparative study of the one atomic and two atomic systems are done and the main highlighting differences have been noted. The reduced subsystem density matrix shows entanglement between the two atoms constituting the system whereas the one atomic subsystem is not entangled. It is also noted that for the case of one atomic case the equilibrium

Parameters	Best entanglement measure	Remarks
Rescaled time (T)	Collision Entropy (\mathcal{H}_2)	The long range correlation at late time scale can be best understood.
Frequency (ω)	Min entropy (\mathcal{H}_∞)	In the chosen frequency range it has the maximum amplitude showing maximum entanglement.
Euclidean distance (L)	Except Log negativity (E_N) others are appropriate	In the large length scale it shows fluctuations unlike other entanglement measures.
Inverse curvature (κ)	Collision entropy (\mathcal{H}_2), Min entropy (\mathcal{H}_∞) and Logarithmic negativity (E_N)	In the chosen κ range it has the maximum normalized amplitude showing maximum entanglement.

Table 1. A comparative study of various entanglement measures for our two atomic OQS setup

Parameters	One atomic system	Two atomic system
Reduced subsystem density matrix	Not entangled	Entangled
Equilibrium temperature of bath	$T = T_{\text{GH}} = \frac{1}{2\pi\alpha}$	$T = \sqrt{T_{\text{GH}}^2 + T_{\text{Unruh}}^2}$ $= \frac{1}{2\pi\sqrt{\alpha^2 - r^2}}$
Inverse curvature κ	$\kappa = \alpha$	$\kappa = \sqrt{\alpha^2 - r^2} \neq \alpha$
Nature of Wightman function	One body Wightman function $G(\tau - \tau') = \langle \Phi(\tau)\Phi(\tau') \rangle$	Many body Wightman function $G_{\alpha\beta}(\tau - \tau') = \langle \Phi(\tau, x_\alpha)\Phi(\tau', x_\beta) \rangle$
Quantum states $\Psi\rangle$	Ground ($ G\rangle = g\rangle$), Excited ($ E\rangle = e\rangle$).	Ground ($ G\rangle = g_1\rangle \otimes g_2\rangle$), Excited ($ E\rangle = e_1\rangle \otimes e_2\rangle$), Symmetric ($ S\rangle = \frac{1}{\sqrt{2}}(e_1\rangle \otimes g_2\rangle + g_1\rangle \otimes e_2\rangle)$), Anti-symmetric ($ A\rangle = \frac{1}{\sqrt{2}}(e_1\rangle \otimes g_2\rangle - g_1\rangle \otimes e_2\rangle)$).
Position of atom	The bath correlation function does not depend on the position of the atom.	The bath correlation function depends on the position of the atoms.
Difference in entanglement measures	Can be observed with very less magnitude, due to interaction with bath.	Observed in larger proportions due to entanglement between the two atoms besides interaction with the bath.
Lamb shift $\delta E_{\text{LS}} = \langle \Psi H_{\text{LS}} \Psi \rangle$	At $\omega \gg \omega_c$ (Bethe cut-off) no Lamb shift observed.	At $\omega \gg \omega_c$ (Bethe cut-off) a finite Lamb shift is observed

Table 2. Comparative study of one atomic and two atomic OQS setup.

temperature of the bath is exactly equal to the Gibbons Hawking temperature whereas for the two atomic case the equilibrium temperature is written in terms of Gibbons Hawking and Unruh temperature. Due to this difference in temperature the curvature of the background spacetime appears to be different for the two cases. The Wightman function has only one component (G_{11}) for the one atomic case as the correlation function is independent of the position of the atom whereas for the two atomic case the Wightman function has four components given by G_{11}, G_{12}, G_{21} and G_{22} corresponding to the dependence of the bath correlation functions on the positions of the atoms. Entanglement measure observed (if any) in case of one atomic system is mainly due to its interactions with the bath whereas for the two atomic case significant amount of entanglement measures are observed due to their mutual entanglement besides interaction with the bath.

15 Conclusion

To summarize, in this work, we have addressed the following issues to study the quantum entanglement phenomenon from two entangled atomic OQS set up:

- To begin with we have started our discussion with two entangled atomic OQS set up. In this framework the two entangled atoms mimic the role of Unruh-De-Witt detectors, conformally coupled to a thermal bath which is modelled by a massless scalar field in this specific problem. Apart from that, within this OQS set up, a non adiabatic Resonant Casimir Polder interaction (RCPI) takes place between the Unruh-De-Witt detectors and the thermal bath. Most importantly this interaction is effected by the background De-Sitter space time in which the probe massless scalar field is fluctuating.
- Since we are only interested in the dynamics of the reduced two entangled atomic subsystem, we partially trace over the probe massless scalar field or thermal bath degrees of freedom. Consequently without solving the total (system+bath+interaction) quantum liouville equation for the total density matrix, we actually solve the Gorini-Kossakowski-Sudarshan-Lindblad equation (Master equation) to explicitly know about the time evolution of the reduced subsystem density matrix. However, solving GSKL master equation with proper initial condition is an extremely complicated task, as it involves two non trivial components in the equation of motion. These are the effective hamiltonian and Quantum dissipator or lindbladian operator. Due to the complicated structure of both of them it is obvious that the analytical solution of the GSKL master equation is not possible for all type of OQS setup. In our two atomic entangled OQS setup we represent the density matrix corresponding to each of the atom through bloch sphere representation. However, the reduced subsystem density matrix, which can be constructed by taking the tensor product of two atomic density matrices, cannot be parametrized by a bloch sphere. Instead of that we found the reduced subsystem density matrix is actually parametrized by three time dependent coefficients $a_{0i}(\tau)$, $a_{i0}(\tau)$ and $a_{ij}(\tau) \forall i, j = 1, 2, 3$. this implies that solving GSKL master equation for the present OQS set up is actually determining the time dependent behaviour of the above mentioned coefficients, which are appearing in the expressions for the reduced subsystem density matrix. We found that this leads to huge number

of coupled differential equations of all these time dependent coefficients, which are not analytically solvable for given appropriate initial condition. To solve this problem next we transformed the basis from $\{1, 2, 3\}$ to $\{+, -, 3\}$. In this new basis we get simplified form of the linear differential equation which are less in number compared to the previous case. Also using the large time equilibrium behaviour of the reduced density matrix, which plays the role of initial condition in our problem, we have found the explicit analytical solution of $a_{ij} \forall i, j = \pm 3$.

- Using the analytical density matrix of the reduced subsystem we further computed various measure of quantum entanglement i.e Von Neumann entropy, Re'nyi entropy, Logarithmic negativity, Quantum discord, Entanglement of formation and Concurrence, which are commonly used in the context of Quantum information theory these days. From the time dependent behaviour of all the measure of quantum entanglement we have found out almost the similar behaviour which states that for initial time $t = 0$, the measure of quantum entanglement is 0 and as time goes on the subsystem gets more entangled and after a certain time it increases very slowly i.e it almost saturates. Apart from these as we have obtained the similar feature both in the case of Von Neumann entropy and in the case of Quantum discord, this imply existence of long range quantum correlation at the late time scale, satisfying the necessary and sufficient condition for quantum entanglement. Similarly we have obtained the time dependent feature of logarithmic negativity, entanglement of formation and concurrence which strongly imply that at initial time $t = 0$ our two atomic OQS setup do not show any signature of quantum entanglement as in all the cases the quantum measure is zero. As time goes on we have found out all of these measures significantly increase and at very late time scale it almost saturates. This is obviously a significant finding of our two atomic entangled OQS setup from which one can extract the existence of long range quantum correlation in late time scale, which is a very common topic of study in the context of quantum information theory.
- Last but not the least we have studied Bell-CHSH inequality ⁸ violation from our present setup in De-Sitter space. Though these kind of violation of Bell-CHSH inequality in de-Sitter space is not very trivial, with axion we and other authors have constructed cosmological setup in which this violation can be established. Most importantly, without introducing any axion in a more model independent way we have established the violation of Bell-CHSH inequality in De-sitter space, which is the necessary ingredient to study the non local effect in correlations in quantum mechanics.

The future prospect of this work is as follows.

- In this work we have restricted our subsystem which is made up of two entangled atoms. One can further generalize the same problem with arbitrary even or odd number of atoms within the framework of OQS.
- In this work we did our computation in the background static De-Sitter metric. However this framework can be implemented in any curved spacetime metric. One can even carry forward the calculations in other patches of De-Sitter space like the global

⁸Bell CHSH inequality in quantum mechanics is the most generalized version of the bell's inequality.

and inflationary (planer) patch. It is expected to get significant modifications in the cosmological correlation functions. Within the framework of OQS and particularly for inflationary patch [50, 51] of the De-Sitter space, one can exactly compare these results with the known cosmological correlation functions computed within the framework of closed quantum system. Such comparative analysis between the obtained cosmological correlation functions obtained from OQS and CQS will help us to know about the correct quantum mechanical picture of early universe cosmology. Additionally, by comparing this result with the data obtained from the observational probe for the early universe cosmology one may further rule out one of the possible quantum pictures mentioned here.

- In this paper we have computed the signature of Quantum entanglement from various Quantum information theoretic measure. However we have not done the calculation for all possible measure. For more completeness and also to conclude about the existence of long range quantum correlations at the late time scale one can further compute squashed entangled entropy [53], entanglement of distillation [54], relative entropy [55] etc. Additionally, one can also compute fisher information from the present OQS set up to know about the difference between the results obtained in the classical and quantum limiting situations.
- Very recently the phenomena of quantum teleportation has been observed with qutrit states [58, 59] for the first time, which is obviously a outstanding finding in the context of quantum information theory. The authors have succeeded in teleporting three-dimensional quantum states for the first time. High-dimensional teleportation could play an important role in future quantum computers. In this direction our future plan is to study such possibilities from the present OQS set up in De Sitter space.

Acknowledgements

SC would like to thank Quantum Gravity and Unified Theory and Theoretical Cosmology Group, Max Planck Institute for Gravitational Physics, Albert Einstein Institute (AEI) for providing the Post-Doctoral Research Fellowship. SC take this opportunity to thank sincerely to Jean-Luc Lehnars for their constant support and inspiration. SC thank the organisers of Summer School on Cosmology 2018, International Centre for Theoretical Physics (ICTP), Trieste, 15 th Marcel Grossman Meeting, Rome, The European Einstein Toolkit meeting 2018, Centra, Instituto Superior Tecnico, Lisbon and The Universe as a Quantum Lab, APC, Paris, Nordic String Meeting 2019, AEI, Potsdam, Tensor networks: from simulations to holography, DESY Zeuthen and AEI, Potsdam, XXXI Workshop Beyond the Standard Model, Physikzentrum Bad Honnef, Workshop in String Theory and Cosmology, NISER, Bhubaneswar for providing the local hospitality during the work. Additionally, SC would like to acknowledge AEI, Potsdam for funding the India trip to present this work at ISI Kolkata, SINP Kolkata, IACS Kolkata, NISER Bhubaneswar, RRI Bengaluru, IISC Bengaluru and DTP, TIFR, Mumbai. Also, SC thank Guruprasad Kar, Shibaji Roy, Arnab Kundu, Soumitra Sengupta, Sudhakar Panda, Anjan Sarkar, Sandip Trivedi, Gautam Mandal and Shiraz Minwalla for inviting to present this work and to provide the local hospitality

during the visit. SC also acknowledge the discussion regarding this work with Shiraz Minwalla, Sandip Trivedi, Joseph Samuel, Madhavan Varadarajan, Aninda Sinha, Justin Raju David, Arnab Kundu, Shibaji Roy, Soumitra Sengupta, T. R. Govindarajan, Naresh Dadich, Banibrata Mukhopadhyay, Subhasish Banerjee, which help us significantly to improve the discussions as well as the presentation of the work. Most significantly, SC is thankful to Shiraz Minwalla for giving the opportunity to present this work in very prestigious seminar series, "Quantum Space-time Seminar" at DTP, TIFR. We also thank all the members of our newly formed virtual international non-profit consortium "Quantum Structures of the Space-Time & Matter" (QASTM) for elaborative discussions and suggestions to improve the presentation of the article. SP acknowledges the J. C. Bose National Fellowship for support of his research. Last but not the least, we would like to acknowledge our debt to the people belonging to the various part of the world for their generous and steady support for research in natural sciences.

A Geometry of Static Patch of De Sitter space time

In this section we are going to discuss about the geometry of De Sitter space time and particularly about the static patch which we have used for background space time for our computation in this paper.

For this purpose let us consider a $(D + 1)$ dimensional De Sitter space time which is represented by the following equation:

$$-\eta_{AB}z^A z^B = -(z^0)^2 + (z^1)^2 + \dots + (z^{D+1})^2 = \alpha^2, \quad \forall \mathcal{A}, \mathcal{B} = 0, 1, \dots, (D + 1), \quad (\text{A.1})$$

where α is a dimensionful parameter, which has the dimension of length.

Now we consider the situation where this $(D + 1)$ dimensional De Sitter space is embedded in $(D + 2)$ dimensional Minkowski space time which is represented by the following infinitesimal line element:

$$ds_{D+2}^2 = \eta_{AB} dz^A dz^B. \quad (\text{A.2})$$

It is a very well known fact that the symmetry group of De Sitter space is $SO(1, D + 1)$, which has $\frac{1}{2}(D + 1)(D + 2)$ number of parameters. In this paper we particularly consider the situation for $D = 3$. However, for generality we have provided the details for any arbitrary $(D + 1)$ dimensional De Sitter space.

Now we know that:

$$z_{D+1}^2 = \eta_{\mu\nu} z^\mu z^\nu + \alpha^2 \implies dz_{D+1}^2 = \frac{\eta_{\mu\delta}\eta_{\nu\beta} z^\delta z^\beta}{\eta_{\gamma\lambda} z^\gamma z^\lambda + \alpha^2} dz^\mu dz^\nu. \quad (\text{A.3})$$

Further, excluding the contribution from the z_{D+1} coordinate from the expression for the $(D + 2)$ dimensional Minkowski infinitesimal line element we get the following result for the new line element:

$$ds^2 = \eta_{\mu\nu} dz^\mu dz^\nu - dz_{D+1}^2 = g_{\mu\nu} dz^\mu dz^\nu, \quad (\text{A.4})$$

where $g_{\mu\nu}$ is the induced metric on the hyperboloid, which is defined as:

$$g_{\mu\nu} = \left(\eta_{\mu\nu} - \frac{\eta_{\mu\delta}\eta_{\nu\kappa} z^\delta z^\kappa}{\eta_{\gamma\lambda} z^\gamma z^\lambda + \alpha^2} \right) \implies g^{\mu\nu} = \left(\eta^{\mu\nu} + \frac{z^\mu z^\nu}{\alpha^2} \right), \quad (\text{A.5})$$

which satisfy the following constraint condition always:

$$\begin{aligned}
g_{\mu\nu}g^{\nu\beta} &= \left(\eta_{\mu\nu} - \frac{\eta_{\mu\delta}\eta_{\nu\kappa}z^\delta z^\kappa}{\eta_{\gamma\lambda}z^\gamma z^\lambda + \alpha^2} \right) \left(\eta^{\nu\beta} + \frac{z^\nu z^\beta}{\alpha^2} \right) \\
&= \eta_{\mu\nu}\eta^{\nu\beta} - \frac{\eta_{\mu\delta}\eta_{\nu\kappa}\eta^{\nu\beta}z^\delta z^\kappa}{\eta_{\gamma\lambda}z^\gamma z^\lambda + \alpha^2} + \frac{\eta_{\mu\nu}z^\nu z^\beta}{\alpha^2} - \frac{\eta_{\mu\delta}\eta_{\nu\kappa}z^\delta z^\kappa}{\eta_{\gamma\lambda}z^\gamma z^\lambda + \alpha^2} \frac{z^\nu z^\beta}{\alpha^2} \\
&= \delta_\mu^\beta - \frac{\alpha^2\eta_{\mu\delta}\delta_\kappa^\beta z^\delta z^\kappa - \eta_{\mu\nu}z^\nu z^\beta(\eta_{\gamma\lambda}z^\gamma z^\lambda + \alpha^2)}{\alpha^2(\eta_{\gamma\lambda}z^\gamma z^\lambda + \alpha^2)} - \frac{\eta_{\mu\delta}\eta_{\nu\kappa}z^\delta z^\kappa z^\nu z^\beta}{\alpha^2(\eta_{\gamma\lambda}z^\gamma z^\lambda + \alpha^2)} \\
&= \delta_\mu^\beta - \frac{\alpha^2\eta_{\mu\delta}z^\delta z^\beta - \eta_{\mu\nu}\eta_{\gamma\lambda}z^\nu z^\beta z^\gamma z^\lambda - \alpha^2\eta_{\mu\nu}z^\nu z^\beta}{\alpha^2(\eta_{\gamma\lambda}z^\gamma z^\lambda + \alpha^2)} - \frac{\eta_{\mu\delta}\eta_{\nu\kappa}z^\delta z^\kappa z^\nu z^\beta}{\alpha^2(\eta_{\gamma\lambda}z^\gamma z^\lambda + \alpha^2)} \\
&= \delta_\mu^\beta + \frac{\eta_{\mu\nu}\eta_{\gamma\lambda}z^\nu z^\beta z^\gamma z^\lambda - \eta_{\mu\delta}\eta_{\nu\kappa}z^\delta z^\kappa z^\nu z^\beta}{\alpha^2(\eta_{\gamma\lambda}z^\gamma z^\lambda + \alpha^2)} \\
&= \delta_\mu^\beta.
\end{aligned} \tag{A.6}$$

Here we have used the fact that for Minkowski flat space time:

$$\eta_{\mu\nu}\eta^{\nu\beta} = \delta_\mu^\beta. \tag{A.7}$$

Now one can compute the *Riemann tensor*, *Ricci tensor* and *Ricci scalar* or *curvature scalar* in maximally symmetric $(D + 1)$ dimensional space in presence of cosmological constant Λ , which are given by the following expressions:

$$R_{\mu\nu\alpha\beta} = \frac{2\Lambda}{D(D-1)} (g_{\mu\alpha}g_{\nu\beta} - g_{\mu\beta}g_{\nu\alpha}) \tag{A.8}$$

$$R_{\mu\nu} = \frac{2\Lambda}{(D-1)}g_{\mu\nu}, \tag{A.9}$$

$$R = \frac{2\Lambda(D+1)}{(D-1)}, \tag{A.10}$$

where in De Sitter space time cosmological constant $\Lambda > 0$. Here the number of Killing vectors are basically $\frac{1}{2}(D+1)(D+2)$ which is exactly same as the number of parameters appearing in $SO(1, D+1)$ De Sitter isometry group.

On the other hand, using the previously mentioned definition of the induced metric $g_{\mu\nu}$ one can also compute the *Ricci scalar* or *curvature scalar*, which are given by the following expression:

$$R = \frac{D(D+1)}{\alpha^2}. \tag{A.11}$$

Now comparing Eq (A.11) and Eq (A.10), we get the following expression for the cosmological constant Λ in terms of the parameter α :

$$\Lambda = \frac{D(D-1)}{2\alpha^2}. \tag{A.12}$$

Since in this paper we are interested in $D = 3$, then we get:

$$R = \frac{12}{\alpha^2} = 4\Lambda > 0, \quad \Lambda = \frac{3}{\alpha^2} > 0. \tag{A.13}$$

Now we introduce radial coordinate r which is defined through the following equation:

$$\sum_{i=1}^D (z^i)^2 = r^2. \quad (\text{A.14})$$

Using Eq (A.14), the equation for the hyperboloid can be described by the following equation:

$$\begin{aligned} & -(z^0)^2 + (z^1)^2 + \dots + (z^{D+1})^2 = \alpha^2 \\ \Rightarrow & -(z^0)^2 + (z^{D+1})^2 = \alpha^2 - r^2 = \kappa^2 > 0. \end{aligned} \quad (\text{A.15})$$

Now we can consider the following sets of transformation equations which satisfy the above mentioned equation for the hyperboloid:

$$z^0 = \kappa \sinh\left(\frac{t}{\alpha}\right), \quad (\text{A.16})$$

$$z^i = r\omega^i, \quad \forall \quad i = 1, \dots, D, \quad (\text{A.17})$$

$$z^{D+1} = \kappa \cosh\left(\frac{t}{\alpha}\right), \quad (\text{A.18})$$

where the parameter κ is defined as:

$$\kappa = \sqrt{\alpha^2 - r^2} > 0 \implies r \leq \alpha. \quad (\text{A.19})$$

Here, $r = \alpha$ is the horizon in the present context.

It is important to note that, ω^i satisfies the following equation:

$$\sum_{i=1}^{D+1} (\omega^i)^2 = 1, \quad (\text{A.20})$$

which is the equation for D dimensional unit sphere. Now, we introduce D angular coordinates, $\theta_i \forall i = 1, \dots, D$, which are connected to $\omega^i \forall i = 1, \dots, D + 1$ by the following sets of transformation equations:

$$\begin{aligned} \omega^1 &= \cos \theta_1, \\ \omega^2 &= \sin \theta_1 \cos \theta_2, \\ &\dots \quad \dots \quad \dots \quad \dots \quad \dots \quad \dots \\ \omega^D &= \sin \theta_1 \cos \theta_2 \cdots \sin \theta_{D-1} \cos \theta_D, \\ \omega^{D+1} &= \sin \theta_1 \cos \theta_2 \cdots \sin \theta_{D-1} \sin \theta_D. \end{aligned} \quad (\text{A.21})$$

This will give rise to the following line element describing the static patch of De Sitter space in arbitrary $(D + 1)$ dimensional space time, given by:

$$ds_{D+1}^2 = \left(1 - \frac{r^2}{\alpha^2}\right) dt^2 - \left(1 - \frac{r^2}{\alpha^2}\right)^{-1} dr^2 - r^2 d\Omega_{D-1}^2 \quad \text{where } \alpha = \sqrt{\frac{D(D-1)}{2\Lambda}} > 0. \quad (\text{A.22})$$

Here $d\Omega_{D-1}^2$ represents the line element for unit $(D - 1)$ dimensional sphere, which is given by the following expression:

$$d\Omega_{D-1}^2 = (d\theta_1)^2 + \sum_{i=2}^{D-1} \left(\prod_{k=1}^{i-1} \sin^2 \theta_k \right) (d\theta_i)^2. \quad (\text{A.23})$$

B Solution for the bath field equation for probe massless scalar field in Static Patch of De Sitter Space

In this context, our prime objective is to solve the bath field equation for probe massless scalar field in $(D + 1)$ dimensional static patch of De Sitter Space. It is important to note that, in this paper we have restricted our analysis to the situation where the probe scalar field is minimally coupled to gravity. However, one can generalise this calculation for massive and conformally coupled scalar field with gravity. After deriving the result once we put the conformal or sometimes called, the non-minimal coupling parameter equal to zero and the mass equal to zero then we will get back the required result expected in $(D + 1)$ dimensional static patch of De Sitter Space.

B.1 Finding un-normalized total solution for probe scalar field

Let us start with the following $(D + 1)$ dimensional action, which is characterised by a scalar field conformally coupled with the gravity, given by the following expression:

$$S_{D+1}[m, \xi] = \int d^{D+1}x \sqrt{-g_{D+1}} \left[\xi R \Phi^2(x) + g^{\mu\nu} (\partial_\mu \Phi(x)) (\partial_\nu \Phi(x)) - \frac{m_\Phi^2}{2} \Phi^2(x) \right], \quad (\text{B.1})$$

where ξ is the conformal or non-minimal coupling parameter which couples the scalar field with the background gravity and m_Φ is the mass of the scalar field under consideration. Now after deriving the result once we substitute $\xi = 0$ and $m = 0$ then we will get back the required result in $(D + 1)$ space time which is used in this paper.

Now after taking the variation of the above mentioned action with respect to the scalar field $\Phi(x)$ we get the following field equation describes the thermal bath in any arbitrary $(D + 1)$ dimensional space time:

$$(\square_{D+1} + m_\Phi^2 + \xi R) \Phi(x) = 0, \quad (\text{B.2})$$

which is also known as the *Klein-Gordon equation*. In $(D + 1)$ dimensional space time the *D'Alembertian operator* (\square_{D+1}) is defined as:

$$\square_{D+1} := \frac{1}{\sqrt{-g_{D+1}}} \partial_\mu (\sqrt{-g_{D+1}} g^{\mu\nu} \partial_\nu). \quad (\text{B.3})$$

Now in the case of $(D + 1)$ dimensional static patch of De Sitter space the above mentioned *D'Alembertian operator* takes the following mathematical structure:

$$\square_{D+1} = \left[\partial_t \left(\frac{1}{(1 - \frac{r^2}{\alpha^2})} \partial_t \right) - \frac{1}{r^{D-1}} \partial_r \left(r^{D-1} \left(1 - \frac{r^2}{\alpha^2} \right) \partial_r \right) - \frac{1}{r^2} \mathbf{L}_{D-1}^2 \right], \quad (\text{B.4})$$

where \mathbf{L}_{D-1}^2 is the *Laplacian operator* described in $(D - 1)$ dimensional sphere.

The most general solution of Eq (B.2) is given by the following expression:

$$\Phi(x) = \Phi(t; r; \theta_1, \dots, \theta_{D-1} := \mathcal{V}) = R \left(\frac{r}{\alpha} \right) Y^{(D-1)}(m_k; \mathcal{V}) e^{-i\omega t}. \quad (\text{B.5})$$

Here $Y^{(D-1)}(m_k; \mathcal{V})$ represents the spherical harmonics in $(D - 1)$ dimensional sphere which satisfy the following eigen value equation:

$$\mathbf{L}_{D-1}^2 Y^{(D-1)}(m_k; \mathcal{V}) = -l(l + D - 2) Y^{(D-1)}(m_k; \mathcal{V}). \quad (\text{B.6})$$

Here $m_k = l, m_i \forall i = 1, 2, \dots, D-2$ are the quantum numbers associated with the system, if we want to interpret this solution quantum mechanically.

Now, just considering the radial part of the solution and substituting back in the classical field equation we get the following differential equation:

$$\frac{1}{\mathcal{Z}} \partial_{\mathcal{Z}} (\mathcal{Z}^{D-1} (1 - \mathcal{Z}^2) \partial_{\mathcal{Z}} R(\mathcal{Z})) + \left\{ \frac{\alpha^2 \omega^2}{1 - \mathcal{Z}^2} - \frac{l(L + D - 2)}{\mathcal{Z}^2} - m_{\Phi}^2 \alpha^2 - D(D + 1)\xi \right\} R(\mathcal{Z}) = 0, \quad (\text{B.7})$$

where we have introduced a new rescaled radial coordinate, \mathcal{Z} , which is defined as:

$$\mathcal{Z} := \frac{r}{\alpha} = \sin u, \quad \text{where } 0 \leq u \leq \frac{\pi}{2}. \quad (\text{B.8})$$

For more convenience, one can further re-express the above equation in terms the newly defined variable u as:

$$\frac{1}{\sin^{D-1} u \cos u} \partial_u (\sin^{D-1} u \cos u \partial_u R(u)) + \left\{ \frac{\alpha^2 \omega^2}{\cos^2 u} - \frac{l(L + D - 2)}{\sin^2 u} - m_{\Phi}^2 \alpha^2 - D(D + 1)\xi \right\} R(u) = 0. \quad (\text{B.9})$$

The general solution of this equation can be written as:

$$R(u) = C_1 \mathcal{R}_1^l(u) + C_2 \mathcal{R}_2^l(u), \quad (\text{B.10})$$

where C_1 and C_2 are two arbitrary constants which can be fixed by choosing appropriate boundary conditions. On the other hand, $\mathcal{R}_i^l \forall i = 1, 2$ are the two linearly independent solutions which can be expressed as:

$$\mathcal{R}_1^l(u) = \tan^l u \cos^n u F \left(\frac{l - n + i\alpha\omega}{2}, \frac{l - n - i\alpha\omega}{2}; l + \frac{D}{2}; -\tan^2 u \right) \quad (\text{B.11})$$

$$\mathcal{R}_2^l(u) = \cot^{l+D-2} u \cos^n u \times F \left(1 - \frac{l + n + D - i\alpha\omega}{2}, 1 - \frac{l + n + D + i\alpha\omega}{2}; 2 - l - \frac{D}{2}; -\tan^2 u \right), \quad (\text{B.12})$$

where $F(x, y; z; w)$ represents the hypergeometric function and also we have used the following fact:

$$\left(n + \frac{D}{2} \right)^2 = \frac{D^2}{4} - m_{\Phi}^2 \alpha^2 - D(D + 1)\xi := \nu_{\Phi}^2 \Rightarrow n = n_{\pm} := \left(-\frac{D}{2} \pm \nu_{\Phi} \right). \quad (\text{B.13})$$

Here ν_{Φ} is known as the mass parameter of the scalar field Φ . For massless and minimally coupled scalar field with gravity we get:

$$\nu_{\Phi} = \frac{D}{2} \quad \text{for } D = 3 \quad \text{we get } \nu_{\Phi} = \frac{3}{2}, \quad (\text{B.14})$$

which is applicable to our present model of OQS.

Here further using the fundamental properties of the hypergeometric function one can explicitly show that:

$$n := n_+ = n_- = -\frac{D}{2} + \nu_\Phi = -\frac{D}{2} - \nu_\Phi. \quad (\text{B.15})$$

So we will go with the signature appearing in n_- . Consequently, the two linearly independent solutions takes the following simplified form:

$$\begin{aligned} \mathcal{R}_1^l(u) &= \tan^l u \cos^{-\left(\frac{D}{2} + \nu_\Phi\right)} u \\ &\times F\left(\frac{l + \frac{D}{2} + \nu_\Phi + i\alpha\omega}{2}, \frac{l + \frac{D}{2} + \nu_\Phi - i\alpha\omega}{2}; l + \frac{D}{2}; -\tan^2 u\right), \end{aligned} \quad (\text{B.16})$$

$$\begin{aligned} \mathcal{R}_2^l(u) &= \cot^{l+D-2} u \cos^{-\left(\frac{D}{2} + \nu_\Phi\right)} u \\ &\times F\left(1 - \frac{l + \frac{D}{2} - \nu_\Phi - i\alpha\omega}{2}, 1 - \frac{l + \frac{D}{2} - \nu_\Phi + i\alpha\omega}{2}; 2 - l - \frac{D}{2}; -\tan^2 u\right). \end{aligned} \quad (\text{B.17})$$

B.2 Finding un-normalized regular solution for probe scalar field

Further, to understand the physical implications of these obtained solution one needs to simplify its mathematical form. To serve this purpose we introduce another variable \mathcal{X} , which is defined as:

$$\mathcal{X} := \tan u = \frac{\mathcal{Z}}{\sqrt{1 - \mathcal{Z}^2}}. \quad (\text{B.18})$$

Using this newly defined variable the previously mentioned linearly independent solutions can be further recast as:

$$\begin{aligned} \mathcal{R}_1^l(\mathcal{X}) &= \mathcal{X}^l (1 + \mathcal{X}^2)^{\frac{(D+2\nu_\Phi)}{4}} \\ &\times F\left(\frac{l + \frac{D}{2} + \nu_\Phi + i\alpha\omega}{2}, \frac{l + \frac{D}{2} + \nu_\Phi - i\alpha\omega}{2}; l + \frac{D}{2}; -\mathcal{X}^2\right), \end{aligned} \quad (\text{B.19})$$

$$\begin{aligned} \mathcal{R}_2^l(\mathcal{X}) &= \mathcal{X}^{-(l+D-2)} (1 + \mathcal{X}^2)^{\frac{(D+2\nu_\Phi)}{4}} \\ &\times F\left(1 - \frac{l + \frac{D}{2} - \nu_\Phi - i\alpha\omega}{2}, 1 - \frac{l + \frac{D}{2} - \nu_\Phi + i\alpha\omega}{2}; 2 - l - \frac{D}{2}; -\mathcal{X}^2\right). \end{aligned} \quad (\text{B.20})$$

Here one can observe the following characteristics in these two solutions:

1. Here we have:

$$\lim_{\mathcal{X} \rightarrow 0} \mathcal{R}_2^l(\mathcal{X}) \rightarrow \infty, \quad (\text{B.21})$$

which implies that the second solution is divergent in the limit $\mathcal{X} \rightarrow 0$. So we will not consider this particular solution as we are interested in only regular solution in this context.

2. To simplify the mathematical form of the hypergeometric function one can apply the following transformation rule:

$$F(x, y; z; w) = \frac{1}{(1-w)^x} F\left(x, z-y; z; \frac{w}{w-1}\right). \quad (\text{B.22})$$

Hence one can write down the following regular solution of the classical field equation as given by:

$$\Phi_\sigma(t, r, \mathcal{V}) = C_1 \mathcal{R}_1^l \left(\frac{r}{\alpha} \right) Y^{(D-1)}(m_k; \mathcal{V}) e^{-i\omega t} \quad \text{where } \sigma = \omega, m_k, \quad (\text{B.23})$$

where C_1 is the arbitrary integration constant which we will fix at the later half of this discussion. Also it is important to note that these modes are characterised by both, ω and $m_k = l, m_i \forall i = 1, 2, \dots, D-2$ in this context. Here we have applied the above mentioned transformation rule to simplify the radial solution as given by:

$$\begin{aligned} \mathcal{R}_1^l(\mathcal{Z}) &= \mathcal{Z}^l (1 - \mathcal{Z}^2)^{\frac{i\alpha\omega}{2}} \\ &\times F \left(\frac{l + \frac{D}{2} + \nu_\Phi + i\alpha\omega}{2}, \frac{l + \frac{D}{2} + \nu_\Phi - i\alpha\omega}{2}; l + \frac{D}{2}; \mathcal{Z}^2 \right). \end{aligned} \quad (\text{B.24})$$

Now we will see the behaviour of this solution, particular the radial part, in the vicinity of the De Sitter horizon, which is represented by $\mathcal{Z} \rightarrow 1$ or equivalently $\mathcal{X} \rightarrow \infty$. To implement this fact first we write down the expression for the hypergeometric function by applying the following linear transformation rule, as given by:

$$\begin{aligned} F(x, y; z; -w) &= \frac{\Gamma(z)\Gamma(y-x)}{\Gamma(y)\Gamma(z-x)} w^{-x} F \left(x, 1-z+x; 1-y+x; \frac{1}{w} \right) \\ &+ \frac{\Gamma(z)\Gamma(x-y)}{\Gamma(x)\Gamma(z-y)} w^{-y} F \left(y, 1-z+y; 1-x+y; \frac{1}{w} \right). \end{aligned} \quad (\text{B.25})$$

Then considering the asymptotic behaviour at $z \rightarrow \infty$ we get the following simplified result:

$$F(x, y; z; -w) = \Gamma(z) \left\{ \frac{\Gamma(y-x)w^{-x}}{\Gamma(y)\Gamma(z-x)} + \frac{\Gamma(x-y)w^{-y}}{\Gamma(x)\Gamma(z-y)} \right\}. \quad (\text{B.26})$$

Using this fact the radial part of the solution can be further expressed in the following simplified form:

$$\mathcal{R}^l(\mathcal{Z}) = \mathcal{A}(\omega)(1 - \mathcal{Z}^2)^{-\frac{i\alpha\omega}{2}} + \mathcal{A}^*(\omega)(1 - \mathcal{Z}^2)^{\frac{i\alpha\omega}{2}}, \quad (\text{B.27})$$

where $\mathcal{A}(\omega)$ and its complex conjugate $\mathcal{A}^*(\omega)$ are defined by the following expression:

$$\mathcal{A}(\omega) = \frac{\Gamma \left(l + \frac{D}{2} \right) \Gamma(i\alpha\omega)}{\Gamma \left(\frac{l + \frac{D}{2} + \nu_\Phi + i\alpha\omega}{2} \right) \Gamma \left(\frac{l + \frac{D}{2} - \nu_\Phi + i\alpha\omega}{2} \right)}, \quad (\text{B.28})$$

$$\mathcal{A}^*(\omega) = \frac{\Gamma^* \left(l + \frac{D}{2} \right) \Gamma^*(i\alpha\omega)}{\Gamma^* \left(\frac{l + \frac{D}{2} + \nu_\Phi + i\alpha\omega}{2} \right) \Gamma^* \left(\frac{l + \frac{D}{2} - \nu_\Phi + i\alpha\omega}{2} \right)}. \quad (\text{B.29})$$

B.3 Finding the normalization constant for the regular solution for probe scalar field

Next, our job is to fix the arbitrary integration constant C_1 using the following normalization condition:

$$\mathcal{I}(\omega) := \int d^D x \Phi_\sigma(x) \Phi_{\sigma'}^*(x) = \frac{1}{2\omega} \delta_{\sigma\sigma'}. \quad (\text{B.30})$$

To evaluate C_1 we start with the left side of the integral which we explicitly write in static coordinate patch of the De Sitter space, given by:

$$\begin{aligned}
\mathcal{I}(\omega) &= \int d^D x \Phi_\sigma(x) \Phi_{\sigma'}^*(x) \\
&= |C_1|^2 \underbrace{\int_{r=0}^{\alpha} dr \frac{r^{D-1}}{\left(1 - \frac{r^2}{\alpha^2}\right)} \mathcal{R}_{1;\omega}^l\left(\frac{r}{\alpha}\right) \mathcal{R}_{1;\omega'}^{l*}\left(\frac{r}{\alpha}\right)}_{\text{Radial Integral}} \underbrace{\int d\Omega_{D-1} Y^{(D-1)}(m_k; \mathcal{V}) \left(Y^{(D-1)}(m_k; \mathcal{V})\right)^*}_{\text{Angular Integral}} \\
&= |C_1|^2 \mathcal{J}_2 \mathcal{J}_1,
\end{aligned} \tag{B.31}$$

where the integral \mathcal{J}_1 and \mathcal{J}_2 are given by the following expressions:

$$\mathcal{J}_1 := \int d\Omega_{D-1} Y^{(D-1)}(m_k; \mathcal{V}) \left(Y^{(D-1)}(m_k; \mathcal{V})\right)^* = N(m_k), \tag{B.32}$$

and

$$\begin{aligned}
\mathcal{J}_2 &:= \int_{r=0}^{\alpha} dr \frac{r^{D-1}}{\left(1 - \frac{r^2}{\alpha^2}\right)} \mathcal{R}_{1;\omega}^l\left(\frac{r}{\alpha}\right) \mathcal{R}_{1;\omega'}^{l*}\left(\frac{r}{\alpha}\right) \\
&= \alpha^D \int_{\mathcal{Z}=0}^1 d\mathcal{Z} \frac{\mathcal{Z}^{D-1}}{\left(1 - \mathcal{Z}^2\right)} \mathcal{R}_{1;\omega}^l(\mathcal{Z}) \mathcal{R}_{1;\omega'}^{l*}(\mathcal{Z}) \\
&= \frac{\alpha^D}{2} \int_{u=0}^1 du \frac{u^{\frac{D}{2}-1}}{\left(1 - u\right)} \mathcal{R}_{1;\omega}^l(\sqrt{u}) \mathcal{R}_{1;\omega'}^{l*}(\sqrt{u}).
\end{aligned} \tag{B.33}$$

Now, here it is important to note that, if we consider the limiting situation $\omega \rightarrow \omega'$, then we see that near the upper limit the integral \mathcal{J}_2 is divergent. Also, we see that the dominant contribution of this integral is appearing in the vicinity of the limiting region $\omega \rightarrow \omega'$. For this reason one can write down the following asymptotic expansion of the product of the two conjugate radial solutions as appearing in the numerator of the integral \mathcal{J}_2 i.e.

$$\begin{aligned}
\mathcal{R}_{1;\omega}^l(\sqrt{u}) \mathcal{R}_{1;\omega'}^{l*}(\sqrt{u}) &\approx \mathcal{A}(\omega) \mathcal{A}(\omega') (1-u)^{-\frac{i\alpha(\omega+\omega')}{2}} + \mathcal{A}(\omega) \mathcal{A}^*(\omega') (1-u)^{-\frac{i\alpha(\omega-\omega')}{2}} \\
&\quad + \mathcal{A}^*(\omega) \mathcal{A}(\omega') (1-u)^{\frac{i\alpha(\omega-\omega')}{2}} + \mathcal{A}^*(\omega) \mathcal{A}^*(\omega') (1-u)^{\frac{i\alpha(\omega+\omega')}{2}}.
\end{aligned} \tag{B.34}$$

This asymptotic expansion is very useful to evaluate the integral \mathcal{J}_2 . The detailed steps are given below for better understanding:

$$\begin{aligned}
\mathcal{J}_2 &= \frac{\alpha^D}{2} \int_{u=0}^1 du \frac{u^{\frac{D}{2}-1}}{(1-u)} \mathcal{R}_{1;\omega}^l(\sqrt{u}) \mathcal{R}_{1;\omega'}^{l*}(\sqrt{u}) \\
&= \frac{\alpha^D}{2} \int_{u=0}^1 du \frac{u^{\frac{D}{2}-1}}{(1-u)} \left\{ \mathcal{A}(\omega)\mathcal{A}(\omega')(1-u)^{-\frac{i\alpha(\omega+\omega')}{2}} + \mathcal{A}(\omega)\mathcal{A}^*(\omega')(1-u)^{-\frac{i\alpha(\omega-\omega')}{2}} \right. \\
&\quad \left. + \mathcal{A}^*(\omega)\mathcal{A}(\omega')(1-u)^{\frac{i\alpha(\omega-\omega')}{2}} + \mathcal{A}^*(\omega)\mathcal{A}^*(\omega')(1-u)^{\frac{i\alpha(\omega+\omega')}{2}} \right\} \\
&\approx \frac{\alpha^D}{2} \int_{u=0}^1 d\ln(1-u) \left\{ \mathcal{A}(\omega)\mathcal{A}(\omega')e^{-\frac{i\alpha(\omega+\omega')}{2\ln(1-u)}} + \mathcal{A}(\omega)\mathcal{A}^*(\omega')e^{-\frac{i\alpha(\omega-\omega')}{2\ln(1-u)}} \right. \\
&\quad \left. + \mathcal{A}^*(\omega)\mathcal{A}(\omega')e^{\frac{i\alpha(\omega-\omega')}{2\ln(1-u)}} + \mathcal{A}^*(\omega)\mathcal{A}^*(\omega')e^{\frac{i\alpha(\omega+\omega')}{2\ln(1-u)}} \right\} \\
&= \frac{\alpha^D}{2} \int_{z=0}^{\infty} dz \left\{ \mathcal{A}(\omega)\mathcal{A}(\omega')e^{-\frac{iz\alpha(\omega+\omega')}{2}} + \mathcal{A}(\omega)\mathcal{A}^*(\omega')e^{-\frac{iz\alpha(\omega-\omega')}{2}} \right. \\
&\quad \left. + \mathcal{A}^*(\omega)\mathcal{A}(\omega')e^{\frac{iz\alpha(\omega-\omega')}{2}} + \mathcal{A}^*(\omega)\mathcal{A}^*(\omega')e^{\frac{iz\alpha(\omega+\omega')}{2}} \right\} \\
&= \frac{\pi\alpha^D}{2} \left\{ \mathcal{A}(\omega)\mathcal{A}(\omega')(1-i)\delta\left(\frac{\alpha(\omega+\omega')}{2}\right) + \mathcal{A}(\omega)\mathcal{A}^*(\omega')(1-i)\delta\left(\frac{\alpha(\omega-\omega')}{2}\right) \right. \\
&\quad \left. + \mathcal{A}^*(\omega)\mathcal{A}(\omega')(1+i)\delta\left(\frac{\alpha(\omega-\omega')}{2}\right) + \mathcal{A}^*(\omega)\mathcal{A}^*(\omega')(1+i)\delta\left(\frac{\alpha(\omega+\omega')}{2}\right) \right\} \\
&= 2|\mathcal{A}(\omega)|^2\pi\delta\left(\frac{\alpha(\omega-\omega')}{2}\right) \\
&= \frac{\alpha^D}{2} \frac{4\pi}{\alpha} |\mathcal{A}(\omega)|^2 \delta(\omega-\omega') \tag{B.35}
\end{aligned}$$

Then the previously mentioned $\mathcal{I}(\omega)$ can be computed as:

$$\mathcal{I}(\omega) = |C_1|^2 N(m_k) \frac{\alpha^D}{2} \frac{4\pi}{\alpha} |\mathcal{A}(\omega)|^2 \delta(\omega-\omega') = \frac{1}{2\omega} \delta(\omega-\omega'), \tag{B.36}$$

then the normalization constant can be evaluated as:

$$C_1 = \frac{\alpha^{\frac{1-D}{2}}}{2\sqrt{\pi\omega N(m_k)} |\mathcal{A}(\omega)|} = \frac{\alpha^{\frac{1-D}{2}}}{2\sqrt{\pi\omega N(m_k)} \left| \frac{\Gamma(l+\frac{D}{2})\Gamma(i\alpha\omega)}{\Gamma\left(\frac{l+\frac{D}{2}+\nu_\Phi+i\alpha\omega}{2}\right)\Gamma\left(\frac{l+\frac{D}{2}-\nu_\Phi+i\alpha\omega}{2}\right)} \right|}, \tag{B.37}$$

where we have neglected additional phase factor.

B.4 Finding normalized regular solution for probe scalar field

Finally, the regular solution for the scalar field can be written as:

$$\Phi_\sigma(t, r, \mathcal{V}) = \frac{\alpha^{\frac{1-D}{2}} \mathcal{R}_1^l\left(\frac{r}{\alpha}\right) Y^{(D-1)}(m_k; \mathcal{V}) e^{-i\omega t}}{2\sqrt{\pi\omega N(m_k)} \left| \frac{\Gamma(l+\frac{D}{2})\Gamma(i\alpha\omega)}{\Gamma\left(\frac{l+\frac{D}{2}+\nu_\Phi+i\alpha\omega}{2}\right)\Gamma\left(\frac{l+\frac{D}{2}-\nu_\Phi+i\alpha\omega}{2}\right)} \right|} \quad \text{where } \sigma = \omega, m_k, \tag{B.38}$$

where the explicit form of the radial solution $\mathcal{R}_1^l\left(\frac{r}{\alpha}\right)$ is already derived earlier and the mass parameter ν_Φ is defined as:

$$\nu_\Phi = \sqrt{\frac{D^2}{4} - m_\Phi^2 \alpha^2 - D(D+1)\xi} \quad \text{where} \quad \alpha = \sqrt{\frac{D(D-1)}{2\Lambda}} > 0 \quad \text{as} \quad \Lambda > 0. \quad (\text{B.39})$$

By fixing $m_\Phi = 0 = \xi$ and $D = 3$ we will get the value of the mass parameter $\nu_\Phi = \frac{3}{2}$ applicable to our problem discussed in this paper. Also, in $D = 3$ the solution can be recast as:

$$\Phi_{lm}(t, r, \theta, \phi) = \frac{\mathcal{R}_1^l\left(\frac{r}{\alpha}\right) Y_{lm}(\theta, \phi) e^{-i\omega t}}{2\alpha\sqrt{\pi\omega} \left| \frac{\Gamma(l+\frac{3}{2})\Gamma(i\alpha\omega)}{\Gamma(\frac{l+3+i\alpha\omega}{2})\Gamma(\frac{l+i\alpha\omega}{2})} \right|} \quad \text{where} \quad l = 0, \dots, \infty; \quad m = -l, \dots, +l, \quad (\text{B.40})$$

where the radial solution in $D = 3$ can be written as:

$$\mathcal{R}^l\left(\frac{r}{\alpha}\right) = \left\{ \frac{\Gamma\left(l+\frac{3}{2}\right)\Gamma(i\alpha\omega)}{\Gamma\left(\frac{l+3+i\alpha\omega}{2}\right)\Gamma\left(\frac{l+i\alpha\omega}{2}\right)} \left(1 + \frac{r^2}{\alpha^2}\right)^{\frac{i\alpha\omega}{2}} + \frac{\Gamma^*\left(l+\frac{3}{2}\right)\Gamma^*(i\alpha\omega)}{\Gamma^*\left(\frac{l+3+i\alpha\omega}{2}\right)\Gamma^*\left(\frac{l+i\alpha\omega}{2}\right)} \left(1 + \frac{r^2}{\alpha^2}\right)^{-\frac{i\alpha\omega}{2}} \right\}. \quad (\text{B.41})$$

Also the angular part of the solution, the spherical harmonics $Y_{lm}(\theta, \phi)$ is defined in the present context as:

$$Y_{lm}(\theta, \phi) = (-1)^m \sqrt{\frac{(2l+1)(l-m)!}{4\pi(l+m)!}} P_{lm}(\cos\theta) e^{im\phi}. \quad (\text{B.42})$$

Further, summing over all l and m we get the following complete solution for the massless minimally coupled scalar field with gravity:

$$\begin{aligned} \Phi(t, r, \theta, \phi) &= \sum_{l=0}^{\infty} \sum_{m=-l}^{+l} \Phi_{lm}(t, r, \theta, \phi) \\ &= \frac{1}{2\alpha\sqrt{\pi\omega}} \sum_{l=0}^{\infty} \sum_{m=-l}^{+l} \frac{Y_{lm}(\theta, \phi) e^{-i\omega t}}{\left| \frac{\Gamma(l+\frac{3}{2})\Gamma(i\alpha\omega)}{\Gamma(\frac{l+3+i\alpha\omega}{2})\Gamma(\frac{l+i\alpha\omega}{2})} \right|} \\ &\quad \times \left\{ \frac{\Gamma\left(l+\frac{3}{2}\right)\Gamma(i\alpha\omega)}{\Gamma\left(\frac{l+3+i\alpha\omega}{2}\right)\Gamma\left(\frac{l+i\alpha\omega}{2}\right)} \left(1 + \frac{r^2}{\alpha^2}\right)^{\frac{i\alpha\omega}{2}} \right. \\ &\quad \left. + \frac{\Gamma^*\left(l+\frac{3}{2}\right)\Gamma^*(i\alpha\omega)}{\Gamma^*\left(\frac{l+3+i\alpha\omega}{2}\right)\Gamma^*\left(\frac{l+i\alpha\omega}{2}\right)} \left(1 + \frac{r^2}{\alpha^2}\right)^{-\frac{i\alpha\omega}{2}} \right\}. \quad (\text{B.43}) \end{aligned}$$

This classical solution of the field equation for the probe massless scalar field is very useful once we want to quantize the bath modes in the static patch of De Sitter space. In the next Appendix we discuss this in detail.

C Quantization of bath modes for probe massless scalar field in Static Patch of De Sitter Space

In this Appendix our prime objective is to quantize the bath modes for probe massless scalar field in the static patch of De Sitter space-time considering configuration space. Now, using

the classical solution in $D = 3$ for the massless probe scalar field derived in the previous section in the static patch of De Sitter Space, one can promote this as a quantum field by the following equation:

$$\hat{\Phi}(t, r, \theta, \phi) = \sum_{l=0}^{\infty} \sum_{m=-l}^{+l} \left[a_{lm} \Phi_{lm}(t, r, \theta, \phi) + a_{lm}^{\dagger} \Phi_{lm}^*(t, r, \theta, \phi) \right]. \quad (\text{C.1})$$

where the quantum states are defined through the following relation:

$$a_{lm} |\Psi\rangle = 0, \quad \text{where } l = 0, \dots, \infty; \quad m = -l, \dots, +l. \quad (\text{C.2})$$

Here, the field $\Phi_{lm}(t, r, \theta, \phi)$ is defined as:

$$\Phi_{lm}(t, r, \theta, \phi) = \frac{1}{2\alpha\sqrt{\pi\omega}} \frac{Y_{lm}(\theta, \phi) e^{-i\omega t}}{\left| \frac{\Gamma(l+\frac{3}{2})\Gamma(i\alpha\omega)}{\Gamma(\frac{l+3+i\alpha\omega}{2})\Gamma(\frac{l+i\alpha\omega}{2})} \right|} \left\{ \frac{\Gamma(l+\frac{3}{2})\Gamma(i\alpha\omega)}{\Gamma(\frac{l+3+i\alpha\omega}{2})\Gamma(\frac{l+i\alpha\omega}{2})} \left(1 + \frac{r^2}{\alpha^2}\right)^{\frac{i\alpha\omega}{2}} \right. \\ \left. + \frac{\Gamma^*(l+\frac{3}{2})\Gamma^*(i\alpha\omega)}{\Gamma^*(\frac{l+3+i\alpha\omega}{2})\Gamma^*(\frac{l+i\alpha\omega}{2})} \left(1 + \frac{r^2}{\alpha^2}\right)^{-\frac{i\alpha\omega}{2}} \right\}. \quad (\text{C.3})$$

Quantization of this quantum field demands the following equal time commutation relations:

$$\left[\hat{\Phi}(t, r, \theta, \phi), \hat{\Pi}_{\Phi}(t, r', \theta', \phi') \right] = \frac{1}{r^2} \delta(r - r') \delta(\cos \theta - \cos \theta') \delta(\phi - \phi'), \quad (\text{C.4})$$

$$\left[\hat{\Phi}(t, r, \theta, \phi), \hat{\Phi}(t, r', \theta', \phi') \right] = 0, \quad (\text{C.5})$$

$$\left[\hat{\Pi}_{\Phi}(t, r, \theta, \phi), \hat{\Pi}_{\Phi}(t, r', \theta', \phi') \right] = 0. \quad (\text{C.6})$$

Here $\hat{\Pi}_{\Phi}(t, r, \theta, \phi)$ is the canonically conjugate momentum of the quantum field $\hat{\Phi}(t, r, \theta, \phi)$, which in the static patch of De Sitter space can be computed as:

$$\hat{\Pi}_{\Phi}(t, r, \theta, \phi) = \sum_{l=0}^{\infty} \sum_{m=-l}^{+l} \left[a_{lm} \Pi_{lm, \Phi}(t, r, \theta, \phi) + a_{lm}^{\dagger} \Pi_{lm, \Phi}^*(t, r, \theta, \phi) \right], \quad (\text{C.7})$$

where $\Pi_{lm, \Phi}(t, r, \theta, \phi)$ can be expressed as:

$$\Pi_{lm, \Phi}(t, r, \theta, \phi) = r^2 \sin \theta \left(1 - \frac{r^2}{\alpha^2}\right)^{-1} \dot{\Phi}_{lm}(t, r, \theta, \phi), \quad (\text{C.8})$$

which in the limit $\alpha \rightarrow \infty$ exactly matches with the result obtained on a sphere. Here the symbol, ' \cdot ' is defined as, $\dot{X} = \partial_0 X = \partial_t X$.

Further, substituting this result back in the expression for the canonically conjugate quantum momentum operator of the scalar field we get:

$$\hat{\Pi}_{\Phi}(t, r, \theta, \phi) = r^2 \sin \theta \left(1 - \frac{r^2}{\alpha^2}\right)^{-1} \sum_{l=0}^{\infty} \sum_{m=-l}^{+l} \left[a_{lm} \dot{\Phi}_{lm}(t, r, \theta, \phi) + a_{lm}^{\dagger} \dot{\Phi}_{lm}^*(t, r, \theta, \phi) \right], \quad (\text{C.9})$$

where $\dot{\Phi}_{lm}(t, r, \theta, \phi)$ can be computed as:

$$\begin{aligned} \dot{\Phi}_{lm}(t, r, \theta, \phi) &= -i\omega\Phi_{lm}(t, r, \theta, \phi) \\ &= \frac{1}{2i\alpha} \sqrt{\frac{\omega}{\pi}} \frac{Y_{lm}(\theta, \phi) e^{-i\omega t}}{\left| \frac{\Gamma(l+\frac{3}{2})\Gamma(i\alpha\omega)}{\Gamma(\frac{l+3+i\alpha\omega}{2})\Gamma(\frac{l+i\alpha\omega}{2})} \right|} \left\{ \frac{\Gamma(l+\frac{3}{2})\Gamma(i\alpha\omega)}{\Gamma(\frac{l+3+i\alpha\omega}{2})\Gamma(\frac{l+i\alpha\omega}{2})} \left(1 + \frac{r^2}{\alpha^2}\right)^{\frac{i\alpha\omega}{2}} \right. \\ &\quad \left. + \frac{\Gamma^*(l+\frac{3}{2})\Gamma^*(i\alpha\omega)}{\Gamma^*(\frac{l+3+i\alpha\omega}{2})\Gamma^*(\frac{l+i\alpha\omega}{2})} \left(1 + \frac{r^2}{\alpha^2}\right)^{-\frac{i\alpha\omega}{2}} \right\}. \end{aligned} \quad (\text{C.10})$$

This will finally give rise to the following commutation relation which can be written previously mentioned creation and annihilation operators as:

$$[a_{lm}, a_{l'm'}^\dagger] = \delta_{ll'}\delta_{mm'}, \quad [a_{lm}^\dagger, a_{l'm'}^\dagger] = \delta_{ll'}\delta_{mm'}, \quad [a_{lm}, a_{l'm'}] = \delta_{ll'}\delta_{mm'}. \quad (\text{C.11})$$

Now, using the classical solution in $D = 3$ for the massless probe scalar field derived in the previous section in the static patch of De Sitter Space, one can promote this as a quantum field by the following equation in Fourier space as:

$$\begin{aligned} \hat{\Phi}(t, k_r) &= \int \frac{d^3x}{(2\pi)^3} e^{-i\mathbf{k}\cdot\mathbf{r}} \hat{\Phi}(t, r, \theta, \phi) \\ &= \frac{1}{(2\pi)^3} \int_0^\alpha dr \int_0^\pi d\theta \int_0^{2\pi} d\phi r^2 \sin\theta \left(1 - \frac{r^2}{\alpha^2}\right)^{-1} e^{-ik_r\alpha\sin^{-1}(\frac{r}{\alpha})\cos\theta} \hat{\Phi}(t, r, \theta, \phi) \\ &= \frac{1}{(2\pi)^3} \int_0^\alpha dr \int_0^\pi d\theta \int_0^{2\pi} d\phi r^2 \sin\theta \left(1 - \frac{r^2}{\alpha^2}\right)^{-1} e^{-ik_r\alpha\sin^{-1}(\frac{r}{\alpha})\cos\theta} \\ &\quad \times \sum_{l=0}^{\infty} \sum_{m=-l}^{+l} \left[a_{lm}\Phi_{lm}(t, r, \theta, \phi) + a_{lm}^\dagger\Phi_{lm}^*(t, r, \theta, \phi) \right]. \end{aligned} \quad (\text{C.12})$$

Here we have written the three part of the metric in the static coordinate patch of De Sitter space as given by the following expression:

$$\begin{aligned} ds_3^2 &= \left(1 - \frac{r^2}{\alpha^2}\right)^{-1} dr^2 + r^2(d\theta^2 + \sin^2\theta d\phi^2) \quad \text{where } \alpha = \sqrt{\frac{3}{\Lambda}} > 0 \\ &= \left\| \left(1 - \frac{r^2}{\alpha^2}\right)^{-1/2} dr \hat{\mathbf{r}} + r(d\theta \hat{\theta} + \sin\theta d\phi \hat{\phi}) \right\|^2 \\ &= d\mathbf{r}\cdot d\mathbf{r}, \end{aligned} \quad (\text{C.13})$$

where the infinitesimal change in the radial coordinate vector can be expressed as:

$$\begin{aligned} d\mathbf{r} &= \left(1 - \frac{r^2}{\alpha^2}\right)^{-1/2} dr \hat{\mathbf{r}} + r(d\theta \hat{\theta} + \sin\theta d\phi \hat{\phi}) \\ &= d\left(\alpha \sin^{-1}\left(\frac{r}{\alpha}\right)\right) \hat{\mathbf{r}} + \alpha \sin^{-1}\left(\frac{r}{\alpha}\right) d\hat{\mathbf{r}} \\ &= d\left(\alpha \sin^{-1}\left(\frac{r}{\alpha}\right) \hat{\mathbf{r}}\right), \end{aligned} \quad (\text{C.14})$$

which after integration on both the sides gives the following simplified expression for the radial coordinate vector describing the three part of the static coordinate patch of De Sitter space:

$$\mathbf{r} = \alpha \sin^{-1} \left(\frac{r}{\alpha} \right) \hat{\mathbf{r}}. \quad (\text{C.15})$$

It is important to note that for this derivation we have identified the infinitesimal change in the radial unit vector by the following expression:

$$d\hat{\mathbf{r}} = \frac{r}{\alpha} \frac{1}{\sin^{-1} \left(\frac{r}{\alpha} \right)} (d\theta \hat{\theta} + \sin \theta d\phi \hat{\phi}). \quad (\text{C.16})$$

Now, to check the physical consistency of the derived result we further take the limit $\alpha \rightarrow \infty$, in which we get the following expression:

$$\begin{aligned} \lim_{\alpha \rightarrow \infty} \alpha \sin^{-1} \left(\frac{r}{\alpha} \right) &= \lim_{\alpha \rightarrow \infty} \alpha \left[\left(\frac{r}{\alpha} \right) + \frac{1}{6} \left(\frac{r}{\alpha} \right)^3 + \frac{3}{40} \left(\frac{r}{\alpha} \right)^5 \dots \right] \\ &= r + \lim_{\alpha \rightarrow \infty} \left[\frac{r^3}{6\alpha^2} + \frac{3r^5}{40\alpha^4} + \dots \right] = r, \end{aligned} \quad (\text{C.17})$$

for which in the the limit $\alpha \rightarrow \infty$ we get, $\mathbf{r} = r \hat{\mathbf{r}}$.

D Bath Hamiltonian for probe massless scalar field in Static Patch of De Sitter Space

D.1 Constructing classical bath Hamiltonian

The bath is described by a massless probe scalar field, which is given by the following action:

$$S_{\text{Bath}} = \frac{1}{2} \int d^4x \sqrt{-g} g^{\mu\nu} (\partial_\mu \Phi(x)) (\partial_\nu \Phi(x)) = \int dt d^3x \mathcal{L}(g^{\mu\nu}, g, \partial_\mu \Phi), \quad (\text{D.1})$$

where $\mathcal{L}(g^{\mu\nu}, g, \partial_\mu \Phi)$ is the Lagrangian density in presence of background gravity, which can be explicitly written as:

$$\mathcal{L}(g^{\mu\nu}, g, \partial_\mu \Phi(x)) = \frac{1}{2} \sqrt{-g} g^{\mu\nu} (\partial_\mu \Phi(x)) (\partial_\nu \Phi(x)) \quad (\text{D.2})$$

Here the scalar field is embedded in static patch of the De Sitter space which is described by the following infinitesimal line element:

$$ds^2 = \left(1 - \frac{r^2}{\alpha^2} \right) dt^2 - \left(1 - \frac{r^2}{\alpha^2} \right)^{-1} dr^2 - r^2 (d\theta^2 + \sin^2 \theta d\phi^2) \quad \text{where } \alpha = \sqrt{\frac{3}{\Lambda}} > 0. \quad (\text{D.3})$$

Here $r = \alpha$ represents the horizon where we have space like singularity in the metric of static De Sitter space time.

The canonically conjugate momentum for this massless probe scalar field is given by the following expression:

$$\begin{aligned} \Pi_\Phi(x) &\equiv \frac{\partial \mathcal{L}(g^{\mu\nu}, g, \partial_\mu \Phi(x))}{\partial (\partial_0 \Phi(x))} \\ &= \frac{\partial \mathcal{L}(g^{\mu\nu}, g, \partial_\mu \Phi(x))}{\partial \dot{\Phi}(x)} \\ &= \sqrt{-g} g^{00} \dot{\Phi}(x) \end{aligned} \quad (\text{D.4})$$

and in static patch of De Sitter space we get:

$$\Pi_{\Phi}(t, r, \theta, \phi) = r^2 \sin \theta \left(1 - \frac{r^2}{\alpha^2}\right)^{-1} \dot{\Phi}(t, r, \theta, \phi). \quad (\text{D.5})$$

Here we have used the fact that:

$$\sqrt{-g} = r^2 \sin \theta \quad \text{and} \quad g^{00} = \left(1 - \frac{r^2}{\alpha^2}\right)^{-1}. \quad (\text{D.6})$$

From Eq (D.4), one can further write:

$$\dot{\Phi}(t, r, \theta, \Phi) = \frac{\Pi_{\Phi}(t, r, \theta, \phi)}{r^2 \sin \theta} \left(1 - \frac{r^2}{\alpha^2}\right), \quad (\text{D.7})$$

which we will use further to compute the expression for the bath Hamiltonian density.

Further, using Legendre transformation the Hamiltonian density in the static patch of the De Sitter space can be written as:

$$\begin{aligned} \mathcal{H}_{\text{Bath}} &= \Pi_{\Phi}(x) \dot{\Phi}(x) - \mathcal{L}(g^{\mu\nu}, g, \partial_{\mu}\Phi(x)) \\ &= \frac{\Pi_{\Phi}^2(t, r, \theta, \phi)}{r^2 \sin \theta} \left(1 - \frac{r^2}{\alpha^2}\right) - \mathcal{L}(g^{\mu\nu}, g, \partial_{\mu}\Phi(x)). \end{aligned} \quad (\text{D.8})$$

Now, in the static patch of the De Sitter space the Lagrangian density can be explicitly written as:

$$\begin{aligned} \mathcal{L}(g^{\mu\nu}, g, \partial_{\mu}\Phi(x)) &= \frac{1}{2} \sqrt{-g} g^{\mu\nu} (\partial_{\mu}\Phi(x)) (\partial_{\nu}\Phi(x)) \\ &= \frac{1}{2} r^2 \sin \theta \left\{ \frac{\Pi_{\Phi}^2(t, r, \theta, \phi)}{r^4 \sin^2 \theta} \left(1 - \frac{r^2}{\alpha^2}\right) - \left(1 - \frac{r^2}{\alpha^2}\right) (\partial_r \Phi(t, r, \theta, \phi))^2 \right. \\ &\quad \left. - \frac{1}{r^2} (\partial_{\theta} \Phi(t, r, \theta, \phi))^2 - \frac{1}{r^2 \sin^2 \theta} (\partial_{\phi} \Phi(t, r, \theta, \phi))^2 \right\} \\ &= \frac{1}{2} \left\{ \frac{\Pi_{\Phi}^2(t, r, \theta, \phi)}{r^2 \sin \theta} \left(1 - \frac{r^2}{\alpha^2}\right) - \left(1 - \frac{r^2}{\alpha^2}\right) r^2 \sin \theta (\partial_r \Phi(t, r, \theta, \phi))^2 \right. \\ &\quad \left. - \sin \theta (\partial_{\theta} \Phi(t, r, \theta, \phi))^2 - \frac{1}{\sin \theta} (\partial_{\phi} \Phi(t, r, \theta, \phi))^2 \right\}. \end{aligned} \quad (\text{D.9})$$

Using Eq (D.9), we get the following simplified expression for the Hamiltonian density in the static patch of De Sitter space:

$$\begin{aligned} \mathcal{H}_{\text{Bath}} &= \frac{\Pi_{\Phi}^2(t, r, \theta, \phi)}{2r^2 \sin \theta} \left(1 - \frac{r^2}{\alpha^2}\right) + \frac{1}{2} \left\{ \left(1 - \frac{r^2}{\alpha^2}\right) r^2 \sin \theta (\partial_r \Phi(t, r, \theta, \phi))^2 \right. \\ &\quad \left. + \sin \theta (\partial_{\theta} \Phi(t, r, \theta, \phi))^2 + \frac{1}{\sin \theta} (\partial_{\phi} \Phi(t, r, \theta, \phi))^2 \right\}. \end{aligned} \quad (\text{D.10})$$

Now the 3D spatial volume element in the static patch of the De Sitter space is given by the following expression:

$$d^3x = r^2 \sin \theta \left(1 - \frac{r^2}{\alpha^2}\right)^{-1} dr d\theta d\phi. \quad (\text{D.11})$$

Hence using this 3D spatial volume element the Hamiltonian of the bath in the static patch of the De Sitter space is given by the following expression:

$$\begin{aligned}
H_{\text{Bath}} &= \int d^3x \mathcal{H}_{\text{Bath}} \\
&= \int_0^\alpha dr \int_0^\pi d\theta \int_0^{2\pi} d\phi r^2 \sin\theta \left(1 - \frac{r^2}{\alpha^2}\right)^{-1} \\
&\quad \times \left[\frac{\Pi_\Phi^2(t, r, \theta, \phi)}{2r^2 \sin\theta} \left(1 - \frac{r^2}{\alpha^2}\right) + \frac{1}{2} \left\{ \left(1 - \frac{r^2}{\alpha^2}\right) r^2 \sin\theta (\partial_r \Phi(t, r, \theta, \phi))^2 \right. \right. \\
&\quad \left. \left. + \sin\theta (\partial_\theta \Phi(t, r, \theta, \phi))^2 + \frac{1}{\sin\theta} (\partial_\phi \Phi(t, r, \theta, \phi))^2 \right\} \right] \\
&= \int_0^\alpha dr \int_0^\pi d\theta \int_0^{2\pi} d\phi \left[\frac{\Pi_\Phi^2(\tau, r, \theta, \phi)}{2} \right. \\
&\quad \left. + \frac{r^2 \sin^2\theta}{2} \left\{ r^2 (\partial_r \Phi(\tau, r, \theta, \phi))^2 + \frac{\left((\partial_\theta \Phi(\tau, r, \theta, \phi))^2 + \frac{(\partial_\phi \Phi(\tau, r, \theta, \phi))^2}{\sin^2\theta} \right)}{\left(1 - \frac{r^2}{\alpha^2}\right)} \right\} \right]. \quad (\text{D.12})
\end{aligned}$$

In this description, $r = \alpha$, which is the upper limit of the radial integral physically represents the horizon in static patch of De Sitter space.

Here it is important to note that, if we further take the $\alpha \rightarrow \infty$ limit then we get the following result:

$$\begin{aligned}
H_{\text{Bath}} &= \int_0^\infty dr \int_0^\pi d\theta \int_0^{2\pi} d\phi \left[\frac{\Pi_\Phi^2(\tau, r, \theta, \phi)}{2} \right. \\
&\quad \left. + \frac{r^2 \sin^2\theta}{2} \left\{ r^2 (\partial_r \Phi(\tau, r, \theta, \phi))^2 + \left((\partial_\theta \Phi(\tau, r, \theta, \phi))^2 + \frac{(\partial_\phi \Phi(\tau, r, \theta, \phi))^2}{\sin^2\theta} \right) \right\} \right], \quad (\text{D.13})
\end{aligned}$$

which represents the Hamiltonian of a sphere with radius R .

D.2 Constructing quantized bath Hamiltonian

In this subsection our prime objective is to express the classical Hamiltonian derived in the previous section. Here we start with the following expression for the quantum Hamiltonian written for bath in the background of static patch of De Sitter space as given by:

$$\begin{aligned}
\hat{H}_{\text{Bath}} &= \int_0^\alpha dr \int_0^\pi d\theta \int_0^{2\pi} d\phi \left[\frac{\hat{\Pi}_\Phi^2(\tau, r, \theta, \phi)}{2} \right. \\
&\quad \left. + \frac{r^2 \sin^2\theta}{2} \left\{ r^2 (\partial_r \hat{\Phi}(\tau, r, \theta, \phi))^2 + \frac{\left((\partial_\theta \hat{\Phi}(\tau, r, \theta, \phi))^2 + \frac{(\partial_\phi \hat{\Phi}(\tau, r, \theta, \phi))^2}{\sin^2\theta} \right)}{\left(1 - \frac{r^2}{\alpha^2}\right)} \right\} \right]. \quad (\text{D.14})
\end{aligned}$$

To write the Hamiltonian in terms the creation and annihilation operators we write down the quantized solution for the scalar field as:

$$\hat{\Phi}(t, r, \theta, \phi) = \sum_{l=0}^{\infty} \sum_{m=-l}^{+l} \left[a_{lm} \Phi_{lm}(t, r, \theta, \phi) + a_{lm}^\dagger \Phi_{lm}^*(t, r, \theta, \phi) \right]. \quad (\text{D.15})$$

where the quantum states are defined through the following relation:

$$a_{lm}|\Psi\rangle = 0, \quad \text{where } l = 0, \dots, \infty; \quad m = -l, \dots, +l. \quad (\text{D.16})$$

Here, the field $\Phi_{lm}(t, r, \theta, \phi)$ is defined as:

$$\begin{aligned} \Phi_{lm}(t, r, \theta, \phi) = \frac{1}{2\alpha\sqrt{\pi\omega}} \frac{Y_{lm}(\theta, \phi) e^{-i\omega t}}{\left| \frac{\Gamma(l+\frac{3}{2})\Gamma(i\alpha\omega)}{\Gamma(\frac{l+3+i\alpha\omega}{2})\Gamma(\frac{l+i\alpha\omega}{2})} \right|} & \left\{ \frac{\Gamma(l+\frac{3}{2})\Gamma(i\alpha\omega)}{\Gamma(\frac{l+3+i\alpha\omega}{2})\Gamma(\frac{l+i\alpha\omega}{2})} \left(1 + \frac{r^2}{\alpha^2}\right)^{\frac{i\alpha\omega}{2}} \right. \\ & \left. + \frac{\Gamma^*(l+\frac{3}{2})\Gamma^*(i\alpha\omega)}{\Gamma^*(\frac{l+3+i\alpha\omega}{2})\Gamma^*(\frac{l+i\alpha\omega}{2})} \left(1 + \frac{r^2}{\alpha^2}\right)^{-\frac{i\alpha\omega}{2}} \right\}. \quad (\text{D.17}) \end{aligned}$$

Further, substituting this result back in the expression for the square of the canonically conjugate quantum momentum operator of the scalar field we get:

$$\hat{\Pi}_{\Phi}^2(t, r, \theta, \phi) = r^4 \sin^2 \theta \left(1 - \frac{r^2}{\alpha^2}\right)^{-2} \left(\sum_{l=0}^{\infty} \sum_{m=-l}^{+l} \left[a_{lm} \dot{\Phi}_{lm}(t, r, \theta, \phi) + a_{lm}^{\dagger} \dot{\Phi}_{lm}^*(t, r, \theta, \phi) \right] \right)^2, \quad (\text{D.18})$$

where $\dot{\Phi}_{lm}(t, r, \theta, \phi)$ can be computed as:

$$\begin{aligned} \dot{\Phi}_{lm}(t, r, \theta, \phi) &= -i\omega \Phi_{lm}(t, r, \theta, \phi) \\ &= \frac{1}{2i\alpha} \sqrt{\frac{\omega}{\pi}} \frac{Y_{lm}(\theta, \phi) e^{-i\omega t}}{\left| \frac{\Gamma(l+\frac{3}{2})\Gamma(i\alpha\omega)}{\Gamma(\frac{l+3+i\alpha\omega}{2})\Gamma(\frac{l+i\alpha\omega}{2})} \right|} \left\{ \frac{\Gamma(l+\frac{3}{2})\Gamma(i\alpha\omega)}{\Gamma(\frac{l+3+i\alpha\omega}{2})\Gamma(\frac{l+i\alpha\omega}{2})} \left(1 + \frac{r^2}{\alpha^2}\right)^{\frac{i\alpha\omega}{2}} \right. \\ & \quad \left. + \frac{\Gamma^*(l+\frac{3}{2})\Gamma^*(i\alpha\omega)}{\Gamma^*(\frac{l+3+i\alpha\omega}{2})\Gamma^*(\frac{l+i\alpha\omega}{2})} \left(1 + \frac{r^2}{\alpha^2}\right)^{-\frac{i\alpha\omega}{2}} \right\}. \quad (\text{D.19}) \end{aligned}$$

Additionally, $(\partial_r \Phi(t, r, \theta, \phi))$, $(\partial_{\theta} \Phi(t, r, \theta, \phi))$ and $(\partial_{\phi} \Phi(t, r, \theta, \phi))$ can be computed as:

$$\begin{aligned} \partial_r \Phi(t, r, \theta, \phi) &= \frac{r}{\alpha^2} \sqrt{\frac{\omega}{\pi}} \frac{Y_{lm}(\theta, \phi) e^{-i\omega t}}{\left| \frac{\Gamma(l+\frac{3}{2})\Gamma(i\alpha\omega)}{\Gamma(\frac{l+3+i\alpha\omega}{2})\Gamma(\frac{l+i\alpha\omega}{2})} \right|} \left\{ \frac{\Gamma(l+\frac{3}{2})\Gamma(i\alpha\omega)}{\Gamma(\frac{l+3+i\alpha\omega}{2})\Gamma(\frac{l+i\alpha\omega}{2})} \left(1 + \frac{r^2}{\alpha^2}\right)^{\frac{i\alpha\omega}{2}-1} \right. \\ & \quad \left. - \frac{\Gamma^*(l+\frac{3}{2})\Gamma^*(i\alpha\omega)}{\Gamma^*(\frac{l+3+i\alpha\omega}{2})\Gamma^*(\frac{l+i\alpha\omega}{2})} \left(1 + \frac{r^2}{\alpha^2}\right)^{-\left(\frac{i\alpha\omega}{2}+1\right)} \right\}, \quad (\text{D.20}) \end{aligned}$$

$$\begin{aligned} \partial_{\theta} \Phi(t, r, \theta, \phi) &= \frac{1}{2\alpha\sqrt{\pi\omega}} \frac{\partial_{\theta} Y_{lm}(\theta, \phi) e^{-i\omega t}}{\left| \frac{\Gamma(l+\frac{3}{2})\Gamma(i\alpha\omega)}{\Gamma(\frac{l+3+i\alpha\omega}{2})\Gamma(\frac{l+i\alpha\omega}{2})} \right|} \left\{ \frac{\Gamma(l+\frac{3}{2})\Gamma(i\alpha\omega)}{\Gamma(\frac{l+3+i\alpha\omega}{2})\Gamma(\frac{l+i\alpha\omega}{2})} \left(1 + \frac{r^2}{\alpha^2}\right)^{\frac{i\alpha\omega}{2}} \right. \\ & \quad \left. + \frac{\Gamma^*(l+\frac{3}{2})\Gamma^*(i\alpha\omega)}{\Gamma^*(\frac{l+3+i\alpha\omega}{2})\Gamma^*(\frac{l+i\alpha\omega}{2})} \left(1 + \frac{r^2}{\alpha^2}\right)^{-\frac{i\alpha\omega}{2}} \right\}, \quad (\text{D.21}) \end{aligned}$$

$$\begin{aligned} \partial_\phi \Phi(t, r, \theta, \phi) = \frac{1}{2\alpha\sqrt{\pi\omega}} \frac{\partial_\phi Y_{lm}(\theta, \phi) e^{-i\omega t}}{\left| \frac{\Gamma(l+\frac{3}{2})\Gamma(i\alpha\omega)}{\Gamma(\frac{l+3+i\alpha\omega}{2})\Gamma(\frac{l+i\alpha\omega}{2})} \right|} \left\{ \frac{\Gamma(l+\frac{3}{2})\Gamma(i\alpha\omega)}{\Gamma(\frac{l+3+i\alpha\omega}{2})\Gamma(\frac{l+i\alpha\omega}{2})} \left(1 + \frac{r^2}{\alpha^2}\right)^{\frac{i\alpha\omega}{2}} \right. \\ \left. + \frac{\Gamma^*(l+\frac{3}{2})\Gamma^*(i\alpha\omega)}{\Gamma^*(\frac{l+3+i\alpha\omega}{2})\Gamma^*(\frac{l+i\alpha\omega}{2})} \left(1 + \frac{r^2}{\alpha^2}\right)^{-\frac{i\alpha\omega}{2}} \right\}. \quad (\text{D.22}) \end{aligned}$$

Consequently, the corresponding quantum operators can be computed as:

$$\begin{aligned} \partial_r \hat{\Phi}(t, r, \theta, \phi) &= \sum_{l=0}^{\infty} \sum_{m=-l}^{+l} \left[a_{lm} \partial_r \Phi_{lm}(t, r, \theta, \phi) + a_{lm}^\dagger \partial_r \Phi_{lm}^*(t, r, \theta, \phi) \right] \\ &= \frac{r}{\alpha^2} \sqrt{\frac{\omega}{\pi}} \sum_{l=0}^{\infty} \sum_{m=-l}^{+l} \left[a_{lm} \frac{Y_{lm}(\theta, \phi) e^{-i\omega t}}{\left| \frac{\Gamma(l+\frac{3}{2})\Gamma(i\alpha\omega)}{\Gamma(\frac{l+3+i\alpha\omega}{2})\Gamma(\frac{l+i\alpha\omega}{2})} \right|} \left\{ \frac{\Gamma(l+\frac{3}{2})\Gamma(i\alpha\omega)}{\Gamma(\frac{l+3+i\alpha\omega}{2})\Gamma(\frac{l+i\alpha\omega}{2})} \left(1 + \frac{r^2}{\alpha^2}\right)^{\frac{i\alpha\omega}{2}-1} \right. \right. \\ &\quad \left. \left. - \frac{\Gamma^*(l+\frac{3}{2})\Gamma^*(i\alpha\omega)}{\Gamma^*(\frac{l+3+i\alpha\omega}{2})\Gamma^*(\frac{l+i\alpha\omega}{2})} \left(1 + \frac{r^2}{\alpha^2}\right)^{-\left(\frac{i\alpha\omega}{2}+1\right)} \right\} \right. \\ &\quad \left. + a_{lm}^\dagger \frac{Y_{lm}^*(\theta, \phi) e^{i\omega t}}{\left| \frac{\Gamma^*(l+\frac{3}{2})\Gamma^*(i\alpha\omega)}{\Gamma^*(\frac{l+3+i\alpha\omega}{2})\Gamma^*(\frac{l+i\alpha\omega}{2})} \right|} \left\{ \frac{\Gamma^*(l+\frac{3}{2})\Gamma^*(i\alpha\omega)}{\Gamma^*(\frac{l+3+i\alpha\omega}{2})\Gamma^*(\frac{l+i\alpha\omega}{2})} \left(1 + \frac{r^2}{\alpha^2}\right)^{-\left(\frac{i\alpha\omega}{2}+1\right)} \right. \right. \\ &\quad \left. \left. - \frac{\Gamma(l+\frac{3}{2})\Gamma(i\alpha\omega)}{\Gamma(\frac{l+3+i\alpha\omega}{2})\Gamma(\frac{l+i\alpha\omega}{2})} \left(1 + \frac{r^2}{\alpha^2}\right)^{\frac{i\alpha\omega}{2}-1} \right\} \right], \quad (\text{D.23}) \end{aligned}$$

$$\begin{aligned} \partial_\theta \hat{\Phi}(t, r, \theta, \phi) &= \sum_{l=0}^{\infty} \sum_{m=-l}^{+l} \left[a_{lm} \partial_\theta \Phi_{lm}(t, r, \theta, \phi) + a_{lm}^\dagger \partial_\theta \Phi_{lm}^*(t, r, \theta, \phi) \right] \\ &= \frac{1}{2\alpha\sqrt{\pi\omega}} \sum_{l=0}^{\infty} \sum_{m=-l}^{+l} \left[a_{lm} \frac{\partial_\theta Y_{lm}(\theta, \phi) e^{-i\omega t}}{\left| \frac{\Gamma(l+\frac{3}{2})\Gamma(i\alpha\omega)}{\Gamma(\frac{l+3+i\alpha\omega}{2})\Gamma(\frac{l+i\alpha\omega}{2})} \right|} \left\{ \frac{\Gamma(l+\frac{3}{2})\Gamma(i\alpha\omega)}{\Gamma(\frac{l+3+i\alpha\omega}{2})\Gamma(\frac{l+i\alpha\omega}{2})} \left(1 + \frac{r^2}{\alpha^2}\right)^{\frac{i\alpha\omega}{2}} \right. \right. \\ &\quad \left. \left. + \frac{\Gamma^*(l+\frac{3}{2})\Gamma^*(i\alpha\omega)}{\Gamma^*(\frac{l+3+i\alpha\omega}{2})\Gamma^*(\frac{l+i\alpha\omega}{2})} \left(1 + \frac{r^2}{\alpha^2}\right)^{-\frac{i\alpha\omega}{2}} \right\} \right. \\ &\quad \left. + a_{lm}^\dagger \frac{(\partial_\theta Y_{lm}(\theta, \phi))^* e^{i\omega t}}{\left| \frac{\Gamma^*(l+\frac{3}{2})\Gamma^*(i\alpha\omega)}{\Gamma^*(\frac{l+3+i\alpha\omega}{2})\Gamma^*(\frac{l+i\alpha\omega}{2})} \right|} \left\{ \frac{\Gamma^*(l+\frac{3}{2})\Gamma^*(i\alpha\omega)}{\Gamma^*(\frac{l+3+i\alpha\omega}{2})\Gamma^*(\frac{l+i\alpha\omega}{2})} \left(1 + \frac{r^2}{\alpha^2}\right)^{-\frac{i\alpha\omega}{2}} \right. \right. \\ &\quad \left. \left. + \frac{\Gamma(l+\frac{3}{2})\Gamma(i\alpha\omega)}{\Gamma(\frac{l+3+i\alpha\omega}{2})\Gamma(\frac{l+i\alpha\omega}{2})} \left(1 + \frac{r^2}{\alpha^2}\right)^{\frac{i\alpha\omega}{2}} \right\} \right], \quad (\text{D.24}) \end{aligned}$$

$$\begin{aligned}
\partial_\phi \hat{\Phi}(t, r, \theta, \phi) &= \sum_{l=0}^{\infty} \sum_{m=-l}^{+l} \left[a_{lm} \partial_\phi \Phi_{lm}(t, r, \theta, \phi) + a_{lm}^\dagger \partial_\phi \Phi_{lm}^*(t, r, \theta, \phi) \right] \\
&= \frac{1}{2\alpha\sqrt{\pi\omega}} \sum_{l=0}^{\infty} \sum_{m=-l}^{+l} \left[a_{lm} \frac{\partial_\phi Y_{lm}(\theta, \phi) e^{-i\omega t}}{\left| \frac{\Gamma(l+\frac{3}{2})\Gamma(i\alpha\omega)}{\Gamma(\frac{l+3+i\alpha\omega}{2})\Gamma(\frac{l+i\alpha\omega}{2})} \right|} \left\{ \frac{\Gamma(l+\frac{3}{2})\Gamma(i\alpha\omega)}{\Gamma(\frac{l+3+i\alpha\omega}{2})\Gamma(\frac{l+i\alpha\omega}{2})} \left(1 + \frac{r^2}{\alpha^2}\right)^{\frac{i\alpha\omega}{2}} \right. \right. \\
&\quad \left. \left. + \frac{\Gamma^*(l+\frac{3}{2})\Gamma^*(i\alpha\omega)}{\Gamma^*(\frac{l+3+i\alpha\omega}{2})\Gamma^*(\frac{l+i\alpha\omega}{2})} \left(1 + \frac{r^2}{\alpha^2}\right)^{-\frac{i\alpha\omega}{2}} \right\} \right. \\
&\quad \left. + a_{lm}^\dagger \frac{(\partial_\phi Y_{lm}(\theta, \phi))^* e^{i\omega t}}{\left| \frac{\Gamma^*(l+\frac{3}{2})\Gamma^*(i\alpha\omega)}{\Gamma^*(\frac{l+3+i\alpha\omega}{2})\Gamma^*(\frac{l+i\alpha\omega}{2})} \right|} \left\{ \frac{\Gamma^*(l+\frac{3}{2})\Gamma^*(i\alpha\omega)}{\Gamma^*(\frac{l+3+i\alpha\omega}{2})\Gamma^*(\frac{l+i\alpha\omega}{2})} \left(1 + \frac{r^2}{\alpha^2}\right)^{-\frac{i\alpha\omega}{2}} \right. \right. \\
&\quad \left. \left. + \frac{\Gamma(l+\frac{3}{2})\Gamma(i\alpha\omega)}{\Gamma(\frac{l+3+i\alpha\omega}{2})\Gamma(\frac{l+i\alpha\omega}{2})} \left(1 + \frac{r^2}{\alpha^2}\right)^{\frac{i\alpha\omega}{2}} \right\} \right]. \tag{D.25}
\end{aligned}$$

Consequently, the quantized version of the bath Hamiltonian can be expressed in terms of the creation and annihilation operators as:

$$\begin{aligned}
\hat{H}_{\text{Bath}} &= \int_0^\alpha dr \int_0^\pi d\theta \int_0^{2\pi} d\phi \\
&\quad \left[\frac{1}{2} r^4 \sin^2 \theta \left(1 - \frac{r^2}{\alpha^2}\right)^{-2} \left(\sum_{l=0}^{\infty} \sum_{m=-l}^{+l} \left[a_{lm} \dot{\Phi}_{lm}(t, r, \theta, \phi) + a_{lm}^\dagger \dot{\Phi}_{lm}^*(t, r, \theta, \phi) \right] \right)^2 \right. \\
&\quad + \frac{r^2 \sin^2 \theta}{2} \left\{ r^2 \left(\sum_{l=0}^{\infty} \sum_{m=-l}^{+l} \left[a_{lm} \partial_r \Phi_{lm}(t, r, \theta, \phi) + a_{lm}^\dagger \partial_r \Phi_{lm}^*(t, r, \theta, \phi) \right] \right)^2 \right. \\
&\quad \quad \left. + \left(1 - \frac{r^2}{\alpha^2}\right)^{-1} \left(\sum_{l=0}^{\infty} \sum_{m=-l}^{+l} \left[a_{lm} \partial_\phi \Phi_{lm}(t, r, \theta, \phi) + a_{lm}^\dagger \partial_\phi \Phi_{lm}^*(t, r, \theta, \phi) \right] \right)^2 \right. \\
&\quad \left. + \frac{1}{\sin^2 \theta} \left(1 - \frac{r^2}{\alpha^2}\right)^{-1} \left(\sum_{l=0}^{\infty} \sum_{m=-l}^{+l} \left[a_{lm} \partial_\phi \Phi_{lm}(t, r, \theta, \phi) + a_{lm}^\dagger \partial_\phi \Phi_{lm}^*(t, r, \theta, \phi) \right] \right)^2 \right\}. \tag{D.26}
\end{aligned}$$

Further, considering only the normal ordered contribution we get the following simplified expression for the bath Hamiltonian, as given by:

$$\hat{H}_{\text{Bath}}(t) = \sum_{l=0}^{\infty} \sum_{m=-l}^{+l} \frac{\omega_{lm}(t)}{2} a_{lm}^\dagger a_{lm}, \tag{D.27}$$

where the quantization frequency $\omega_{lm}(t)$ is defined as:

$$\begin{aligned}
\omega_{lm}(t) &= 2 \int_0^\alpha dr \int_0^\pi d\theta \int_0^{2\pi} d\phi \left[r^4 \sin^2 \theta \left(1 - \frac{r^2}{\alpha^2} \right)^{-2} \left| \dot{\Phi}_{lm}(t, r, \theta, \phi) \right|^2 \right. \\
&\quad + r^2 \sin^2 \theta \left\{ r^2 \left| \partial_r \Phi_{lm}(t, r, \theta, \phi) \right|^2 + 2 \left(1 - \frac{r^2}{\alpha^2} \right)^{-1} \left| \partial_\theta \Phi_{lm}(t, r, \theta, \phi) \right|^2 \right. \\
&\quad \left. \left. + \frac{1}{\sin^2 \theta} \left(1 - \frac{r^2}{\alpha^2} \right)^{-1} \left| \partial_\phi \Phi_{lm}(t, r, \theta, \phi) \right|^2 \right\} \right] \\
&= 2 \int_0^\alpha dr \int_0^\pi d\theta \int_0^{2\pi} d\phi \\
&\quad \left[r^4 \sin^2 \theta \left(1 - \frac{r^2}{\alpha^2} \right)^{-2} \left| \frac{1}{2i\alpha} \sqrt{\frac{\omega}{\pi}} \frac{Y_{lm}(\theta, \phi) e^{-i\omega t}}{\left| \frac{\Gamma(l+\frac{3}{2})\Gamma(i\alpha\omega)}{\Gamma(\frac{l+3+i\alpha\omega}{2})\Gamma(\frac{l+i\alpha\omega}{2})} \right|} \left\{ \frac{\Gamma(l+\frac{3}{2})\Gamma(i\alpha\omega)}{\Gamma(\frac{l+3+i\alpha\omega}{2})\Gamma(\frac{l+i\alpha\omega}{2})} \left(1 + \frac{r^2}{\alpha^2} \right)^{\frac{i\alpha\omega}{2}} \right. \right. \right. \\
&\quad \left. \left. \left. + \frac{\Gamma^*(l+\frac{3}{2})\Gamma^*(i\alpha\omega)}{\Gamma^*(\frac{l+3+i\alpha\omega}{2})\Gamma^*(\frac{l+i\alpha\omega}{2})} \left(1 + \frac{r^2}{\alpha^2} \right)^{-\frac{i\alpha\omega}{2}} \right\} \right|^2 \right. \\
&\quad + r^2 \sin^2 \theta \left\{ r^2 \left| \frac{r}{\alpha^2} \sqrt{\frac{\omega}{\pi}} \frac{Y_{lm}(\theta, \phi) e^{-i\omega t}}{\left| \frac{\Gamma(l+\frac{3}{2})\Gamma(i\alpha\omega)}{\Gamma(\frac{l+3+i\alpha\omega}{2})\Gamma(\frac{l+i\alpha\omega}{2})} \right|} \left\{ \frac{\Gamma(l+\frac{3}{2})\Gamma(i\alpha\omega)}{\Gamma(\frac{l+3+i\alpha\omega}{2})\Gamma(\frac{l+i\alpha\omega}{2})} \left(1 + \frac{r^2}{\alpha^2} \right)^{\frac{i\alpha\omega}{2}-1} \right. \right. \right. \\
&\quad \left. \left. \left. - \frac{\Gamma^*(l+\frac{3}{2})\Gamma^*(i\alpha\omega)}{\Gamma^*(\frac{l+3+i\alpha\omega}{2})\Gamma^*(\frac{l+i\alpha\omega}{2})} \left(1 + \frac{r^2}{\alpha^2} \right)^{-\frac{i\alpha\omega}{2}+1} \right\} \right|^2 \right. \\
&\quad + 2 \left(1 - \frac{r^2}{\alpha^2} \right)^{-1} \left| \frac{1}{2\alpha\sqrt{\pi\omega}} \frac{\partial_\theta Y_{lm}(\theta, \phi) e^{-i\omega t}}{\left| \frac{\Gamma(l+\frac{3}{2})\Gamma(i\alpha\omega)}{\Gamma(\frac{l+3+i\alpha\omega}{2})\Gamma(\frac{l+i\alpha\omega}{2})} \right|} \left\{ \frac{\Gamma(l+\frac{3}{2})\Gamma(i\alpha\omega)}{\Gamma(\frac{l+3+i\alpha\omega}{2})\Gamma(\frac{l+i\alpha\omega}{2})} \left(1 + \frac{r^2}{\alpha^2} \right)^{\frac{i\alpha\omega}{2}} \right. \right. \\
&\quad \left. \left. \left. + \frac{\Gamma^*(l+\frac{3}{2})\Gamma^*(i\alpha\omega)}{\Gamma^*(\frac{l+3+i\alpha\omega}{2})\Gamma^*(\frac{l+i\alpha\omega}{2})} \left(1 + \frac{r^2}{\alpha^2} \right)^{-\frac{i\alpha\omega}{2}} \right\} \right|^2 \right. \\
&\quad + \frac{1}{\sin^2 \theta} \left(1 - \frac{r^2}{\alpha^2} \right)^{-1} \left| \frac{1}{2\alpha\sqrt{\pi\omega}} \frac{\partial_\phi Y_{lm}(\theta, \phi) e^{-i\omega t}}{\left| \frac{\Gamma(l+\frac{3}{2})\Gamma(i\alpha\omega)}{\Gamma(\frac{l+3+i\alpha\omega}{2})\Gamma(\frac{l+i\alpha\omega}{2})} \right|} \left\{ \frac{\Gamma(l+\frac{3}{2})\Gamma(i\alpha\omega)}{\Gamma(\frac{l+3+i\alpha\omega}{2})\Gamma(\frac{l+i\alpha\omega}{2})} \left(1 + \frac{r^2}{\alpha^2} \right)^{\frac{i\alpha\omega}{2}} \right. \right. \\
&\quad \left. \left. \left. + \frac{\Gamma^*(l+\frac{3}{2})\Gamma^*(i\alpha\omega)}{\Gamma^*(\frac{l+3+i\alpha\omega}{2})\Gamma^*(\frac{l+i\alpha\omega}{2})} \left(1 + \frac{r^2}{\alpha^2} \right)^{-\frac{i\alpha\omega}{2}} \right\} \right|^2 \right] \Bigg], \quad (D.28)
\end{aligned}$$

which one can explicitly compute for our problem by substituting the classical solution of the probe scalar field $\Phi_{lm}(t, r, \theta, \phi)$.

E Quantum states for many body (two atomic) entangled states

Set of eigenstates ($|g_1\rangle, |e_1\rangle$) and ($|g_2\rangle, |e_2\rangle$) of the two body (atomic) system are described by the following expressions:

A. For atom 1 :

$$H_1 = \frac{\omega}{2} (\sigma_1^1 \cos \alpha^1 + \sigma_2^1 \cos \beta^1 + \sigma_3^1 \cos \gamma^1)$$

$$= \frac{\omega}{2} \begin{pmatrix} \sigma_0 \cos \gamma^1 & \sigma_0 (\cos \alpha^1 - i \cos \beta^1) \\ \sigma_0 (\cos \alpha^1 + i \cos \beta^1) & -\sigma_0 \cos \gamma^1 \end{pmatrix}$$

Ground state \Rightarrow

$$|g_1\rangle = \frac{1}{\sqrt{2}} \sqrt{1 + \cos \gamma^1} \begin{pmatrix} -\frac{(\cos \alpha^1 - i \cos \beta^1)}{1 + \cos \gamma^1} \\ 1 \end{pmatrix} \Rightarrow \text{Eigenvalue } E_G^{(2)} = -\frac{\omega}{2}, \quad (\text{E.1})$$

Excited state \Rightarrow

$$|e_1\rangle = \frac{1}{\sqrt{2}} \sqrt{1 + \cos \gamma^1} \begin{pmatrix} 1 \\ \frac{(\cos \alpha^1 + i \cos \beta^1)}{1 + \cos \gamma^1} \end{pmatrix} \Rightarrow \text{Eigenvalue } E_E^{(2)} = \frac{\omega}{2}. \quad (\text{E.2})$$

B. For atom 2 :

$$H_1 = \frac{\omega}{2} (\sigma_1^2 \cos \alpha^1 + \sigma_2^2 \cos \beta^1 + \sigma_3^2 \cos \gamma^1)$$

$$= \frac{\omega}{2} \begin{pmatrix} \sigma_1 \cos \alpha^2 + \sigma_2 \cos \beta^2 + \sigma_3 \cos \gamma^2 & 0 \\ 0 & \sigma_1 \cos \alpha^2 + \sigma_2 \cos \beta^2 + \sigma_3 \cos \gamma^2 \end{pmatrix}$$

Ground state \Rightarrow

$$|g_2\rangle = \frac{1}{\sqrt{2}} \sqrt{1 + \cos \gamma^2} \begin{pmatrix} -\frac{(\cos \alpha^2 - i \cos \beta^2)}{1 + \cos \gamma^2} \\ 1 \end{pmatrix} \Rightarrow \text{Eigenvalue } E_G^{(2)} = -\frac{\omega}{2}, \quad (\text{E.3})$$

Excited state \Rightarrow

$$|e_2\rangle = \frac{1}{\sqrt{2}} \sqrt{1 + \cos \gamma^2} \begin{pmatrix} 1 \\ \frac{(\cos \alpha^2 + i \cos \beta^2)}{1 + \cos \gamma^2} \end{pmatrix} \Rightarrow \text{Eigenvalue } E_E^{(2)} = \frac{\omega}{2}. \quad (\text{E.4})$$

In the collective state representation the ground state ($|G\rangle$), excited state ($|E\rangle$), symmetric state ($|S\rangle$) and the anti-symmetric state ($|A\rangle$) of the two-entangled atomic system can be

expressed by the following expression:

1. Ground state : \Rightarrow

$$|G\rangle = |g_1\rangle \otimes |g_2\rangle = \frac{1}{2} \sqrt{(1 + \cos \gamma^1)(1 + \cos \gamma^2)} \begin{pmatrix} -\frac{(\cos \alpha^1 - i \cos \beta^1)(\cos \alpha^2 - i \cos \beta^2)}{1 + \cos \gamma^1} \\ -\frac{(\cos \alpha^1 - i \cos \beta^1)}{1 + \cos \gamma^1} \\ -\frac{(\cos \alpha^2 - i \cos \beta^2)}{1 + \cos \gamma^2} \\ 1 \end{pmatrix}, \quad (\text{E.5})$$

2. Excited state : \Rightarrow

$$|E\rangle = |e_1\rangle \otimes |e_2\rangle = \frac{1}{2} \sqrt{(1 + \cos \gamma^1)(1 + \cos \gamma^2)} \begin{pmatrix} 1 \\ \frac{(\cos \alpha^2 + i \cos \beta^2)}{1 + \cos \gamma^2} \\ \frac{(\cos \alpha^1 + i \cos \beta^1)}{1 + \cos \gamma^1} \\ \frac{(\cos \alpha^1 + i \cos \beta^1)(\cos \alpha^2 + i \cos \beta^2)}{1 + \cos \gamma^1} \end{pmatrix}, \quad (\text{E.6})$$

3. Symmetric state : \Rightarrow

$$\begin{aligned} |S\rangle &= \frac{1}{\sqrt{2}} [|e_1\rangle \otimes |g_2\rangle + |g_1\rangle \otimes |e_2\rangle] \\ &= \frac{1}{2\sqrt{2}} \sqrt{(1 + \cos \gamma^1)(1 + \cos \gamma^2)} \begin{pmatrix} -\frac{(\cos \alpha^1 - i \cos \beta^1)}{1 + \cos \gamma^1} - \frac{(\cos \alpha^2 - i \cos \beta^2)}{1 + \cos \gamma^2} \\ 1 - \frac{(\cos \alpha^1 - i \cos \beta^1)(\cos \alpha^2 + i \cos \beta^2)}{1 + \cos \gamma^1} \\ 1 - \frac{(\cos \alpha^1 + i \cos \beta^1)(\cos \alpha^2 - i \cos \beta^2)}{1 + \cos \gamma^1} \\ \frac{(\cos \alpha^1 + i \cos \beta^1)}{1 + \cos \gamma^1} + \frac{(\cos \alpha^2 + i \cos \beta^2)}{1 + \cos \gamma^2} \end{pmatrix}, \quad (\text{E.7}) \end{aligned}$$

4. Antisymmetric state : \Rightarrow

$$\begin{aligned} |S\rangle &= \frac{1}{\sqrt{2}} [|e_1\rangle \otimes |g_2\rangle + |g_1\rangle \otimes |e_2\rangle] \\ &= \frac{1}{2\sqrt{2}} \sqrt{(1 + \cos \gamma^1)(1 + \cos \gamma^2)} \begin{pmatrix} \frac{(\cos \alpha^1 - i \cos \beta^1)}{1 + \cos \gamma^1} - \frac{(\cos \alpha^2 - i \cos \beta^2)}{1 + \cos \gamma^2} \\ 1 + \frac{(\cos \alpha^1 - i \cos \beta^1)(\cos \alpha^2 + i \cos \beta^2)}{1 + \cos \gamma^1} \\ -1 - \frac{(\cos \alpha^1 + i \cos \beta^1)(\cos \alpha^2 - i \cos \beta^2)}{1 + \cos \gamma^1} \\ \frac{(\cos \alpha^1 + i \cos \beta^1)}{1 + \cos \gamma^1} - \frac{(\cos \alpha^2 + i \cos \beta^2)}{1 + \cos \gamma^2} \end{pmatrix}, \quad (\text{E.8}) \end{aligned}$$

Out of all these states the entangled ground state ($|G\rangle$) is very useful to define the two point many body (two atomic) correlation function, which are described by the Wightman function described by the following equation:

$$G_{\alpha\beta}(\tau - \tau') = \langle G|\Phi(\tau, x^\alpha)\Phi(\tau', x^\beta)|G\rangle$$

$$= \begin{cases} \langle G|\Phi(\tau, x^1)\Phi(\tau', x^2)|G\rangle = G_{11}(\tau - \tau') & \alpha = 1, \beta = 1 \\ \langle G|\Phi(\tau, x^2)\Phi(\tau', x^1)|G\rangle = G_{12}(\tau - \tau') & \alpha = 1, \beta = 2 \\ \langle G|\Phi(\tau, x^2)\Phi(\tau', x^2)|G\rangle = G_{21}(\tau - \tau') & \alpha = 2, \beta = 1. \\ \langle G|\Phi(\tau, x^\alpha)\Phi(\tau', x^\beta)|G\rangle = G_{22}(\tau - \tau') & \alpha = 2, \beta = 2. \end{cases}$$

On the other hand, all of these entangled quantum states contribute to the computation of the Lamb shift from the Heisenberg spin chain interaction considered in the effective Hamiltonian of the OQS considered in the present context. Technically, by taking $\alpha^1 = \beta^1 = \pi/2, \gamma^1 = 0$ and $\alpha^2 = \beta^2 = \pi/2, \gamma^2 = 0$ this is quantified as:

$$\delta E_{\text{LS}} = \langle \Psi | H_{\text{LS}} | \Psi \rangle = \begin{cases} 0 & |\Psi\rangle = |G\rangle \\ 0 & |\Psi\rangle = |E\rangle \\ Q(L, \kappa, \omega_0) & |\Psi\rangle = |S\rangle. \\ -Q(L, \kappa, \omega_0) & |\Psi\rangle = |A\rangle. \end{cases} \quad (\text{E.9})$$

where we define the a new function $Q(L, \kappa, \omega_0)$ as:

$$Q(L, \kappa, \omega_0) = -\frac{\mu^2}{4\pi} \frac{1}{L\sqrt{1 + \left(\frac{L}{2k}\right)^2}} \cos\left(2\omega_0 k \sinh^{-1}\left(\frac{L}{2k}\right)\right). \quad (\text{E.10})$$

F Many body (two atomic) Wightman function for probe massless scalar field in Static Patch of De Sitter Space

In this section we compute the two atomic Wightman correlation function for a massless probe scalar field in static De Sitter spacer characterised by the following infinitesimal line element:

$$ds^2 = \left(1 - \frac{r^2}{\alpha^2}\right) dt^2 - \left(1 - \frac{r^2}{\alpha^2}\right)^{-1} dr^2 - r^2(d\theta^2 + \sin^2\theta d\phi^2) \quad \text{where } \alpha = \sqrt{\frac{3}{\Lambda}} > 0. \quad (\text{F.1})$$

To compute the expression for the each of the entries of the two body Wightman function of the probe scalar field present in the external thermal bath we use the four dimensional

static De Sitter geometry of our space-time. In this set of coordinate system in four dimension, the Klein-Gordon field equation for the massless conformally coupled external probe scalar field for the non-adiabatic environment can be expressed as:

$$\left[\frac{1}{\cosh^3\left(\frac{t}{\alpha}\right)} \frac{\partial}{\partial t} \left(\cosh^3\left(\frac{t}{\alpha}\right) \frac{\partial}{\partial t} \right) - \frac{1}{\alpha^2 \cosh^2\left(\frac{t}{\alpha}\right)} \mathbf{L}^2 \right] \Phi(t, \chi, \theta, \phi) = 0 \quad , \quad (\text{F.2})$$

where \mathbf{L}^2 is the *Laplacian differential operator* in the three dimensions characterised by the coordinate (χ, θ, ϕ) , which is explicitly defined as:

$$\mathbf{L}^2 = \frac{1}{\sin^2 \chi} \left[\frac{\partial}{\partial \chi} \left(\sin^2 \chi \frac{\partial}{\partial \chi} \right) + \frac{1}{\sin \theta} \frac{\partial}{\partial \theta} \left(\sin \theta \frac{\partial}{\partial \theta} \right) + \frac{1}{\sin^2 \theta} \frac{\partial^2}{\partial \phi^2} \right] \quad , \quad (\text{F.3})$$

where we introduce a new coordinate χ which is related to the radial coordinate r as:

$$r = \sin \chi. \quad (\text{F.4})$$

The corresponding two body Wightman function between two space-time points for massless probe scalar field can be expressed as:

$$\begin{aligned} G(x, x') &= \begin{pmatrix} G^{11}(x, x') & G^{12}(x, x') \\ G^{21}(x, x') & G^{22}(x, x') \end{pmatrix} \\ &= \begin{pmatrix} \langle \Phi(\mathbf{x}_1, \tau) \Phi(\mathbf{x}_1, \tau') \rangle & \langle \Phi(\mathbf{x}_1, \tau) \Phi(\mathbf{x}_2, \tau') \rangle \\ \langle \Phi(\mathbf{x}_2, \tau) \Phi(\mathbf{x}_1, \tau') \rangle & \langle \Phi(\mathbf{x}_2, \tau) \Phi(\mathbf{x}_2, \tau') \rangle \end{pmatrix} \\ &= \frac{1}{Z_{\text{Bath}}} \begin{pmatrix} \text{Tr} [\rho_{\text{Bath}}(\tau - \tau') \Phi(\mathbf{x}_1, \tau) \Phi(\mathbf{x}_1, \tau')] & \text{Tr} [\rho_{\text{Bath}}(\tau - \tau') \Phi(\mathbf{x}_1, \tau) \Phi(\mathbf{x}_2, \tau')] \\ \text{Tr} [\rho_{\text{Bath}}(\tau - \tau') \Phi(\mathbf{x}_2, \tau) \Phi(\mathbf{x}_1, \tau')] & \text{Tr} [\rho_{\text{Bath}}(\tau - \tau') \Phi(\mathbf{x}_2, \tau) \Phi(\mathbf{x}_2, \tau')] \end{pmatrix}, \quad (\text{F.5}) \end{aligned}$$

where the Partition function for the bath is given by:

$$Z_{\text{Bath}} = \text{Tr} [\rho_{\text{Bath}}(\tau - \tau')]. \quad (\text{F.6})$$

Also, the components of the two atomic Wightman function can be expressed as:

$$\begin{aligned} G^{11}(x, x') = G^{22}(x, x') &= \langle \Phi(\mathbf{x}_1, \tau) \Phi(\mathbf{x}_1, \tau') \rangle = \langle \Phi(\mathbf{x}_2, \tau) \Phi(\mathbf{x}_2, \tau') \rangle \\ &= -\frac{1}{16\pi^2 k^2} \frac{1}{\sinh^2\left(\frac{\Delta\tau}{2k} - i\epsilon\right)}, \quad (\text{F.7}) \end{aligned}$$

$$\begin{aligned} G^{12}(x, x') = G^{21}(x, x') &= \langle \Phi(\mathbf{x}_1, \tau) \Phi(\mathbf{x}_2, \tau') \rangle = \langle \Phi(\mathbf{x}_2, \tau) \Phi(\mathbf{x}_1, \tau') \rangle \\ &= -\frac{1}{16\pi^2 k^2} \frac{1}{\left\{ \sinh^2\left(\frac{\Delta\tau}{2k} - i\epsilon\right) - \frac{r^2}{k^2} \sin^2\left(\frac{\Delta\theta}{2}\right) \right\}}. \quad (\text{F.8}) \end{aligned}$$

Here we have introduced few parameters, which are defined as:

$$k = \sqrt{g_{00}}\alpha = \sqrt{\alpha^2 - r^2}, \quad (\text{F.9})$$

$$\Delta\tau = \tau - \tau' = \sqrt{g_{00}}(t - t') = k \left(\frac{t - t'}{\alpha} \right). \quad (\text{F.10})$$

G Gorini Kossakowski Sudarshan Lindblad (GSKL) ($C_{ij}^{\alpha\beta}$) matrix

In this appendix, we explicitly write down the entries of the Gorini Kossakowski Sudarshan Lindblad (GSKL) ($C_{ij}^{\alpha\beta}$) matrix which is appearing in the expression for the quantum dissipator or *Lindbladian* operator as given by the following expression:

$$\mathcal{L}[\rho_{\text{System}}(\tau)] = \frac{1}{2} \sum_{i,j=\pm}^3 \sum_{\alpha,\beta=1}^2 C_{ij}^{\alpha\beta} \left[2\sigma_j^\beta \rho_{\text{System}}(\tau) \sigma_i^\alpha - \left\{ \sigma_i^\alpha \sigma_j^\beta, \rho_{\text{System}}(\tau) \right\} \right], \quad (\text{G.1})$$

where we have written the expression in a transformed basis span by $(+, -, 3)$ for two entangled OQS set up. The components of $C_{ij}^{\alpha\beta}$ matrix are very crucial to solve the time evolution equation of the reduced subsystem density matrix when we partially trace out the bath degrees of freedom from our two atomic entangled OQS set up. In general, Gorini Kossakowski Sudarshan Lindblad (GSKL) ($C_{ij}^{\alpha\beta}$) can be expressed as:

$$C_{ij}^{\alpha\beta} := \tilde{A}^{\alpha\beta} \delta_{ij} - i \tilde{B}^{\alpha\beta} \epsilon_{ijk} \delta_{3k} - \tilde{A}^{\alpha\beta} \delta_{3i} \delta_{3j} \quad \forall i, j = +, -, 3 \text{ and } \forall \alpha, \beta = 1(\text{Atom 1}), 2(\text{Atom 2}). \quad (\text{G.2})$$

In terms of explicit components the entries of the $C_{ij}^{\alpha\beta}$ matrix can be written as:

$$C_{++}^{\alpha\beta} = \tilde{A}^{\alpha\beta} \quad (\text{G.3})$$

$$C_{+-}^{\alpha\beta} = -i \tilde{B}^{\alpha\beta} \quad (\text{G.4})$$

$$C_{+3}^{\alpha\beta} = C_{-3}^{\alpha\beta} = C_{3+}^{\alpha\beta} = C_{3-}^{\alpha\beta} = C_{33}^{\alpha\beta} = 0 \quad (\text{G.5})$$

$$C_{-+}^{\alpha\beta} = i \tilde{B}^{\alpha\beta} \quad (\text{G.6})$$

$$C_{--}^{\alpha\beta} = \tilde{A}^{\alpha\beta} \quad (\text{G.7})$$

In the next two subsections, we will explicitly compute each of the components of $\tilde{A}^{\alpha\beta}$ and $\tilde{B}^{\alpha\beta}$ for the two atomic OQS in $(+, -, 3)$ transformed basis.

G.1 Calculation of $\tilde{A}^{\alpha\beta}$

The general expression of $\tilde{A}^{\alpha\beta}$ can be written in terms of the Fourier transformed two atomic Wightman functions as given below:

$$\tilde{A}^{\alpha\beta} = \frac{\mu^2}{4} [\mathcal{G}^{\alpha\beta}(\omega_0) + \mathcal{G}^{\alpha\beta}(-\omega_0)] \quad (\text{G.8})$$

where $\mathcal{G}^{\alpha\beta}(\pm\omega_0)$ is defined as:

$$\mathcal{G}^{\alpha\beta}(\pm\omega_0) = \int_{-\infty}^{\infty} d\Delta\tau e^{\pm i\Delta\tau\omega_0} G^{\alpha\beta}(\Delta\tau), \quad (\text{G.9})$$

where $G^{\alpha\beta}(\Delta\tau)$ is the two point two atomic Wightman function which is explicitly computed in the previous Appendix.

In this context, all the components of the Fourier transformed Wightman function can be written as:

$$\mathcal{G}^{11}(\pm\omega_0) = \mathcal{G}^{22}(\pm\omega_0) = \pm \frac{1}{2\pi} \frac{\omega_0}{1 - e^{\mp 2\pi\kappa\omega_0}}, \quad (\text{G.10})$$

$$\mathcal{G}^{12}(\pm\omega_0) = \mathcal{G}^{21}(\pm\omega_0) = \pm \frac{1}{2\pi} \frac{\omega_0}{1 - e^{\mp 2\pi\kappa\omega_0}} f\left(\pm\omega_0, \frac{L}{2}\right). \quad (\text{G.11})$$

Further, using this above mentioned expression for the Fourier transformed two point Wightman function the components of the $\tilde{A}^{\alpha\beta}$ can be written as:

$$\begin{aligned}\tilde{A}^{11} = \tilde{A}^{22} &= \frac{\mu^2}{4} \left[\frac{\omega_0}{2\pi(1 - e^{-2\pi\kappa\omega_0})} - \frac{\omega_0}{2\pi(1 - e^{2\pi\kappa\omega_0})} \right] \\ &= \frac{\mu^2\omega_0}{8\pi} \coth(\pi\kappa\omega_0),\end{aligned}\tag{G.12}$$

$$\begin{aligned}\tilde{A}^{12} = \tilde{A}^{21} &= \frac{\mu^2}{4} \left[\frac{\omega_0}{2\pi(1 - e^{-2\pi\kappa\omega_0})} f\left(\omega_0, \frac{L}{2}\right) - \frac{\omega_0}{2\pi(1 - e^{2\pi\kappa\omega_0})} f\left(-\omega_0, \frac{L}{2}\right) \right] \\ &= \frac{\mu^2\omega_0}{8\pi} \coth(\pi\kappa\omega_0) f\left(\omega_0, \frac{L}{2}\right).\end{aligned}\tag{G.13}$$

where we have introduced a new function $f\left(\pm\omega_0, \frac{L}{2}\right)$ which is defined as:

$$f\left(\pm\omega_0, \frac{L}{2}\right) = \pm \frac{1}{L\omega_0 \sqrt{1 + \left(\frac{L}{2\kappa}\right)^2}} \sin\left(\pm 2\kappa\omega_0 \sinh^{-1} \frac{L}{2\kappa}\right) = f\left(\mp\omega_0, \frac{L}{2}\right).\tag{G.14}$$

Here L characterises the Euclidean distance between the two atoms placed at the coordinates (r, θ, ϕ) and (r, θ', ϕ) , which is defined as:

$$L = 2r \sin\left(\frac{|\Delta\theta|}{2}\right),\tag{G.15}$$

where $\Delta\theta = \theta - \theta'$ represents the angular separation.

Now we are interested in the following limit where the following condition is satisfied ⁹:

$$\coth(\pi\kappa\omega_0) = 0 \implies \kappa\omega_0 = i \left(n + \frac{1}{2}\right) \quad \text{where } n \in \mathbb{Z},\tag{G.16}$$

in which we found the following simplified expression for the components of the $\tilde{A}^{\alpha\beta}$, as given by:

$$\tilde{A}^{11} = \tilde{A}^{22} = 0,\tag{G.17}$$

$$\tilde{A}^{12} = \tilde{A}^{21} = 0.\tag{G.18}$$

This is really very useful to fix the elements of the GSKL matrix elements and to further solve the GSKL master equation.

⁹To simplify the solutions we have considered this assumption. However, the similar kind of feature one can get in the sub horizon time scale in De Sitter space itself. Particularly in sub horizon scale one can neglect the contribution for the mode momentum which is appearing in the frequency of the fluctuating modes and for De Sitter inflationary patch of the metric one can explicitly show that ω is imaginary and controlled by conformal time scale. In our case the parameter $\kappa = \sqrt{\frac{3}{\Lambda} - r^2} > 0$ as for De Sitter space the cosmological constant $\Lambda > 0$. This implies that in our case we get imaginary frequency if we respect this specific constraint condition and it is physically justifiable.

G.2 Calculation of $\tilde{B}^{\alpha\beta}$

The general expression of $\tilde{B}^{\alpha\beta}$ can be written in terms of the Fourier transformed two atomic Wightman functions as given below:

$$\tilde{B}^{\alpha\beta} = \frac{\mu^2}{4} [\mathcal{G}^{\alpha\beta}(\omega_0) - \mathcal{G}^{\alpha\beta}(-\omega_0)] \quad (\text{G.19})$$

Further, using the previously expression for the Fourier transformed two point Wightman function the components of the $\tilde{B}^{\alpha\beta}$ can be written as:

$$\begin{aligned} \tilde{B}^{11} = \tilde{B}^{22} &= \frac{\mu^2}{4} \left[\frac{\omega_0}{2\pi(1 - e^{-2\pi\kappa\omega_0})} + \frac{\omega_0}{2\pi(1 - e^{2\pi\kappa\omega_0})} \right], \\ &= \frac{\mu^2\omega_0}{8\pi}, \end{aligned} \quad (\text{G.20})$$

$$\begin{aligned} \tilde{B}^{12} = \tilde{B}^{21} &= \frac{\mu^2}{4} \left[\frac{\omega_0}{2\pi(1 - e^{-2\pi\kappa\omega_0})} f\left(\omega_0, \frac{L}{2}\right) + \frac{\omega_0}{2\pi(1 - e^{2\pi\kappa\omega_0})} f\left(-\omega_0, \frac{L}{2}\right) \right] \\ &= \frac{\mu^2\omega_0}{8\pi} f\left(\omega_0, \frac{L}{2}\right). \end{aligned} \quad (\text{G.21})$$

G.3 Calculation of $C_{ij}^{\alpha\beta}$ matrix elements

Finally, substituting the explicit forms of $\tilde{A}^{\alpha\beta}$ and $\tilde{B}^{\alpha\beta}$ which we have derived in the previous sub section, we get the following expressions for the entries of the GSKL matrix:

$$C_{+3}^{\alpha\beta} = C_{-3}^{\alpha\beta} = C_{3+}^{\alpha\beta} = C_{3-}^{\alpha\beta} = C_{33}^{\alpha\beta} = 0 \quad (\text{G.22})$$

$$C_{-+}^{11} = C_{-+}^{22} = -C_{+-}^{11} = -C_{+-}^{22} = i\tilde{B}^{11} = i\tilde{B}^{22} = \frac{\mu^2\omega_0 i}{8\pi}, \quad (\text{G.23})$$

$$C_{-+}^{12} = C_{-+}^{21} = -C_{+-}^{12} = -C_{+-}^{21} = i\tilde{B}^{12} = i\tilde{B}^{21} = \frac{\mu^2\omega_0 i}{8\pi} f\left(\omega_0, \frac{L}{2}\right) \quad (\text{G.24})$$

$$C_{++}^{11} = C_{++}^{11} = C_{--}^{11} = C_{--}^{22} = \tilde{A}^{11} = \tilde{A}^{22} = \frac{\mu^2\omega_0}{8\pi} \coth(\pi\kappa\omega_0), \quad (\text{G.25})$$

$$C_{++}^{12} = C_{++}^{21} = C_{--}^{12} = C_{--}^{21} = \tilde{A}^{12} = \tilde{A}^{21} = \frac{\mu^2\omega_0}{8\pi} \coth(\pi\kappa\omega_0) f\left(\omega_0, \frac{L}{2}\right). \quad (\text{G.26})$$

Further, using the assumption, $\kappa\omega_0 = i\left(n + \frac{1}{2}\right)$ where $n \in \mathbb{Z}$, we get the following simplified expressions for the entries of the GSKL matrix:

$$C_{+3}^{\alpha\beta} = C_{-3}^{\alpha\beta} = C_{3+}^{\alpha\beta} = C_{3-}^{\alpha\beta} = C_{33}^{\alpha\beta} = 0 \quad (\text{G.27})$$

$$C_{-+}^{11} = C_{-+}^{22} = -C_{+-}^{11} = -C_{+-}^{22} = i\tilde{B}^{11} = i\tilde{B}^{22} = -\frac{\mu^2}{8\pi\kappa} \left(n + \frac{1}{2}\right), \quad (\text{G.28})$$

$$C_{-+}^{12} = C_{-+}^{21} = -C_{+-}^{12} = -C_{+-}^{21} = i\tilde{B}^{12} = i\tilde{B}^{21} = -\frac{\mu^2}{8\pi\kappa} \left(n + \frac{1}{2}\right) f\left(\omega_0, \frac{L}{2}\right) \quad (\text{G.29})$$

$$C_{++}^{11} = C_{++}^{11} = C_{--}^{11} = C_{--}^{22} = \tilde{A}^{11} = \tilde{A}^{22} = 0, \quad (\text{G.30})$$

$$C_{++}^{12} = C_{++}^{21} = C_{--}^{12} = C_{--}^{21} = \tilde{A}^{12} = \tilde{A}^{21} = 0, \quad (\text{G.31})$$

where, the parameter

$$\kappa = \sqrt{\frac{3}{\Lambda} - r^2} = \sqrt{\left(\frac{12}{R_{\text{DS}}}\right)^2 - r^2} > 0, \quad (\text{G.32})$$

for De Sitter space. Here we use the fact that, the curvature of static De Sitter space is given by the following expression:

$$R_{\text{DS}} = \sqrt{48\Lambda} > 0 \quad \text{as } \Lambda > 0 \text{ De Sitter.} \quad (\text{G.33})$$

H Effective Hamiltonian ($H_{ij}^{\alpha\beta}$) matrix

In this appendix, we explicitly write down the entries of the Effective Hamiltonian ($H_{ij}^{\alpha\beta}$) matrix which is appearing in the expression for the *Lamb Shift* part of the Hamiltonian as given by the following expression:

$$H_{\text{Lamb Shift}} = -\frac{i}{2} \sum_{\alpha, \beta=1}^2 \sum_{i, j=1}^3 H_{ij}^{\alpha\beta} (n_i^\alpha \cdot \sigma_i^\alpha) (n_j^\beta \cdot \sigma_j^\beta). \quad (\text{H.1})$$

where this Hamiltonian is constructed by partially tracing over bath degrees of freedom, which is in our problem a probe massless scalar field. Technically, the Effective Hamiltonian ($H_{ij}^{\alpha\beta}$) matrix represent here the strength of the spin chain interaction mentioned above. The general expression of $H_{ij}^{\alpha\beta}$ matrix is given by the following expression:

$$H_{\alpha\beta}^{ij} = \mathcal{A}^{\alpha\beta} \delta_{ij} - i\mathcal{B}^{\alpha\beta} \epsilon_{ijk} \delta_{3k} - \mathcal{A}^{\alpha\beta} \delta_{3i} \delta_{3j} \quad \forall i, j = +, -, 3 \text{ and } \forall \alpha, \beta = 1(\text{Atom 1}), 2(\text{Atom 2}). \quad (\text{H.2})$$

In terms of explicit components the entries of the $H_{ij}^{\alpha\beta}$ matrix can be written as:

$$H_{++}^{\alpha\beta} = H_{--}^{\alpha\beta} = A^{\alpha\beta} \quad \forall \alpha, \beta = 1, 2, \quad (\text{H.3})$$

$$H_{+-}^{\alpha\beta} = -iB^{\alpha\beta} \quad \forall \alpha, \beta = 1, 2, \quad (\text{H.4})$$

$$H_{-+}^{\alpha\beta} = iB^{\alpha\beta} \quad \forall \alpha, \beta = 1, 2, \quad (\text{H.5})$$

$$H_{+3}^{\alpha\beta} = H_{-3}^{\alpha\beta} = 0 \quad \forall \alpha, \beta = 1, 2, \quad (\text{H.6})$$

$$H_{3j}^{\alpha\beta} = 0 \quad \forall j = +, -, 3 \text{ and } \forall \alpha, \beta = 1, 2. \quad (\text{H.7})$$

H.1 Calculation of $A^{\alpha\beta}$

The general expression of $A^{\alpha\beta}$ can be written in terms of the Fourier transformed two atomic Wightman functions as given below:

$$A^{\alpha\beta} = \frac{\mu^2}{4} [\mathcal{K}^{\alpha\beta}(\omega_0) + \mathcal{K}^{\alpha\beta}(-\omega_0)] \quad (\text{H.8})$$

where $\mathcal{K}^{\alpha\beta}(\pm\omega_0)$ is defined as:

$$\mathcal{K}^{\alpha\beta}(\pm\omega_0) = \frac{P}{\pi i} \int_{-\infty}^{\infty} d\omega \frac{\mathcal{G}(\pm\omega)}{\omega \pm \omega_0} = \frac{P}{\pi i} \int_{-\infty}^{\infty} d\omega \int_{-\infty}^{\infty} d\Delta\tau \frac{e^{\pm i\Delta\tau\omega}}{\omega \pm \omega_0} G^{\alpha\beta}(\Delta\tau), \quad (\text{H.9})$$

where $G^{\alpha\beta}(\Delta\tau)$ is the two point two atomic Wightman function which is explicitly computed in the previous Appendix. Here P represents the principal value of the integral.

In this context, all the components of the Hilbert transformed principal part of the Wightman function can be expressed as:

$$\mathcal{K}^{11}(\pm\omega_0) = \mathcal{K}^{22}(\pm\omega_0) = \frac{P}{2\pi^2 i} \int_{-\infty}^{\infty} d\omega \frac{1}{(\omega \pm \omega_0)} \frac{\omega}{(1 - e^{-2\pi\kappa\omega})}, \quad (\text{H.10})$$

$$\mathcal{K}^{12}(\pm\omega_0) = \mathcal{K}^{21}(\pm\omega_0) = \frac{P}{2\pi^2 i} \int_{-\infty}^{\infty} d\omega \frac{1}{(\omega \pm \omega_0)} \frac{\omega}{(1 - e^{-2\pi\kappa\omega})} f\left(\omega, \frac{L}{2}\right), \quad (\text{H.11})$$

where we have introduced a new function $f\left(\omega, \frac{L}{2}\right)$ which is defined as:

$$f\left(\omega, \frac{L}{2}\right) = \pm \frac{1}{L\omega\sqrt{1 + \left(\frac{L}{2\kappa}\right)^2}} \sin\left(\pm 2\kappa\omega \sinh^{-1} \frac{L}{2\kappa}\right). \quad (\text{H.12})$$

Further, using this above mentioned expressions for Hilbert transformed principal part of the Wightman function the components of the $A^{\alpha\beta}$ can be written as:

$$\begin{aligned} A^{11} = A^{22} &= \frac{\mu^2 P}{8\pi^2 i} \int_{-\infty}^{\infty} d\omega \left[\frac{1}{(\omega + \omega_0)} + \frac{1}{(\omega - \omega_0)} \right] \frac{\omega}{(1 - e^{-2\pi\kappa\omega})} \\ &= \frac{\mu^2 P}{4\pi^2 i} \int_{-\infty}^{\infty} d\omega \frac{\omega^2}{(\omega + \omega_0)(\omega - \omega_0)(1 - e^{-2\pi\kappa\omega})}, \end{aligned} \quad (\text{H.13})$$

$$\begin{aligned} A^{12} = A^{21} &= \frac{\mu^2 P}{8\pi^2 i} \int_{-\infty}^{\infty} d\omega \left[\frac{1}{(\omega + \omega_0)} + \frac{1}{(\omega - \omega_0)} \right] \frac{\omega}{(1 - e^{-2\pi\kappa\omega})} f\left(\omega, \frac{L}{2}\right) \\ &= \frac{\mu^2 P}{4\pi^2 i} \int_{-\infty}^{\infty} d\omega \frac{\omega^2}{(\omega + \omega_0)(\omega - \omega_0)(1 - e^{-2\pi\kappa\omega})} f\left(\omega, \frac{L}{2}\right). \end{aligned} \quad (\text{H.14})$$

Next, using the approximation $2\pi\kappa\omega \gg 1$, we get the following simplified expressions for the components of the $A^{\alpha\beta}$ as given by:

$$A^{11} = A^{22} = \frac{\mu^2 P}{4\pi^2 i} \int_{-\infty}^{\infty} d\omega \frac{\omega^2}{(\omega + \omega_0)(\omega - \omega_0)}, \quad (\text{H.15})$$

$$A^{12} = A^{21} = \frac{\mu^2 P}{4\pi^2 i} \int_{-\infty}^{\infty} d\omega \frac{\omega^2}{(\omega + \omega_0)(\omega - \omega_0)} f\left(\omega, \frac{L}{2}\right). \quad (\text{H.16})$$

H.2 Calculation of $B^{\alpha\beta}$

The general expression of $B^{\alpha\beta}$ can be written in terms of the Fourier transformed two atomic Wightman functions as given below:

$$B^{\alpha\beta} = \frac{\mu^2}{4} [\mathcal{K}^{\alpha\beta}(\omega_0) - \mathcal{K}^{\alpha\beta}(-\omega_0)] \quad (\text{H.17})$$

where $\mathcal{K}^{\alpha\beta}(\pm\omega_0)$ is defined earlier.

Further, using this above mentioned expressions for Hilbert transformed principal part of the Wightman function the components of the $B^{\alpha\beta}$ can be written as:

$$\begin{aligned} B^{11} = B^{22} &= \frac{\mu^2 P}{8\pi^2 i} \int_{-\infty}^{\infty} d\omega \left[\frac{1}{(\omega + \omega_0)} - \frac{1}{(\omega - \omega_0)} \right] \frac{\omega}{(1 - e^{-2\pi\kappa\omega})} \\ &= \frac{\mu^2 P}{4\pi^2 i} \int_{-\infty}^{\infty} d\omega \frac{\omega\omega_0}{(\omega + \omega_0)(\omega - \omega_0)(1 - e^{-2\pi\kappa\omega})}, \end{aligned} \quad (\text{H.18})$$

$$\begin{aligned} B^{12} = B^{21} &= \frac{\mu^2 P}{8\pi^2 i} \int_{-\infty}^{\infty} d\omega \left[\frac{1}{(\omega + \omega_0)} - \frac{1}{(\omega - \omega_0)} \right] \frac{\omega}{(1 - e^{-2\pi\kappa\omega})} f\left(\omega, \frac{L}{2}\right) \\ &= \frac{\mu^2 P}{4\pi^2 i} \int_{-\infty}^{\infty} d\omega \frac{\omega\omega_0}{(\omega + \omega_0)(\omega - \omega_0)(1 - e^{-2\pi\kappa\omega})} f\left(\omega, \frac{L}{2}\right). \end{aligned} \quad (\text{H.19})$$

Next, using the approximation $2\pi\kappa\omega \gg 1$, we get the following simplified expressions for the components of the $A^{\alpha\beta}$ as given by:

$$B^{11} = B^{22} = \frac{\mu^2 P}{4\pi^2 i} \int_{-\infty}^{\infty} d\omega \frac{\omega\omega_0}{(\omega + \omega_0)(\omega - \omega_0)}, \quad (\text{H.20})$$

$$B^{12} = B^{21} = \frac{\mu^2 P}{4\pi^2 i} \int_{-\infty}^{\infty} d\omega \frac{\omega\omega_0}{(\omega + \omega_0)(\omega - \omega_0)} f\left(\omega, \frac{L}{2}\right). \quad (\text{H.21})$$

H.3 Calculation of $H_{ij}^{\alpha\beta}$ matrix elements

Finally, substituting the explicit forms of $A^{\alpha\beta}$ and $B^{\alpha\beta}$ which we have derived in the previous sub section, we get the following expressions for the entries of the effective Hamiltonian matrix:

$$H_{ij}^{11} = H_{ij}^{22} = \frac{\mu^2 P}{4\pi^2 i} [(\delta_{ij} - \delta_{3i}\delta_{3j})\Theta_1 - i\epsilon_{ijk}\delta_{3k}\Theta_2], \quad (\text{H.22})$$

$$H_{ij}^{12} = H_{ij}^{21} = \frac{\mu^2 P}{4\pi^2 i} [(\delta_{ij} - \delta_{3i}\delta_{3j})\Theta_3 - i\epsilon_{ijk}\delta_{3k}\Theta_4]. \quad (\text{H.23})$$

Therefore, all the various entries of $H_{ij}^{\alpha\beta}$ can be written as:

$$H_{++}^{11} = H_{++}^{22} = H_{--}^{11} = H_{--}^{22} = A^{11} = A^{22} = \frac{\mu^2 P}{4\pi^2 i} \Theta_1 \quad (\text{H.24})$$

$$H_{-+}^{11} = H_{-+}^{22} = -H_{+-}^{11} = -H_{+-}^{22} = iB^{11} = iB^{22} = \frac{\mu^2 P}{4\pi^2} \Theta_2 \quad (\text{H.25})$$

$$H_{++}^{12} = H_{++}^{21} = H_{--}^{12} = H_{--}^{21} = A^{12} = A^{21} = \frac{\mu^2 P}{4\pi^2 i} \Theta_3 \quad (\text{H.26})$$

$$H_{-+}^{12} = H_{-+}^{21} = -H_{+-}^{12} = -H_{+-}^{21} = iB^{12} = iB^{21} = \frac{\mu^2 P}{4\pi^2} \Theta_4 \quad (\text{H.27})$$

The function $f\left(\omega, \frac{L}{2}\right)$ has already been defined in the previous section. Here we introduce four integral functions $\Theta_i \forall i = 1, 2, 3, 4$, which is defined as:

Integral I :

$$\Theta_1 := \int_{-\infty}^{\infty} d\omega \frac{\omega^2}{(1 - e^{-2\pi k\omega})(\omega + \omega_0)(\omega - \omega_0)}. \quad (\text{H.28})$$

Integral II :

$$\Theta_2 := \int_{-\infty}^{\infty} d\omega \frac{\omega\omega_0}{(1 - e^{-2\pi k\omega})(\omega + \omega_0)(\omega - \omega_0)}. \quad (\text{H.29})$$

Integral III :

$$\Theta_3 := \int_{-\infty}^{\infty} d\omega \frac{\omega^2}{(1 - e^{-2\pi k\omega})(\omega + \omega_0)(\omega - \omega_0)} f\left(\omega, \frac{L}{2}\right) \quad (\text{H.30})$$

Integral IV :

$$\Theta_4 := \int_{-\infty}^{\infty} d\omega \frac{\omega\omega_0}{(1 - e^{-2\pi k\omega})(\omega + \omega_0)(\omega - \omega_0)} f\left(\omega, \frac{L}{2}\right). \quad (\text{H.31})$$

In the next section we explicitly compute the contributions from all of these integrals.

I Calculation of useful integrals

In this section, we explicitly compute the analytical expression for the useful integrals $\Theta_i \forall i = 1, 2, 3, 4$, which are very useful to compute the expressions for the effective Hamiltonian matrix elements.

I.1 Integral I

In this subsection we explicitly compute the finite contribution from the following integral:

$$\Theta_1 := \int_{-\infty}^{\infty} d\omega \frac{\omega^2}{(1 - e^{-2\pi k\omega})(\omega + \omega_0)(\omega - \omega_0)}. \quad (\text{I.1})$$

In the limiting approximation $2\pi k\omega \gg 1$, one can further expand the integrand by taking large $\kappa\omega$ approximation as:

$$\mathcal{V}(\omega_0, \omega, k) := \frac{\omega^2}{(1 - e^{-2\pi k\omega})(\omega + \omega_0)(\omega - \omega_0)} \xrightarrow{2\pi k\omega \gg 1} \frac{\omega^2}{(\omega + \omega_0)(\omega - \omega_0)} := \mathcal{V}(\omega_0, \omega). \quad (\text{I.2})$$

This implies that, after taking large $\kappa\omega$ approximation the integrand of Θ_1 becomes independent of the parameter k .

Now, further using this approximation the integral Θ_1 can be further simplified as:

$$\Theta_2 \approx \int_{-\infty}^{\infty} d\omega \mathcal{V}(\omega_0, \omega) = \underbrace{\int_{-\infty}^0 d\omega \mathcal{V}(\omega_0, \omega)}_{\equiv \mathcal{D}_1(\omega_0)} + \underbrace{\int_0^{\infty} d\omega \mathcal{V}(\omega_0, \omega)}_{\equiv \mathcal{D}_2(\omega_0)}, \quad (\text{I.3})$$

where we have written the integrals into two parts, represented by $\mathcal{D}_1(\omega_0)$ and $\mathcal{D}_2(\omega_0)$. Now, here we see that in the $2\pi\kappa \gg 1$ limit we get:

$$\mathcal{D}_1(\omega_0) = \int_{-\infty}^0 d\omega \mathcal{V}(\omega_0, \omega) = - \int_0^{\infty} d\omega \mathcal{V}(\omega_0, \omega) = -\mathcal{D}_2(\omega_0). \quad (\text{I.4})$$

Now, here $\mathcal{D}_1(\omega_0)$ and $\mathcal{D}_2(\omega_0)$ gives divergent contributions in the frequency range, $-\infty < \omega < 0$ and $0 < \omega < \infty$. To get the finite regularised contributions from these integrals we introduce a cut-off regulator ω_c , by following *Bethe regularisation* procedure. After introducing this cut-off we get the following result:

$$\mathcal{D}_1(\omega_0, \omega_c) = \int_{-\omega_c}^0 d\omega \mathcal{V}(\omega_0, \omega) = \int_0^{\omega_c} d\omega \mathcal{V}(\omega_0, \omega) = \mathcal{D}_2(\omega_0, \omega_c) = \frac{1}{2} \left[\omega_c - \omega_0 \tanh^{-1} \left(\frac{\omega_c}{\omega_0} \right) \right]. \quad (\text{I.5})$$

Consequently, we get the following regularised expression for the integral Θ_1 , as given by:

$$\Theta_1 = \mathcal{D}_1(\omega_0, \omega_c) + \mathcal{D}_2(\omega_0, \omega_c) = \left[\omega_c - \omega_0 \tanh^{-1} \left(\frac{\omega_c}{\omega_0} \right) \right]. \quad (\text{I.6})$$

Now, if we further use the approximation that the cut-off is small compared to ω_0 i.e. $\omega_c \ll \omega_0$, then we get ¹⁰:

$$\text{Integral I: } \Theta_2 = \mathcal{D}_1(\omega_0, \omega_c) + \mathcal{D}_2(\omega_0, \omega_c) = \left[\omega_c - \omega_0 \left(\frac{\omega_c}{\omega_0} \right) \right] \approx 0. \quad (\text{I.8})$$

I.2 Integral II

In this subsection we explicitly compute the finite contribution from the following integral:

$$\Theta_2 := \int_{-\infty}^{\infty} d\omega \frac{\omega \omega_0}{(1 - e^{-2\pi k \omega}) (\omega + \omega_0) (\omega - \omega_0)}. \quad (\text{I.9})$$

It is important to note that in the limit, $2\pi\kappa\omega \gg 1$, one can further expand the integrand given by the following approximation as:

$$\mathcal{M}(\omega_0, \omega, k) := \frac{\omega_0 \omega}{(1 - e^{-2\pi k \omega}) (\omega + \omega_0) (\omega - \omega_0)} \xrightarrow{2\pi\kappa\omega \gg 1} \frac{\omega_0 \omega}{(\omega + \omega_0) (\omega - \omega_0)} := \mathcal{M}(\omega_0, \omega). \quad (\text{I.10})$$

This implies that, after taking limit $2\pi\kappa\omega \gg 1$ the integrand of Θ_2 becomes independent of the parameter k .

Now, further using this approximation the integral Θ_1 can be expressed as:

$$\Theta_1 \approx \int_{-\infty}^{\infty} d\omega \mathcal{M}(\omega_0, \omega) = \underbrace{\int_{-\infty}^0 d\omega \mathcal{M}(\omega_0, \omega)}_{\equiv \mathcal{N}_1(\omega_0)} + \underbrace{\int_0^{\infty} d\omega \mathcal{M}(\omega_0, \omega)}_{\equiv \mathcal{N}_2(\omega_0)}, \quad (\text{I.11})$$

¹⁰In the limit, $\omega_c \ll \omega_0$ we can approximate the Taylor series expansion of the following function as:

$$\tanh^{-1} \left(\frac{\omega_c}{\omega_0} \right) = \left(\frac{\omega_c}{\omega_0} \right) + \frac{1}{3} \left(\frac{\omega_c}{\omega_0} \right)^3 + \dots \approx \left(\frac{\omega_c}{\omega_0} \right) \ll 1. \quad (\text{I.7})$$

where we have written the integrals into two parts, indicated by $\mathcal{N}_1(\omega_0)$ and $\mathcal{N}_2(\omega_0)$. Now, in the limit $2\pi\kappa\omega \gg 1$, we get:

$$\mathcal{N}_1(\omega_0) = \int_{-\infty}^0 d\omega \mathcal{M}(\omega_0, \omega) = - \int_0^{\infty} d\omega \mathcal{M}(\omega_0, \omega) = -\mathcal{N}_2(\omega_0). \quad (\text{I.12})$$

Now, here $\mathcal{N}_1(\omega_0)$ and $\mathcal{N}_2(\omega_0)$ gives divergent contributions in the frequency range, $-\infty < \omega < 0$ and $0 < \omega < \infty$. To get the finite contributions from these integrals we introduce a cut-off regulator ω_c , by following *Bethe regularisation* procedure. After introducing this cut-off we get the following finite contribution:

$$\mathcal{N}_1(\omega_0, \omega_c) = \int_{-\omega_c}^0 d\omega \mathcal{M}(\omega_0, \omega) = - \int_0^{\omega_c} d\omega \mathcal{M}(\omega_0, \omega) = -\mathcal{N}_2(\omega_0, \omega_c) = -\frac{\omega_0}{2} \ln \left[1 - \left(\frac{\omega_c}{\omega_0} \right)^2 \right]. \quad (\text{I.13})$$

Consequently, we get the following expression for the integral Θ_2 , as given by:

$$\text{Integral II : } \Theta_1 = \mathcal{U}_1(\omega_0, \omega_c) + \mathcal{U}_2(\omega_0, \omega_c) = \frac{\omega_0}{2} \ln \left[1 - \left(\frac{\omega_c}{\omega_0} \right)^2 \right] - \frac{\omega_0}{2} \ln \left[1 - \left(\frac{\omega_c}{\omega_0} \right)^2 \right] = 0. \quad (\text{I.14})$$

I.3 Integral III

In this subsection we explicitly compute the finite contribution from the following integral:

$$\Theta_3 := \int_{-\infty}^{\infty} d\omega \frac{\omega^2}{(1 - e^{-2\pi\kappa\omega})(\omega + \omega_0)(\omega - \omega_0)} f\left(\omega, \frac{L}{2}\right), \quad (\text{I.15})$$

where, we define the function $f\left(\omega, \frac{L}{2}\right)$ given by the following expression:

$$f\left(\omega, \frac{L}{2}\right) = \frac{1}{L\omega\sqrt{1 + \left(\frac{L}{2k}\right)^2}} \sin\left(2k\omega \sinh^{-1}\left(\frac{L}{2k}\right)\right). \quad (\text{I.16})$$

In the limit $2\pi\kappa \gg 1$, one can further expand the integrand as:

$$\mathcal{Z}(\omega_0, \omega, k) := \frac{\omega^2 f\left(\omega, \frac{L}{2}\right)}{(1 - e^{-2\pi\kappa\omega})(\omega + \omega_0)(\omega - \omega_0)} \xrightarrow{2\pi\kappa\omega > 1} \frac{\omega^2 f\left(\omega, \frac{L}{2}\right)}{(\omega + \omega_0)(\omega - \omega_0)} := \mathcal{Z}(\omega_0, \omega, k). \quad (\text{I.17})$$

This implies that, in the limit $2\pi\kappa \gg 1$ the integrand of Θ_3 is not independent of the parameter k .

Now, further using this approximation the integral Θ_3 can be further simplified as:

$$\Theta_3 \approx \int_{-\infty}^{\infty} d\omega \mathcal{Z}(\omega_0, \omega, k) = \underbrace{\int_{-\infty}^0 d\omega \mathcal{Z}(\omega_0, \omega, k)}_{\equiv \mathcal{R}_1^l(\omega_0, k)} + \underbrace{\int_0^{\infty} d\omega \mathcal{Z}(\omega_0, \omega, k)}_{\equiv \mathcal{R}_2^l(\omega_0, k)}, \quad (\text{I.18})$$

where we have written the integrals into two parts, indicated by $\mathcal{R}_1^l(\omega_0, k)$ and $\mathcal{R}_2^l(\omega_0, k)$. Now, here in the limit $2\pi\kappa \gg 1$ we get:

$$\begin{aligned} \mathcal{R}_1^l(\omega_0, k) &= \int_{-\infty}^0 d\omega \mathcal{Z}(\omega_0, \omega, k) = \int_0^{\infty} d\omega \mathcal{Z}(\omega_0, \omega, k) = \mathcal{R}_2^l(\omega_0, k) \\ &= \frac{\pi}{2L\sqrt{1 + \left(\frac{L}{2k}\right)^2}} \cos\left(2k\omega_0 \sinh^{-1}\left(\frac{L}{2k}\right)\right). \end{aligned} \quad (\text{I.19})$$

Consequently, we get the following expression for the integral Θ_3 , given by:

$$\boxed{\text{Integral III : } \Theta_3 = \mathcal{R}_1^l(\omega_0, k) + \mathcal{R}_2^l(\omega_0, k) = \frac{\pi}{L\sqrt{1 + \left(\frac{L}{2k}\right)^2}} \cos\left(2k\omega_0 \sinh^{-1}\left(\frac{L}{2k}\right)\right)}. \quad (\text{I.20})$$

Further, substituting $\kappa\omega_0 = i\left(n + \frac{1}{2}\right) \forall n \in \mathbb{Z}$, we get the following simplified expression for the integral Θ_3 , given by:

$$\boxed{\text{Integral III : } \Theta_3 = \mathcal{R}_1(\omega_0, k) + \mathcal{R}_2(\omega_0, k) = \frac{\pi}{L\sqrt{1 + \left(\frac{L}{2k}\right)^2}} \cosh\left((2n + 1) \sinh^{-1}\left(\frac{L}{2k}\right)\right)}. \quad (\text{I.21})$$

I.4 Integral IV

In this subsection we explicitly compute the finite contribution from the following integral:

$$\Theta_4 := \int_{-\infty}^{\infty} d\omega \frac{\omega\omega_0}{(1 - e^{-2\pi k\omega})(\omega + \omega_0)(\omega - \omega_0)} f\left(\omega, \frac{L}{2}\right), \quad (\text{I.22})$$

where, we define the function $f\left(\omega, \frac{L}{2}\right)$ given by the following expression:

$$f\left(\omega, \frac{L}{2}\right) = \frac{1}{L\omega\sqrt{1 + \left(\frac{L}{2k}\right)^2}} \sin\left(2k\omega \sinh^{-1}\left(\frac{L}{2k}\right)\right). \quad (\text{I.23})$$

In the limit $2\pi\kappa \gg 1$, one can further expand the integrand as:

$$\mathcal{S}(\omega_0, \omega, k) := \frac{\omega\omega_0 f\left(\omega, \frac{L}{2}\right)}{(1 - e^{-2\pi k\omega})(\omega + \omega_0)(\omega - \omega_0)} \xrightarrow{2\pi\kappa \gg 1} \frac{\omega\omega_0 f\left(\omega, \frac{L}{2}\right)}{(\omega + \omega_0)(\omega - \omega_0)} := \mathcal{S}(\omega_0, \omega, k). \quad (\text{I.24})$$

This implies that, in the limit $2\pi\kappa \gg 1$ the integrand of Θ_3 is not independent of the parameter k .

Now, further using this approximation the integral Θ_4 can be further simplified as:

$$\Theta_4 \approx \int_{-\infty}^{\infty} d\omega \mathcal{S}(\omega_0, \omega, k) = \underbrace{\int_{-\infty}^0 d\omega \mathcal{S}(\omega_0, \omega, k)}_{\equiv \mathcal{L}_1(\omega_0, k)} + \underbrace{\int_0^{\infty} d\omega \mathcal{S}(\omega_0, \omega, k)}_{\equiv \mathcal{L}_2(\omega_0, k)}, \quad (\text{I.25})$$

where we have written the integrals into two parts, indicated by $\mathcal{L}_1(\omega_0, k)$ and $\mathcal{L}_2(\omega_0, k)$. Now, here in the limit $2\pi\kappa \gg 1$ we get:

$$\begin{aligned} \mathcal{L}_1(\omega_0, k) &= \int_{-\infty}^0 d\omega \mathcal{S}(\omega_0, \omega, k) = - \int_0^{\infty} d\omega \mathcal{S}(\omega_0, \omega, k) = -\mathcal{L}_2(\omega_0, k) \\ &= - \frac{i\sqrt{\pi}}{2L\sqrt{1 + \left(\frac{L}{2k}\right)^2}} \underbrace{G_{1,3}^{2,1}\left(-\omega_0^2\kappa^2 \sinh^{-1}\left(\frac{L}{2k}\right)^2 \mid \begin{matrix} \frac{1}{2} \\ \frac{1}{2}, \frac{1}{2}, 0 \end{matrix}\right)}_{\text{Meijer G function}}. \end{aligned} \quad (\text{I.26})$$

Consequently, we get the following expression for the integral Θ_4 , as given by:

$$\boxed{\text{Integral IV : } \Theta_4 = \mathcal{L}_1(\omega_0, k) + \mathcal{L}_2(\omega_0, k) = 0}. \quad (\text{I.27})$$

J Functions appearing in the solution of GSKL master equations

The functional form of the terms A_1 , B_1 and B_2 appearing in the solution of the evolution equations of the reduced subsystem density matrix are functions of the components of the GSKL $C_{ij}^{\alpha\beta}$ matrix and effective Hamiltonian $H_{ij}^{\alpha\beta}$ matrix that we have computed explicitly in the previous Appendices. These factors are defined as:

$$\begin{aligned} A_1 &= -\frac{i\mu^2}{4L\sqrt{1+(\frac{L}{2\kappa})^2}} \cos\left(2\kappa\omega_0 \sinh^{-1}\left(\frac{L}{2\kappa}\right)\right) \\ &= -\frac{i\mu^2}{4L\sqrt{1+(\frac{L}{2\kappa})^2}} \cosh\left((2n+1) \sinh^{-1}\left(\frac{L}{2\kappa}\right)\right), \end{aligned} \quad (\text{J.1})$$

$$B_1 = \frac{i\mu^2\omega_0}{4\pi} = -\frac{\mu^2}{4\pi\kappa} \left(n + \frac{1}{2}\right), \quad (\text{J.2})$$

$$\begin{aligned} B_2 &= \frac{i\mu^2}{4L\sqrt{1+(\frac{L}{2\kappa})^2}} \sin\left(2\kappa\omega_0 \sinh^{-1}\left(\frac{L}{2\kappa}\right)\right) \\ &= -\frac{\mu^2}{4L\sqrt{1+(\frac{L}{2\kappa})^2}} \sinh\left((2n+1) \sinh^{-1}\left(\frac{L}{2\kappa}\right)\right). \end{aligned} \quad (\text{J.3})$$

The functions $\Delta_1(\omega)$, $\Delta_2(\omega)$ and $\Delta_3(\omega)$ appearing in the $f_1(\omega)$, $f_2(\omega)$ and $f_3(\omega)$ terms of the solutions of the evolution equations are explicitly written in the following equations. Here the following symbols have been used to write $\Delta_1(\omega)$, $\Delta_2(\omega)$ and $\Delta_3(\omega)$ terms

$$b_1 = -48A_1^2 + 36B_2^2 - 4\omega^2 \quad (\text{J.4})$$

$$b_2 = 288A_1^2\omega + 432B_2^2\omega + 16\omega^3 \quad (\text{J.5})$$

Now we define, $\Delta_1(\omega)$, $\Delta_2(\omega)$ and $\Delta_3(\omega)$ in terms of the predefined factors b_1 , b_2 and b_3 given by the following expression:

$$\Delta_1(\omega) = \frac{2\omega}{3} - 2^{1/3}\frac{b_1}{3}\mathcal{Z}(b_1, b_2) + \frac{1}{3 \times 2^{1/3}}\mathcal{Z}(b_1, b_2), \quad (\text{J.6})$$

$$\Delta_2(\omega) = \frac{2\omega}{3} + \frac{((1+i\sqrt{3}b_1))}{3 \times 2^{2/3}\mathcal{Z}(b_1, b_2)} - \frac{1}{6 \times 2^{1/3}}(1-i\sqrt{3})\mathcal{Z}(b_1, b_2), \quad (\text{J.7})$$

$$\Delta_3(\omega) = \frac{2\omega}{3} + \frac{((1-i\sqrt{3}b_1))}{3 \times 2^{2/3}\mathcal{Z}(b_1, b_2)} - \frac{1}{6 \times 2^{1/3}}(1+i\sqrt{3})\mathcal{Z}(b_1, b_2), \quad (\text{J.8})$$

where we define again a new function $\mathcal{Z}(b_1, b_2)$, which is given by:

$$\mathcal{Z}(b_1, b_2) = \left(b_2 + \sqrt{4b_1^3 + b_2^2}\right)^{1/3}. \quad (\text{J.9})$$

The above equation shows that the function $\Delta_1(\omega)$ is real, whereas $\Delta_2(\omega)$ and $\Delta_3(\omega)$ are complex. The arbitrary constants obtained after using the late time behaviour as the initial

conditions which are written in the earlier section of this paper are explicitly defined by the following expressions:

$$g_1(\omega) = \frac{1}{\left(-\frac{\mathcal{Y}_1 f_2(\omega)}{4(B_1+B_2)} + \frac{\mathcal{Y}_1 f_3(\omega)}{4(B_1+B_2)}\right) \left(-\frac{\mathcal{Y}_2 f_3(\omega)}{\mathcal{Y}_4} + \frac{\mathcal{Y}_3 f_2(\omega)}{\mathcal{Y}_4}\right) + \left(\frac{\mathcal{Y}_1 f_2(\omega)}{4(B_1+B_2)^2} + \frac{3B_2 f_3(\omega)}{4(B_1+B_2)^2}\right) \left(-\frac{\mathcal{Y}_2 f_3(\omega)}{\mathcal{Y}_4} + \frac{\mathcal{Y}_3 f_2(\omega)}{\mathcal{Y}_4}\right)} \times \left[\frac{-\frac{\mathcal{Y}_3}{4A_1(B_1+B_2)} \left(-\frac{\mathcal{Y}_1 f_2(\omega)}{4(B_1+B_2)} + \frac{\mathcal{Y}_1 f_3(\omega)}{4(B_1+B_2)}\right) \tanh(\pi\kappa\omega) - \mathcal{Y}_1 \left(-\frac{\mathcal{Y}_2 f_3}{\mathcal{Y}_4} + \frac{\mathcal{Y}_3 f_2}{\mathcal{Y}_4}\right) \tanh(\pi\kappa\omega)}{\left(-\frac{\mathcal{Y}_1 f_2(\omega)}{4(B_1+B_2)} + \frac{\mathcal{Y}_1 f_2(\omega) f_3(\omega)}{4(B_1+B_2)}\right)} \right], \quad (\text{J.10})$$

$$g_2(\omega) = \frac{4(B_1 + B_2)12B_1B_2^2 + 36B_2^2 + B_1f_1^2 + 3B_2f_3^2 \tanh(\pi\kappa\omega)}{(f_2 - f_3)(12B_1B_2^2 - 36B_2^3 - B_1f_1^2 + B_1f_1f_2 + B_1f_1f_3 + 3B_2f_2f_3)}, \quad (\text{J.11})$$

$$g_3(\omega) = -\frac{4}{(f_2 - f_3)(12B_1B_2^2 - 36B_2^3 - B_1f_1^2 + B_1f_1f_2 + B_1f_1f_3 + 3B_2f_2f_3)} \times [12B_1^2B_2^2 \tanh(\pi\kappa\omega) + 48B_1B_2^3 \tanh(\pi\kappa\omega) + 36B_2^4 \tanh(\pi\kappa\omega) + B_1^2f_1^2 \tanh(\pi\kappa\omega) + B_1B_2f_1^2 \tanh(\pi\kappa\omega) + 3B_1B_2f_2^2 \tanh(\pi\kappa\omega) + 3B_2^2f_2 \tanh(\pi\kappa\omega)], \quad (\text{J.12})$$

$$g_5(\omega) = -\frac{1}{12B_1B_2^2 + 36B_2^3B_1f_2^2 - B_1f_1f_2 - B_1f_1f_3 - 3B_2f_2f_3} \times [4B_1B_2f_2 \tanh(\pi\kappa\omega) + 3B_2^2f_2 \tanh(\pi\kappa\omega) + B_1B_2f_3 \tanh(\pi\kappa\omega) + 3B_2^2f_3 \tanh(\pi\kappa\omega)], \quad (\text{J.13})$$

$$g_6(\omega) = \frac{1}{12B_1B_2^2 + 36B_2^3 + B_1f_1^2 - B_1f_1f_2 - B_1f_1f_3 - 3B_2f_2f_3} \times [4B_1^2f_2 \tanh(\pi\kappa\omega) \tanh(\pi\kappa\omega) + 16B_1B_2(f_2 \tanh(\pi\kappa\omega) + 12B_2^2f_3 \tanh(\pi\kappa\omega) + 4B_1^2f_5 \tanh(\pi\kappa\omega) + 16B_1B_2 \tanh(\pi\kappa\omega) + 12B_2^2f_3 \tanh(\pi\kappa\omega) - 12B_1B_2^2 \tanh^2(\pi\kappa\omega) - 36B_2^3 \tanh^2(\pi\kappa\omega) - B_1f_1^2 \tanh^2(\pi\kappa\omega) + B_1f_1f_2 \tanh^2(\pi\kappa\omega) + B_1f_1f_3 \tanh^2(\pi\kappa\omega) + 3B_2f_2f_3 \tanh^2(\pi\kappa\omega)]. \quad (\text{J.14})$$

where in writing the function $g_1(\omega)$ we have introduced the following symbols:

$$\mathcal{Y}_1 = \left(1 - \frac{B_2}{B_1 + B_2}\right), \quad (\text{J.15})$$

$$\mathcal{Y}_2 = -12B_2^2 - f_2^2, \quad (\text{J.16})$$

$$\mathcal{Y}_3 = -12B_2^2 - f_3^2, \quad (\text{J.17})$$

$$\mathcal{Y}_4 = 16A_1(B_1 + B_2)^2. \quad (\text{J.18})$$

References

- [1] Daniel A. Lidar "Lecture Notes on the Theory of Open Quantum Systems," arXiv:1902.00967
- [2] Subhashish Banerjee, V. Ravishankar and R. Srikanth, "Dynamics of entanglement in two-qubit open quantum system interacting with a squeezed thermal bath via dissipative interaction," Ann. of Phys. (NY): 325, 816 (2010), eprint:arXiv:0901.0404.

- [3] R. Horodecki, P. Horodecki, M. Horodecki and K. Horodecki “Quantum entanglement” *Rev. Mod. Phys.* **81** (2009) 865 [quant-ph/0702225].
- [4] C. H. Bennett, G. Brassard, C. Crepeau, R. Jozsa, A. Peres and W. K. Wootters, “Teleporting an unknown quantum state via dual classical and Einstein-Podolsky-Rosen channels,” *Phys. Rev. Lett.* **70** (1993) 1895.
- [5] Sk Sazim, S. Adhikari, Subhashish Banerjee and T. Pramanik, "Quantification of Entanglement of Teleportation in Arbitrary Dimensions," *Quantum Information Processing* **13**, 863 (2014), arXiv:1208.4200.
- [6] Simon J. Devitt, Kae Nemoto, William J. Munro “Quantum Error Correction for Beginners” *Rep. Prog. Phys.* **76** (2013) 076001,
- [7] S. Omkar, R. Srikanth and Subhashish Banerjee, "Characterization of quantum dynamics using quantum error correction," *Phys. Rev. A* **91**, 012324 (2015), Eprint:arXiv:1405.0964.
- [8] L. Pezze and A. Smerzi “Entanglement, Nonlinear Dynamics, and the Heisenberg Limit,” *Phys. Rev. Lett.* **102** (2009) 100401.
- [9] Frank Jensen “Introduction to Computational Chemistry.” Wiley, 2007,
- [10] Mohan Sarovar, Akihito Ishizaki, Graham R. Fleming, K. Birgitta Whaley “Quantum entanglement in photosynthetic light harvesting complexes” arXiv:0905.3787
- [11] C Marletto and D M Coles and T Farrow and V Vedral “Entanglement between living bacteria and quantized light witnessed by Rabi splitting” *Journal of Physics Communications*
- [12] M. A. Nielsen and I. L. Chuang, "Quantum Computation and Quantum Information", Cambridge University Press, Cambridge (2000)
- [13] Z. Huang and Z. Tian, “Dynamics of quantum entanglement in de Sitter spacetime and thermal Minkowski spacetime,” *Nucl. Phys. B* **923** (2017) 458.
- [14] Z. Tian, J. Wang, J. Jing and A. Dragan, “Detecting the Curvature of de Sitter Universe with Two Entangled Atoms,” *Sci. Rep.* **6**, 35222 (2016) [arXiv:1605.07350 [quant-ph]].
- [15] J. Hu and H. Yu, “Entanglement dynamics for uniformly accelerated two-level atoms,” *Phys. Rev. A* **91**, no. 1, 012327 (2015) [arXiv:1501.03321 [quant-ph]].
- [16] H. Yu, “Open quantum system approach to Gibbons-Hawking effect of de Sitter space-time,” *Phys. Rev. Lett.* **106** (2011) 061101 [arXiv:1101.5235 [gr-qc]].
- [17] G. Lindblad, "On the Generators of Quantum Dynamical Semigroups", *Commun. Math. Phys.* **48** (1976) 119.
- [18] V. Gorini, A. Kossakowski and E. C. G. Sudarshan, "Completely Positive Dynamical Semigroups of N Level Systems", *J. Math. Phys.* **17** (1976) 821.
- [19] Ingemar Bengtsson, Karol Życzkowski, "Geometry of Quantum States: An Introduction to Quantum Entanglement", Cambridge University Press
- [20] Petr Jizba, Toshihico Arimitsu, "On observability of Renyi’s entropy", arXiv:cond-mat/0307698
- [21] M. B. Plenio, "Logarithmic Negativity: A Full Entanglement Monotone That is not Convex", *Phys. Rev. Lett.* **95** (2005) no.9, 090503 [quant-ph/0505071]
- [22] William K. Wootters, "Entanglement of formation and concurrence", *Journal Quantum Information & Computation*

- [23] W. K. Wootters, "Entanglement of formation of an arbitrary state of two qubits," *Phys. Rev. Lett.* **80** (1998) 2245
- [24] Shunlong Luo and Shuangshuang Fu, "Geometric measure of quantum discord", *Phys. Rev. A* **82**, 034302
- [25] S. Kukita and Y. Nambu, "Entanglement dynamics in de Sitter spacetime", *Quant. Grav.* **34** (2017) no.23, 235010 [arXiv:1706.09175 [gr-qc]].
- [26] Angel Rivas and Susana F. Huelga, "Open Quantum Systems:An Introduction", Springer Briefs in Physics, Springer-Verlag Berlin Heidelberg, 2012, doi:-10.1007/978-3-642-23354-8
- [27] S. Bhattacharjee, H. Bohra, S. Choudhury, P. Chauhan, A. Mukherjee, P. Narayan, S. Panda and A. Swain, "Relating the curvature of De Sitter Universe to Open Quantum Lamb Shift Spectroscopy," arXiv:1905.07403 [physics.gen-ph].
- [28] E. T. Akhmedov, "Lecture notes on interacting quantum fields in de Sitter space," *Int. J. Mod. Phys. D* **23** (2014) 1430001 [arXiv:1309.2557 [hep-th]].
- [29] M. Spradlin, A. Strominger and A. Volovich, "Les Houches lectures on de Sitter space," hep-th/0110007.
- [30] D. Baumann, "Inflation," arXiv:0907.5424 [hep-th].
- [31] S. Choudhury, "CMB from EFT," *Universe* **5** (2019) no.6, 155 [arXiv:1712.04766 [hep-th]]
- [32] A. Naskar, S. Choudhury, A. Banerjee and S. Pal, "Inflation to Structures: EFT all the way," arXiv:1706.08051 [astro-ph.CO].
- [33] S. Choudhury and A. Dasgupta, "Effective Field Theory of Dark Matter from membrane inflationary paradigm," *Phys. Dark Univ.* **13** (2016) 35 [arXiv:1510.08195 [hep-th]].
- [34] L. Senatore, "Lectures on Inflation," arXiv:1609.00716 [hep-th].
- [35] I. Chakrabarty, Subhashish Banerjee and N. Siddharth, "A study of Quantum Correlations in Open Quantum Systems," *Quantum Information and Computation*: 11, 0541 (2011), eprint:arXiv:1006.1856.
- [36] Subhashish Banerjee, "Open Quantum Systems: Dynamics of Nonclassical Evolution", *Texts and Readings in Physical Sciences*, Volume 20, Springer-Singapore, 2018, <https://doi.org/10.1007/978-981-13-3182-4>.
- [37] R. Kosloff, "Quantum Thermodynamics," *Entropy* **15** (2013) 2100 [arXiv:1305.2268 [quant-ph]].
- [38] Breuer, Heinz-Peter; F. Petruccione "The Theory of Open Quantum Systems" Oxford University Press. ISBN 978-0-19-921390-0.
- [39] W. Zhou and H. W. Yu, "The Lamb shift in de Sitter spacetime," *Phys. Rev. D* **82**, 124067 (2010) [arXiv:1012.4055 [hep-th]].
- [40] A. Lewkowycz and E. Perlmutter, "Universality in the geometric dependence of Renyi entropy," *JHEP* **1501** (2015) 080 [arXiv:1407.8171 [hep-th]], J. Lee, A. Lewkowycz, E. Perlmutter and B. R. Safdi, "Renyi entropy, stationarity, and entanglement of the conformal scalar," *JHEP* **1503** (2015) 075 [arXiv:1407.7816 [hep-th]].
- [41] J. L. Zhang and H. W. Yu, "Casimir-Polder-like force for an atom in Hartle-Hawking vacuum outside a Schwarzschild black hole," *Chin. Phys. Lett.* **29**, 080403 (2012).
- [42] G. W. Gibbons and S. W. Hawking, "Cosmological Event Horizons, Thermodynamics, and Particle Creation," *Phys. Rev. D* **15**, 2738 (1977). doi:10.1103/PhysRevD.15.2738

- [43] W. Zhou and H. W. Yu, "The Lamb shift in de Sitter spacetime," *Phys. Rev. D* **82**, 124067 (2010) [arXiv:1012.4055 [hep-th]].
- [44] R. F. Werner, "Quantum states with Einstein-Podolsky-Rosen correlations admitting a hidden-variable model," *Phys. Rev. A* **40** (1989) 4277.
- [45] S. Choudhury and S. Panda, "Entangled de Sitter from stringy axionic Bell pair I: an analysis using Bunch-Davies vacuum", *Eur. Phys. J. C* **78** (2018) no.1, 52 [arXiv:1708.02265 [hep-th]].
- [46] S. Choudhury, S. Panda and R. Singh "Bell violation in the Sky," *Eur. Phys. J. C* **77** (2017) no.2, 60 [arXiv:1607.00237 [hep-th]].
- [47] S. Choudhury and S. Panda "Quantum entanglement in de Sitter space from stringy axion: An analysis using α vacua," *Nucl. Phys. B* **943** (2019) 114606 [arXiv:1712.08299 [hep-th]].
- [48] S. Choudhury and S. Panda, "Spectrum of cosmological correlation from vacuum fluctuation of Stringy Axion in entangled De Sitter space," arXiv:1809.02905 [hep-th].
- [49] S. Choudhury, S. Panda and R. Singh, "Bell violation in primordial cosmology," *Universe* **3** (2017) no.1, 13 [arXiv:1612.09445 [hep-th]].
- [50] S. Choudhury and A. Mazumdar, "An accurate bound on tensor-to-scalar ratio and the scale of inflation," *Nucl. Phys. B* **882** (2014) 386 [arXiv:1306.4496 [hep-ph]].
- [51] S. Choudhury and S. Pal, "Brane inflation: A field theory approach in background supergravity," *J. Phys. Conf. Ser.* **405** (2012) 012009 [arXiv:1209.5883 [hep-th]], S. Choudhury and S. Pal, "Brane inflation in background supergravity," *Phys. Rev. D* **85** (2012) 043529 [arXiv:1102.4206 [hep-th]], S. Choudhury and S. Pal, "DBI Galileon inflation in background SUGRA," *Nucl. Phys. B* **874** (2013) 85 [arXiv:1208.4433 [hep-th]], S. Choudhury, A. Mukherjee, P. Chauhan and S. Bhattacharjee, "Quantum Out-of-Equilibrium Cosmology," *Eur. Phys. J. C* **79** (2019) no.4, 320 [arXiv:1809.02732 [hep-th]], S. Choudhury and A. Mukherjee, "Quantum randomness in the Sky," *Eur. Phys. J. C* **79** (2019) no.7, 554 [arXiv:1812.04107 [physics.gen-ph]].
- [52] D. Choudhury, D. Ghoshal, D. P. Jatkar and S. Panda, "Hybrid inflation and brane - anti-brane system," *JCAP* **0307** (2003) 009 [hep-th/0305104].
- [53] Matthias Christandl, Andreas Winter "Squashed Entanglement" - An Additive Entanglement Measure" arXiv:quant-ph/0308088
- [54] Robert R. Tucci "Entanglement of Distillation and Conditional Mutual Information" arXiv:quant-ph/0202144
- [55] Y. O. Nakagawa, G. S. Arosi and T. Ugajin, "Chaos and relative entropy," *JHEP* **1807** (2018) 002 [arXiv:1805.01051 [hep-th]].
- [56] S. Hollands and R. M. Wald, "Quantum fields in curved spacetime," *Phys. Rept.* **574** (2015), [arXiv:1401.2026 [gr-qc]].
- [57] Attal, Stéphane; Joye, Alain; Pillet, Claude-Alain, "Open Quantum Systems II: The Markovian Approach" Springer. ISBN 978-3-540-30992-5.
- [58] See the web link: "<https://www.oeaw.ac.at/en/detail/news/qutrit-complex-quantum-teleportation-achieved-for-the-first-time/>".
- [59] Yi-Han Luo, Han-Sen Zhong, Manuel Erhard, Xi-Lin Wang, Li-Chao Peng, Mario Krenn, Xiao Jiang, Li Li, Nai-Le Liu, Chao-Yang Lu, Anton Zeilinger, Jian-Wei Pan, "Quantum teleportation in high dimensions," *Phys. Rev. Lett.* **123** 070505 (2019), [arXiv:1906.09697 [quant-ph]].